FROM CAR TRAFFIC TO PRODUCTION FLOWS. A GUIDED TOUR THROUGH SOLVABLE STOCHASTIC TRANSPORT PROCESSES

THÈSE N^{O} 3247 (2005)

PRÉSENTÉE À LA FACULTÉ SCIENCES ET TECHNIQUES DE L'INGÉNIEUR

Institut de production et robotique

SECTION DE MICROTECHNIQUE

ÉCOLE POLYTECHNIQUE FÉDÉRALE DE LAUSANNE

POUR L'OBTENTION DU GRADE DE DOCTEUR ÈS SCIENCES

PAR

Roger FILLIGER

mathématicien diplômé de l'Université de Neuchâtel
de nationalité suisse et originaire d'Ennetmoos (NW)

acceptée sur proposition du jury:

Prof. M.-O. Hongler, directeur de thèse
Prof. Y. Dallery, rapporteur
Prof. J. Jacot, rapporteur
Prof. T. Mountford, rapporteur
Prof. C. van den Broeck, rapporteur

Lausanne, EPFL
2005

From car traffic to production flows A guided tour through solvable stochastic transport processes

Lausanne, EPFL
2005
In part supported by the "Fonds National Suisse pour la Recherche Scientifique"

Preface

The matter exposed here is the organized outcome of three years of theoretical research in the fields of production and micro-engineering which were guided by a theoretical physicist and worked out by a mathematician. The work therefore intrinsically inhibits an interdisciplinary flavor and I personally tend to locate it – using a term introduced recently by S. Solomon and E. Shir in [136]– into the realm of "applied theoretical sciences".
When working between disciplines one takes several risks and in exchange, one is offered several advantages. An omnipresent risk is to fall between the disciplines such that the work is not recognized either by the specialists or by the generalists. An advantage is the possibility to use and exploit existing analogies which may suddenly pop up once a dialog between disciplines has taken place. Both aspects, the risky and the advantageous ones, are present in this work. A few chapters for example do have a strong mathematical touch, even so they contain mainly results relevant for the engineering and/or the physicists world. Nevertheless I hope that the chosen presentation of these chapters helps non specialists to go through the argumentation and specialists to appreciate new applications in their field. As far as the advantageous dialog between disciplines is concerned, I am deeply indebted to my adviser Max-Olivier Hongler. The relevant interdisciplinary dialog preceding this work was (and still is) realized through his constant interplay with a varied scientific and engineering community. The present work and my proper forthcoming owe a lot to this dialog.
The fact that I started with this work is basically due to (reinforced) chance. Max turned chance into fruitful work. A wonderful metamorphose for which I am very grateful and for which I like to express my deep gratitude. I further wish to thank the scientific jury the Professors C. van den Broeck, Y. Dallery, J. Jacot and Prof. T. Mountford. Thanks are also due to the national research foundation which partially supported the research project under the grant number 2000-63377.00/1 and 200020-1011572/1. To complete the financial support I had the opportunity to do tutorial work in the LPM lab and the mathematical lab at the University of Neuchâtel. My thanks go to the lab

headers Professor J. Jacot and Professor A. Vallet for employing me. Thanks are further due to all the members of both labs for professional and social interactions. I am indebted to Mark Coggins which greatly helped me through many english revisions to prepare the final version.

Lausanne, January 2005 *Roger Filliger*

Summary

The purpose of this thesis is to show on explicit examples how various theoretical concepts, ranging from statistical mechanics to stochastic control and from traffic theory to queuing systems, can be transferred to transport processes, encountered in particular in manufacturing systems, with benefic implications for their *dynamical* understanding, optimization and control. The thesis collects several articles where such implications are exposed [38]-[43].

We start with the observation that car traffic and production flows share several common dynamical properties (chapter 3). The main reason for the similarities are the presence of non-linear interactions in both settings. In traffic theory the interactions are between *competing cars* and originate from a trade off between safe and fast driving. They directly influence the speed of the cars. In production flow engineering the interactions are between *cooperating work-cells* forming the manufacturing system. They govern the production policy and hence the throughput of the manufacturing system. We exploit this analogy in case of a serial production line where the influence on the production rate of a work-cell is determined by the contents of its adjacent buffers (fig. 0.1) and derive a dictionary between the two fields. As a first result, this analogy allows the recognition of free-flow and jamming-flow regimes –well studied in traffic theory – in the context of production lines.
Applying a linear stability analysis to a given stationary flow regime, we draw a flow diagram which defines the boundary between the free and the jammed regime as a function of the control parameters. The relevant conclusions include the introduction of a dimensionless performance parameter, an enlightening connection between transient and stationary performance measures for production lines, a discussion of both the bull-whip effect and the stabilizing effect of pull production controls in serial production lines.

The traffic models used in the analogy with serial production lines are so-called optimal-velocity car following models which assume that the velocity of a car is adapted to a distance dependent *optimal velocity* which reflects the safety requirements of two neighboring cars. This optimal velocity is chosen

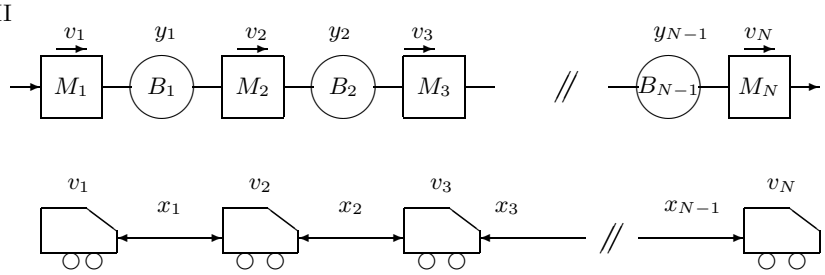

Fig. 0.1. Above: Sketch of a serial production line composed of N machines M_i with production rates v_i and $N-1$ buffers B_i with buffer content y_i. **Below**: Sketch of a one-lane traffic system composed of N cars with velocities v_i and headways x_i. Dynamical similarities between cars and work-cells: the production rates and the car velocities, depend both on their environment e.g., the content of the next nearest buffers $v_i = v_i(y_{i-1}, y_i)$ resp. the distances to the next nearest cars $v_i = v_i(x_{i-1}, x_i)$.

in an ad hoc fashion by traffic engineers and is not related to a cost functional which defines "optimality" via a minimization procedure. Here we calculate in the context of serial production lines the "optimal velocity" (*i.e.*, the optimal production control) based on a specific cost functional. We solve in chapter 4 an optimal control problem for the production rates where the cost structure penalizes the entrance of the buffer content into a boundary state. We show that the optimal control is of four thresholds type and give the optimal position of the thresholds.

The optimal control problem, explicitly discussed for a serial two-stage production line, can not be solved analytically for longer lines. This forces us to look in chapter 5 for other ways to describe relations between the throughput and the work in process of production flows. The analogous quantities in traffic theory – flow of cars and car density – are related in the so-called fundamental diagram (fig. 0.2). It encodes in a single graph the functional

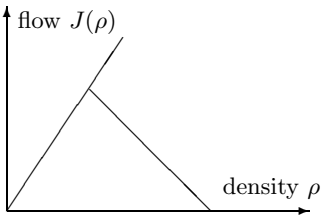

Fig. 0.2. Generic form of the density-flow relation in one-lane car traffic.

relation between the flow of cars and the car-density. Inspired by the micro-macro paradigm of mechanical statistics, we derive from a mesoscopic level the fundamental diagram introduced by Greenshields in 1931. The study is based on the Boltzmann equations introduced by Ruijgrok and Wu, which

we derive from a space discrete interacting particle system. The fundamental kinetic features of the microscopic model are *migration*, *reaction* and *collisions* of particles. Performing the hydrodynamic limit of the model, we have that the macroscopic density distribution ρ is governed by the Burgers equation and that the macroscopic flow J is proportional to the logistic equation.

Another property of production flows shared with cars in traffic is the simple fact that the *circulating items have spatial extensions*. This is of foremost importance especially when multiplexing structures are present in the production line and/or the traffic network. The distribution of items flowing out of a merge structure into a single collecting flow definitely depends on the physical size of the circulating items. In chapter 6 we will study a discrete materials flow merge system connected to a downstream station (fig. 0.3). The outflow process from the merge as a function of the the items extensions is given.

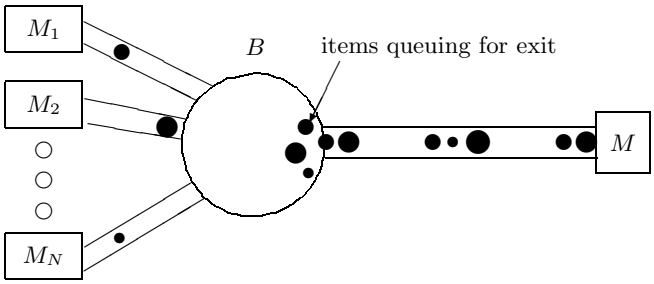

Fig. 0.3. Merging of N streams of items into a buffer B. A conveyor transports the items from B to M. The spatial extensions of the items are crucial for the outflow.

The mentioned discrete velocities Boltzmann equations of Ruijgrok and Wu are related to random evolutions. They are particularly well adapted to model the dynamics of failure prone machines switching between their states (e.g., between "on" and "off"). For the inhomogeneous two-states case (*i.e.*, when the switching rates depend on the environment), we show in chapter 7 that the probability density and the associated probability current are in a supersymmetric relation – a algebraic structure well known in quantum mechanics.

The quest to optimize throughput in stochastic manufacturing systems and vehicles flow in traffic systems can be unified through the following question: *Given the initial distribution of items (of workload or cars) how do I have to influence the noisy dynamics in order to efficiently transport the items involved (workpieces or cars) to a given final distribution?*
This point of view seems natural to us and is directly related to a problem addressed by E. Schrödinger in 1931. He asks for a Markov diffusion process satisfying given initial and final conditions and which minimizes some energy functional. Based on this, we propose in chapter 8 an efficiency measure relevant for a large class of diffusion-mediated transport processes.

Zusammenfassung

Die vorliegende Arbeit hat zum Ziel *dynamische* Vorgänge in stochastischen Transportprozessen zu beschreiben, wie sie speziell in Massenproduktionsprozessen auftreten, wo dynamische Vorgänge entscheiden auf Kontroll- und Optimierungsmöglichkeiten einwirken. Sie zeigt an explizit ausgearbeiteten Beispielen wie Konzepte der statistischen Mechanik, der Kontroll- und Warteschlangentheorie sowie der theoretischen Verkehrsdynamik zum besseren Verständnis solcher Vorgänge beitragen können. Die Arbeit umfasst mehrere Forschungsartikel die sich in diesem Sinne mit entsprechenden theoretischen Konzepten beschäftigen [38, 39, 42, 40, 44, 41, 43].

Wir beginnen mit der Bemerkung, dass verschiedene dynamische Phänomene wie sie im Strassenverkehr auftreten, ihr Analogon in Produktionsprozessen finden (Kapitel 3). Die dynamischen Analogien sind auf Ähnlichkeiten in den nichtlinearen Interaktionen zwischen den Prozessteilnehmer zurückzuführen. In Verkehrssystemen sind diese Interaktionen auf die sich lokal *konkurrierenden Verkehrsteilnehmer* beschränkt, die zwischen schnellem und sicherem Fahren optimieren. Dieses Verhalten ist bestimmend für die Geschwindigkeiten der einzelnen Verkehrsteilnehmer. In Produktionsprozessen werden die Interaktionen zwischen den *kooperierenden Arbeitszellen* lokalisiert, die als Ganzes den Prozess definieren. Sie beeinflussen in entscheidendem Masse die Produktionsstrategie und dadurch die globale Produktionskapazität des Prozesses. Wir bedienen uns dieser Analogie im Fall einer mit Bufferzonen ausgestatteten seriellen Produktionslinie, bei der die Produktionsraten einer Arbeitszelle durch den Lagerbestand der nächstliegenden Bufferzonen determiniert ist (Fig. 0.1). Ein erstes aus dieser Analogie sich ergebendes Resultat für Produktionsprozesse ist die Unterscheidung zwischen laminarem Produktionsfluss und turbulentem Produktionsfluss. Es sind dies Phasenzustände für Materialflüsse die in Verkehrssystemen seit langem intensiv studiert werden. Eine lineare Stabilitätsanalyse ermöglicht die explizite Berechnung eines Phasendiagramms in Abhängigkeit der Kontrollparameter. Eine dimensionslose dy-

namische Kennzahl ähnlich der Reynoldszahl wird eingeführt, der so genannte "bull-whip" Effekt wird angesprochen und der stabilisierende Effekt einer "Pull"-Produktionsstrategie wird disskutiert.

Die zur Beschreibung von seriellen Produktionsprozessen geeigneten Verkehrsmodelle sind so genannte "optimale Geschwindigkeit Fahrzeugfolgemodelle". Die *optimalen Geschwindigkeiten* sich folgender Fahrzeuge sind in aller Regel phänomenologisch angesetzte und von den Distanzen zu den nächsten Fahrzeugen abhängige Funktionen, die die Sicherheitsbedürfnisse der Lenker mit einbeziehen. Die Bezeichnung "optimal" wird von Verkehrsingenieuren nicht an eine Kostenfunktion gekoppelt und bezieht sich deshalb nicht auf ein wohldefiniertes Optimierungsproblem. Diesem Umstand wird in Kapitel 4 Rechnung getragen. Wir berechnen in der produktionstheoretischen Interpretation die Struktur der "optimalen Geschwindigkeit" (genauer, der "optimalen Produktionsraten") durch Einführung einer adäquaten Kostenfunktion und anschliessendem Lösen des Optimierungsproblems. Es wird gezeigt, dass die optimalen Produktionsraten durch vier Lagerbestandniveaus definiert werden können. Die Niveaus werden explizit berechnet.

Das Optimierungsproblem kann explizit nur für serielle Produktionslinien mit (nur) zwei Arbeitszellen disskutiert werden. Dieser Umstand lässt uns in Kapitel 5 andere Wege suchen, um Durchfluss-Lagerbestandrelationen für längere Produktionslinien anzugeben. Die analogen Grössen in Verkehrssystemen – Verkehrsfluss und Verkehrsdichte – werden im so genannten Fundamentaldiagramm zusammengeführt (Fig. 0.2). Es entschlüsselt in einem einzigen Graphen die funktionale Beziehung zwischen dem Fahrzeugfluss und der Verkehrsdichte. Inspiriert durch das Mikro-Makro Paradigma der statistischen Mechanik leiten wir, ausgehend von einer mesoskopischen Beschreibungsebene, das wohlbekannte Fundamentaldiagramm von Greenshields ab. Die Studie basiert auf dem nichtlinearen, Boltzmann-ähnlichen Vielteilchenmodel von Ruijgrok und Wu. Die fundamentalen kinetischen Eigenschaften der Teilchen sind (*i*) *Migration*, (*ii*) *Reaktion* und (*iii*) *Kollisionen*. Folgende Interpretation als einfaches Verkehrsmodel ist möglich: (*i*) Fahren mit zwei möglichen Geschwindigkeiten, (*ii*) spontaner Wechsel zwischen den beiden möglichen Geschwindigkeiten (*iii*) Abbremsen eines schnellen Fahrzeugs das sich einem Langsamen nähert. Interpretiert als einfaches Model für serielle Produktionsprozesse, kann eingesehen werden, dass Migration eines Teilchens dem Weitertransport zu einer nächsten Arbeitszelle entspricht, dass der Reaktionsterm einer spontanen Änderung des Operationszustandes der Zelle zugeordnet werden kann und dass Kollisionen angrenzender Zellen dann eintreffen, wenn der Lagerbestand dazwischen geleert wird. Im hydrodynamischen Limes wird gezeigt, dass die makroskopische Dichte ρ durch die "Burgersgleichung"

gegeben ist und das der makroskopische Fluss proportional zur logistischen Gleichung ist $J \propto \rho(1-\rho)$.

Eine weitere Eigenschaft von Produktionsflüssen die mit Verkehrsflüssen geteilt wird, ist die granulare, platzkonsumierende Struktur der sich bewegenden Teilchen. Diese Bemerkung ist speziell dann von Wichtigkeit, wenn konvergente Strukturen, so genannte Multiplexer, vorhanden sind, die die Flüsse zusammenführen oder teilen. Das Zusammenführen mehrerer Flüsse zu einem gemeinsamen Materienstrom hängt klar von der räumlichen Ausdehnung der Teilchen ab und wird unter diesem Gesichtspunkt in Kapitel 6 untersucht (Fig. 0.3). Wir geben – unter geeigneten Hypothesen – die stationäre Ausflussverteilung als Funktion der granularen Ausdehnung.

Die oben angesprochene Boltzmanngleichung von Ruijgrok und Wu kann, Dank einer logarithmischen Transformation, als "zufallsgesteuertes Evolutionsmodel" (random evolutions) interpretiert werden. Solch evolutive Systeme sind verbreitete Modellierungsmethoden die auch speziell geeignet sind, Maschinenausfälle ("Null-Eins" Dynamik) in die Dynamik aufzunehmen. Wir zeigen in Kapitel 7, dass im Falle einer Dynamik mit zwei möglichen Zuständen, die Wahrscheinlichkeitsdichte und der zugehörige Wahrscheinlichkeitsfluss (also die konstituierenden Grössen des Fundamentaldiagramms) in einer supersymmetrischen Beziehung stehen.

Auf Grund der inhärenten Fluktuationen in Fabrikations- *und* Verkehrssystemen kann den Optimierungsmöglichkeiten beider Systeme folgende probabilistische Fragestellung zu Grunde gelegt werden:
Gegeben eine Anfangsverteilung von Teilchen (von Jobs in den Arbeitszellen oder von Fahrzeugen auf dem Strassennetz), wie braucht die verrauschte Dynamik beeinflusst zu werden um die involvierten Teilchen (Jobs oder Fahrzeuge) effizient auf eine gegebene Endverteilung abzubilden?
Diese Fragestellung scheint natürlich und kann direkt auf ein von E. Schrödinger gestelltes Problem zurückgeführt werden. Es besteht darin, zu gegebenen Anfangs- und Endbedingungen einen Diffusionsprozess zu konstruieren der ein Kostenfunktional minimiert. Basierend auf dieser allgemeinen Betrachtung wird in Kapitel 8 ein konzeptuell neues Effizienzmass für diffusionsunterstützte Transportprozesse eingeführt.

Résumé

La nécessité de maîtriser le pilotage des flux de produits délivrés par les processus de production opérant en environnement aléatoire (les aléas sont essentiellement dus aux enrayages des installations), nous a conduit à développer un ensemble de modèles mathématiques permettant de caractériser la dynamique et le contrôle de flux granulaires hors de l'équilibre thermodynamique. La thèse fait donc un usage intégré de concepts et de méthodes relevant de la mécanique statistique, de la théorie des files d'attentes, du trafic routier et de la théorie du contrôle optimal stochastique. Le travail regroupe et met en relations un ensemble de contributions dédiées aux phénomènes de transports d'objets circulant dans des installations de production [38, 39, 42, 40, 44, 41, 43].

Nous débutons par l'observation que nombreux sont les phénomènes dynamiques propres au trafic routier qui trouvent un analogue dans le domaine des flux de productions (Chapitre 3). Fondamentalement, ces similarités sont dues aux interactions non-linéaires entre les constituants présents dans ces deux types de systèmes. Dans le domaine du trafic routier, les interactions interviennent via les conducteurs qui tentent d'optimiser leur comportement en visant simultanément deux objectifs conflictuels à savoir, conduire avec célérité et sûreté. Dans le domaine des systèmes de production, les interactions interviennent entre les produits délivrés par les unités de production. En effet, les unités de production sont couplées via des convoyeurs et des zones de stockages dans lesquels les produits sont en interaction mutuelle. L'assèchement d'une ou plusieurs zones de stockage ou à l'opposé, leur saturation influe directement la dynamique des flux et détermineront les performances des systèmes de gestion de production. Les similarités formelles entre trafic routier et chaînes de production sont explorées dans le cadre concret d'une installation de type " flow-shop " (fig. 0.1), pour laquelle nous sommes conduit à distinguer entre des flux laminaires et des flux turbulents traversant l'installation. Par une analyse de stabilité, nous dérivons un diagramme de phases qui caractérise l'appartenance à l'un ou l'autre de ces régimes, ceci

en fonction des paramètres de contrôle. Le point de vue interdisciplinaire adopté nous conduit à introduire un nouveau paramètre dynamique, jouant pour les chaînes de production, un rôle similaire au nombre de Reynolds en hydrodynamique.

Les modèles de trafic que nous utilisons pour les flux productions sont connus, dans le domaine du trafic de véhicules, comme étant du type " modèle à vitesse optimale ". Ces modèles, de nature phénoménologique, tiennent compte simultanément de l'évolution en environnement aléatoire et des impératifs de sécurité requis par les conducteurs. Au chapitre 4, nous calculons, pour un dipôle de production, les " vitesses " optimales (i.e. la politique de production optimale) en utilisant un ensemble de critères d'optimisation naturels et pertinents pour les applications usuelles.

Une extension directe du problème à des multipôles de production ne permet plus une approche analytique. C'est la raison pour laquelle nous proposons, au chapitre 5, un nouveau point de vue qui lui offre la possibilité de relier, dans les régimes stationnaires, l'amplitude du flux de production avec la densité locale des entités en circulation. Cette relation s'exprime via un diagramme – flux et densité – connu sous le nom le diagramme fondamental (fig.0.2) qui a été introduit par Greenshields en 1931. A partir de considérations purement microscopiques et en s'inspirant très directement du paradigme "micro-macroscopique" emprunté à la mécanique statistique, nous dérivons ce diagramme fondamental analytiquement. A cette fin, nous sommes amenés à introduire un niveau de description intermédiaire (*i.e.* le point de vue mésoscopique) qui fait appel à des équations de type Boltzmann avec des vitesses discrètes (modèle de Ruijgrok et Wu). Initialement, les propriétés cinétiques fondamentales des particules modélisées sont (*i*) *migration*, (*ii*) *réaction* et (*iii*) *collision* se traduisent en termes de trafic routier par (*i*) conduire avec deux vitesses possibles, (*ii*) modifier sa vitesse (*iii*) ralentir à cause de la présence d'une voiture plus lente en aval. Cette analogie exploitée dans le cadre de la production, nous permet de construire un modèle dynamique – fortement simplifié - qui décrit les multipôles de production. Les migrations et les réactions du modèle initial deviennent respectivement l'avancement d'une pièce et le changement d'état (i.e. marche- arrêt) d'une machine et une unité affamée correspond à une collision dans le domaine du trafic. Dans cette approche, il est remarquable que dans la limite hydrodynamique, la densité ρ obéisse à l'équation de Burgers alors que le flux J lui satisfasse à l'équation logistique $J \propto \rho(1-\rho)$.

Une autre propriété fondamentale commune aux flux de produits et aux flux de véhicules est l'extension spatiale des objets en circulation. La prise en compte de cette extension est tout particulièrement nécessaire lorsque l'on a affaire soit à des aiguillages soit à des multiplexeurs rassemblant plusieurs

flux parallèles en un seul flux émergent. Cette problématique est discutée au chapitre 6, où nous caractérisons le flux de sortie d'un multiplexeur en fonction de la taille des objets en circulation (fig. 0.3).

L'équation de Boltzmann dans sa variante à vitesses discrètes, (i.e. le modèle de Ruijgrok et Wu mentionné précédemment), est très intimement connectée, via une transformation logarithmique, à des modèles d'évolution sujets à des changements aléatoires de vitesses. Ce point de vue est lui également adapté à la modélisation d'une unité de production sujette à des aléas et nous montrons au chapitre 7 que, sous certaines hypothèses, la densité de probabilité et son flux associé conjointement obéissent à une relation super-symétrique bien connue en mécanique quantique.

Tout au long de notre travail, la présence ubiquitaire de fluctuations, nous amène à repenser la nature des problèmes d'optimisation des flux en termes purement probabilistes et directement inspiré par une ancienne mais fondamentale contribution de E. Schrödinger (1925). Comment, à partir d'un état initial aléatoire mais dont la distribution de probabilité est donnée, piloter l'évolution afin de réaliser un état final lui aussi aléatoire mais dont la distribution de probabilités est définie à priori et ceci tout en minimisant une fonction objectif donnée. Ce cadre général appliqué dans le domaine du transport, nous permet de proposer de nouveaux critères de performance pour le pilotage des flux granulaires et en particulier d'avancer une définition rigoureuse de l'efficacité des moteurs browniens.

Contents

Preface V

Summary VII

Zusammenfassung XI

Résumé XV

Part I Introduction

1 Introduction 3
- 1.1 The Industrial Revolution, or the possible outcome of a dynamical system 3
- 1.2 Background and Motivation 7
- 1.3 Original contributions exposed in this thesis 9
- 1.4 Organization 10

2 A brief review of related literature 13
- 2.1 Introduction 13
- 2.2 Directly related literature 13
- 2.3 Related literature on Stochastic modelling and control of MSs 14
- 2.4 Related literature on Traffic theory 16
- 2.5 Related literature on Stochastic control 17
- 2.6 Related literature on Random evolution 18
- 2.7 Related literature on Diffusion mediated transport 18

Part II Flows in Manufacturing and Traffic systems

3 Cooperative Flow dynamics in production lines with buffer level dependent production rates 21
3.1 Introduction 21
3.2 Models 23
3.2.1 Buffered Flow Shop 23
3.2.2 Optimal-Velocity Car Traffic Model 25
3.2.3 Correspondence between Flow Shops and Optimal-Velocity models 26
3.3 Linear stability analysis 29
3.3.1 Time-continuous Analysis 29
3.3.2 A worked example; the stability of a production line following a pull production control. 32
3.3.3 Discrete time analysis 34
3.4 Concluding remarks 36
3.5 Contributions of Chapter 3 37

4 Optimal control for two stage production systems 39
4.1 Introduction 39
4.2 The Model 43
4.2.1 The production planning problem 44
4.3 Chapman-Kolmogorov-equations 48
4.3.1 The absolutely continuous part of the C-K equations 49
4.3.2 The C-K equations at the boundaries 0 and H 49
4.3.3 The C-K equations at the thresholds y and Y 50
4.3.4 The C-K equations at the thresholds z and Z 50
4.3.5 Constants of integration 51
4.4 Stationary probability distribution 52
4.4.1 Solutions for the absolutely continuous part 53
4.4.2 Solutions at 0 and H 54
4.4.3 Solutions at z and Z 55
4.4.4 Solutions at y and Y 55
4.4.5 Matching at z and Z 55
4.4.6 Matching at y and Y 56
4.4.7 The cumulative distribution function 58
4.5 The optimal thresholds 59
4.6 Concluding remarks 61
4.7 Contributions of Chapter 4 62

5 Multi-scale analysis for a traffic model 63
5.1 Introduction 63
5.2 Discrete derivation of Ruijgrok's and Wu's model 64
5.2.1 Space discrete stochastic hopping model 64
5.2.2 Micro-meso link 67
5.3 Application to Traffic modelling 71

5.4 The Mesoscopic derivation of Greenshields fundamental diagram . . . 75
5.4.1 Derivation of Greenshields' Model . . . 76
5.4.2 Discussion . . . 78
5.5 Application to serial production lines . . . 80
5.6 Concluding remarks . . . 82
5.7 Contributions of Chapter 5 . . . 83

6 The outflow process of a merge system . . . 85
6.1 Introduction . . . 85
6.2 Problem Formulation . . . 89
6.3 Exact analysis of the output process from the buffer . . . 90
6.4 Beyond the merge . . . 95
6.5 Concluding remarks . . . 96
6.6 Contributions of Chapter 6 . . . 97

Part III Mesoscopic Modelling of Stochastic Transport

7 Supersymmetric density-flow relations in random two-velocities processes . . . 103
7.1 Introduction . . . 103
7.2 Two-velocities process with inhomogeneous dichotomous noise 105
7.3 Transient behavior and Supersymmetry . . . 107
7.4 Concluding remarks . . . 111
7.5 Contributions of Chapter 7 . . . 112

8 Efficiency Measure for diffusion-mediated transport processes . . . 113
8.1 Introduction . . . 113
8.2 Problem Formulation . . . 116
8.3 Applications for a class of pulsating ratchets . . . 118
8.3.1 The efficiency for a pulsating ratchet in the central limit regime . . . 119
8.3.2 Conceiving efficient Brownian Motors. . . . 121
8.4 Concluding remarks . . . 122
8.5 Contributions of Chapter 8 . . . 122

Part IV Conclusions and Perspectives

9 Conclusions and perspectives in a word on complexity . . . 127

Part V Appendix

10 Appendix Chapter 4 133

11 Appendix Chapter 6 137
11.1 Numerical simulation 137

12 Appendix Chapter 8 139
12.1 Conditioned Probabilities 139

13 Curriculum vitae 143

References 147

Index 155

Part I

Introduction

1

Introduction

1.1 The Industrial Revolution, or the possible outcome of a complex dynamical system

"In the eighteenth century, a series of inventions transformed the manufacture of cotton in England and gave rise to a new mode of production – the ***factory system****. During these years, other branches of industry effected comparable advances, and all these together, mutually reinforcing one another, made possible further gains on an ever-widening front. The abundance and variety of these innovations almost defy compilation, but they may be subsumed under three principles:*

- *the substitution of machines – rapid, regular, precise, tireless – for human skill and effort;*
- *the substitution of inanimate for animate sources of power, in particular, the introduction of engines for converting heat into work, thereby opening to man a new and almost unlimited supply of energy;*
- *the use of new and far more abundant raw materials, in particular, the substitution of mineral for vegetable or animal substances.*

These improvements constitute the Industrial Revolution."
These principles – stated in [92] by David S. Landes, Emeritus Professor of Economics at Harvard University – are doubtless of foremost importance for the emergence of the Industrial Revolution. But still, the phenomenon leaves us with many questions: was the revolution in industry simply an issue of new machinery or mechanical innovation? Was industrial capitalism nothing more than a clever system devised by clever capitalists to exploit the labor of ignorant workers? Was the revolution in industry the product of conscious planning or did it happen spontaneously?

Trying to answer these questions is an interdisciplinary task which goes far beyond the scope of these notes. I will instead state – using Landes' definition – a related and more precise introductory question:

Why can we conceive factory systems?

From a purely philosophical point of view, H. Arendt gives a very concise and convincing answer based on the principle of organization ([10] p.113). Remarking that a factory system is based on a possible partition of a manufacturing process into its essential constituents, she concludes that these constituents have to *co-operate* and must therefore be *organized* (in order to manufacture the desired goods). Hence, it is the capability of *organizing* specific operations which conceptually allows to conceive manufacturing systems (MS).
In modern MSs these specific operations are realized in work-cells (*i.e.* the essential constituents) capable to receive (resp. send) items from (resp. to) other work-cells following the organization scheme. The resulting "flow" of products routed through the cooperating work-cells makes the MS a complex dynamical system.
Coming back to Landes' characterization, we see that it was the interplay of such dynamical systems – interacting either directly with each other or by means of the shared economical environment – which gave rise to the Industrial Revolution.
Yet the Industrial Revolution is a historical fact and we are not going to prove such a macroeconomic outcome out of interconnected (microeconomic) dynamical systems. The point is that, whenever the principle of workforce-organization applies, manufacturers are – from a synergetic point of view – confronted with an open complex physical system, itself organized in a network-like structure which is driven and maintained far from the thermodynamic equilibrium. Short, the flow dynamics of a MS is a complicated thing. It is therefore natural to ask for **theoretical concepts able to explain** at least qualitatively the issuing **dynamical phenomena** such as instabilities, inefficiencies and self-organization **in production processes** and more generally in transportation processes. This is the main theme of the present work.
To be more concrete, let us consider a MS embedded in its environment as depicted in figure 1.1. Flows of matter, energy and information are maintained in the factory and contribute, as an out-of-equilibrium system, to the occurrence of the required finished goods. The production flows present in such systems give emergence to dissipative structures (e.g. flow patterns) including the following **dynamical phenomena**:

1. Clogging at bottlenecks (*i.e.* accumulation of matter at specific work-cells) leading to inefficiencies in the production process due to blocking and starving phenomena (*i.e.* full and empty buffers);
2. The so-called "bull-whip effect" (*i.e.* important oscillations in stock levels due to (small) variations in the consumption rate) which is a hallmark of dynamical instabilities in the production process.

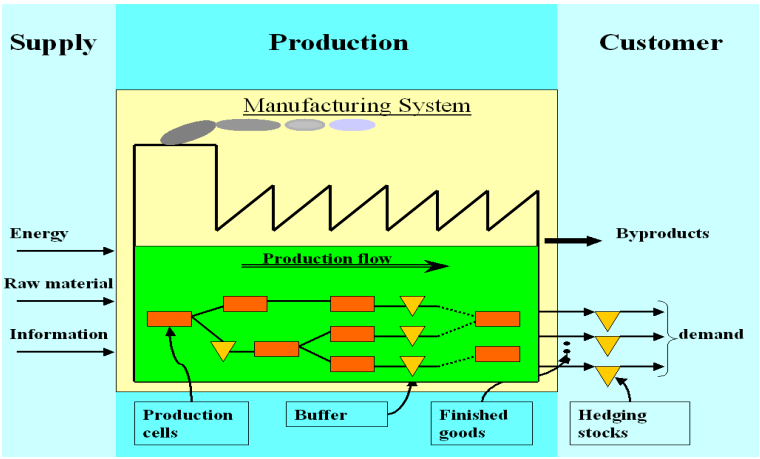

Fig. 1.1. Schematic view of a supply-production-customer chain. Energy, raw material and information are gathered in the supply part, conveniently transformed in the production part and transported towards the downstream-user (e.g. individual customers), where the finished goods are consumed.

3. Self-organizing effects such as the synchronization of stock levels oscillations in buffered manufacturing systems.

The **theoretical concepts** we will use to help understand such dynamical features come from:

1. Statistical Physics. The fundamental task of statistical mechanics indeed culminates in the desire to understand the emergence of macroscopic collective properties from microscopic interactions.
2. Traffic Theory. The observation that several dynamical phenomena of cars in traffic share common properties with production flows is key and will be exploited throughout this work.
3. Queueing Systems. A powerful and well developed modelling tool which is the widely accepted modelling language for stochastic MSs.

Regrouped as a whole, these theoretical tools are concerned with the relationships between entities moving in a network. The precise nature of the moving entities is thereby downplayed in hopes of uncovering deeper laws (e.g. the emergence of instabilities etc.). A simple but fundamental example of such a law, directly relevant for this work, are *current-density relations* which may take the following form:

$$J(x,t) = J(\rho(x,t)). \tag{1.1}$$

The above relation – if it exists for the dynamics of a given system of moving entities – says that $J(x,t)$, the current of the moving entities on a given location x at time t, depends exclusively on $\rho(x,t)$, the density of these entities at a given place x at time t. Such a relation is very rich in content as it encloses

all the dynamic information specific for the system at hand and a large body of theoretical work has been devoted to derive such macroscopic relations starting from microscopic models. Depending on the physical nature of the circulating entities (discrete items or continuous flow of matter), the function ρ takes on values in $\{0, 1\}$ or $[0, 1]$ and we suppose that it describes, up to a multiplicative normalization constant, the distribution of the entities among the network (in view of our examples, one may think of $x \mapsto \rho(x, t)$ as the distribution of cars along the road at time t or as the workload distribution in manufacturing systems at t). Such a relation is of crucial interest in particular if we assume that the quantity of circulating items is conserved (*i.e.* the inflow into and the outflow from the system are balanced). In this case we can add to eq. (1.1), at least formally, the continuity equation:

$$\partial_t \rho(x, t) + \partial_x J(\rho(x, t)) = 0 \tag{1.2}$$

where $\partial_t \rho$ is the variation of ρ with respect to t and where $\partial_x J$ is to be understood as the flow variation in the space variable. From these introductory remarks we see that knowing that the stationary current is a function of the density alone, is crucial for calculating the density profile $\rho(x, t)$.
The point for "flow engineering" is that the knowledge of $\rho(x, t)$ contains the information on the density (e.g., the workload distribution upon the work-cells or the distribution of cars along the road) and $J(x, t)$ encodes the flow behavior at time t on the location x (e.g., the throughput of a specific work cell or the vehicles-flow at x). These are fundamental pieces of information for production engineers and for traffic engineers which have to *organize* and *optimize* production flows in MSs and respectively vehicles-flow in traffic systems. This active influence onto the dynamics lead us, together with the three aforementioned theoretical concepts, to the fourth concept extensively used in this work namely

4. Stochastic optimal control. It is the natural connection between the scientific desire to understand a given process and the engineering need to modify and control it.

The controlled state variables $J_u(x, t)$ and $\rho_u(x, t)$ now both depend on a control u affecting the production rates of the work-cells respectively the speed of the circulating vehicles and which can be chosen within a set U of possible values. It is then mandatory to select the best control u^* with respect to some cost functional *i.e.*, to select the control which minimizes the costs. Such an optimization procedure is performed in Chapter 4 in the context of production engineering.

It is amusing to note that this directed research (transfer from theoretical to applied sciences) has generated two theoretical "by-products" in the opposite direction. Firstly, the study of the mentioned current-density relation for given stochastic dynamics indeed enables us to unveil a supersymmetric relation similar to the one arising in Quantum Mechanics. Secondly, the quest for

optimal transport in stochastic manufacturing systems offered a new understanding of the currently used efficiency concepts employed in the domain of diffusion mediated transport processes. I believe that with these two theoretical results, the thesis gains on interdisciplinary character. This is, I believe, an essential need on the way towards a better understanding of the emerging phenomena of complex systems such as the industrial revolution out of interconnected manufacturing systems.

1.2 Background and Motivation

The increased international competition for manufactured products has made clear that the quality of a product is not the single factor upon which the life of a product depends. The competition indeed has created the need for sophisticated MSs *and* manufacturing processes which has stimulated a lot of academic research for problems related to manufacturing.
Traditionally, the academical problems that have originated from the manufacturing environment belong to the sphere of Operations Research (OR). Queueing theory is one of the many tools used by the OR community to model and study MSs. Here the MS is modelled as a network of queues. Queueing networks originating from manufacturing environments have proved to be anything but trivial. Manufacturing processes seems indeed to be an endless source of challenging problems and the related literature is simply immense and bewildering.
Without checking all the available results in queueing networks, most of the analytical results are and will remain – due to the inherent complexity of manufacturing networks – of stationary character (*i.e.* only stationary performance measures can be calculated). This is a serious *drawback of this approach as it does not account for time localized, transient dynamical phenomena.* Production dynamics however, based on the time localized cooperation of working-cells, show very rich spatio-temporal flow patterns and their understanding is of foremost importance for optimization purposes. An external reference corroborating this point of view is Professor Buzacotts comprehensive lecture on "Analysis and Modelling of Manufacturing Systems". In this lecture, held in Tinos Island Greece 1999, he emphasizes the importance to study *cooperative behaviors in complex manufacturing systems.*
Soon after this lecture, my thesis adviser M.-O. Hongler came up with the idea of using theoretical concepts from traffic theory, statistical mechanics and transportation theory in order to help understanding cooperative behaviors in production processes. The crucial helper for the breakthrough of the idea was a series of discussions with the production engineers of a large chemical group based in Geneva. They drew our attention to their need to understand thoroughly the cooperative effects occurring in their production flows. They observed that a relatively short time interruption in the production flow, (due

for example to a "punctual" strike), induces an extremely robust and long lived *jamming* in their process. The issuing question:

"Can we give critical conditions for the formation of robust jamming together with the characteristic time needed for these perturbations to be faded out?"

was the starting point of this thesis and already demands for concepts capable to deal with phase transitions between flow regimes, time localized perturbations and stability.

Besides the restricted dynamical insight into production dynamics, queueing systems modelling suffers from another drawback. While the modelling concepts of queueing theory naturally takes into account the probabilistic nature of stochastic manufacturing systems, all Markov network models share the property that the circulating items are immaterial tokens. Tokens with vanishing spatial extensions can clearly be superposed or dispatched without any physical constraints. This abstract point of view is often too naive for production processes. Consider indeed the *multiplexing of sever parallel flows* of items into a single stream as sketched in figure 0.3. A consistent description of the flow dynamics at the merging point must imperatively *take into account the finite spacial extension of the items.*

From an interdisciplinary point of view it is interesting to note that the understanding of merging flows of physical objects at bottlenecks is relevant for the modelling of the crowd dynamics of panicking pedestrians – one of the most disastrous forms of collective human behavior (see e.g., http://www.panics.org). Observed and simulated current-density relations of pedestrians jamming in escape situations unveil a *"slower-is-faster effect"* which is to say that for sufficiently high densities, the escape rate (outflow current) decreases when the individuals augment their speeds (see figure 1.2). The driving force behind this effect is the existing discrepancy between the

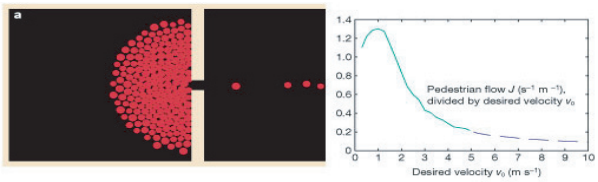

Fig. 1.2. Simulation-analysis of pedestrians moving with identical desired speed v_0 towards the exit. The figure is taken from the article *Simulating dynamical features of escape panics* by D. Helbing et al. in [23]. It shows the slower-is-faster effect due to clogging at the exit.

individual and the collective goals. Minimizing the individual outflow times

does in fact not necessarily maximize the escape rate. The immediate lesson to be learned for production engineering is that whenever the circulating entities take local decisions (think for example of a state dependent local routing through a manufacturing system) they have to be optimized on a global level. Note that the "slower-is-faster" paradigm has already been successfully applied to production processes [122].

Two rather unexpected theoretical results popped up while having a closer look at current-density relations in transport processes. They are exposed in part III of the thesis. The starting point is that MS models with prone-to-failure machines have many similarities with velocity-jump processes (think of the velocity-jumps as sudden switches between production rates). Inspecting a simple two-velocities jump process with space-inhomogeneous switching rates, we became aware of a remarkable symmetry relation between the probability density and the associated probability current which appears to have its analogy in the context of signal processing. This strong relation suggests that one may be able to further reduce the number of relevant variables describing (and/or controlling!) current and density variables. Moreover, the issuing results are suspected to be useable for the numerical studies of a class of hyperbolic partial differential equations [79]. The second theoretical result combines transport with stochastic control which lead naturally to optimal transportation problems. We believe that the field of optimal transportation contains a wealth of results of practical relevance for supply chains and logistics.

1.3 Original contributions exposed in this thesis

The basic contributions of our research can be located in the domains of (*i*) manufacturing modelling, (*ii*) traffic theory, (*iii*) optimal control, (*iv*) random evolution and (*v*) diffusion mediated transport. In this order we:

(i) unveiled and explored a close analogy between the production flows delivered by serial production lines and cars in highway traffic. We draw a phase diagram exhibiting two different flow patterns, namely the free and jamming production regimes and identify the critical production control parameter for stable free flow. We extract a dimensionless dynamic parameter (relevant for design purposes) which quantifies the part of the stationary production inefficiency coming from the linear instabilities of the production dynamics [42]. Moreover, we calculated the outflow process of a merge system feeded by N independent streams of physical items having finite spacial extensions and have drawn conclusions related to production engineering [40].

(ii) derived from a mesoscopic Boltzmann-like traffic model the current-density relation introduced in an ad hoc manner by B.D. Greeshields.

The non-linear Boltzmann-like traffic model is derived from a space discrete particle hopping model and explains on a minimal level of detailed knowledge the kinetic features leading to congestion formation in traffic flows [39, 38].

(iii) solved a production planing problem for a buffered two stage, failure prone production system where the associated cost structure penalizes empty and full buffer states [43].

(iv) discussed a two-velocity process with space dependent drift and show that under some additional conditions, the probability current and the probability density obey a supersymmetric relation [41].

(v) propose an efficiency measure for a large class of diffusion mediated transport processes based on a stochastic optimal control problem [44].

Note that the concluding sections given at the end of every Chapter provide the detailed lists of all the new results and contributions of the corresponding chapter.

1.4 Organization

This thesis is divided into five parts which, in turn, are subdivided into several Chapters. Each Chapter is as self-contained as possible and contains an introductory part which is conceived as an entry point into different ares of the related literature. The different parts regroup the work as follows:

I introduction to the main phenomena of interests and the main concepts necessary for their descriptions;
II modelling and control of production and traffic flows;
III mesoscopic modelling of stochastic transport;
IV conclusions and open research problems;
V a set of appendices providing computations;

Part I consists of Chapter 1 and 2. In Chapter 1 (the one you are actually reading now) we give a gentle introduction to the main theme of the thesis, provide the reader with some background information and industrial motivations, state the main contributions and outline the plan of the thesis. In Chapter 2, we briefly review the literature on related works.
Part II consists of Chapter 3, 4, 5 and 6. Chapter 3 sets out for the dynamical analogies between serial N stage production processes and the flow of N cars described by an ad hoc "optimal velocity" car following model. In Chapter 4 we rigourously calculate the "optimal velocity" in case of a tandem production line with $N = 2$. In Chapter 5 we are looking for current-density relations for N big. In Chapter 6 we study the outflow process of a discrete materials flow merge system connected to a downstream buffer.
Part III consists of two theoretical results exposed in the Chapters 7 and 8. In Chapter 7, we report on a supersymmetric relation in a space inhomogenous

two-velocities transport process and in Chapter 8 we quantify the efficiency of diffusion mediated transport processes using a stochastic optimal control formulation.
Part IV regroups the overall-conclusion and perspectives in a word on complexity.
Part V consists of Appendices. These provide some technical calculations used in the notes.
An extensive bibliography, the subject index and the authors CV and publications follow the appendices. We conclude this section by drawing a flowchart (fig. 1.3) depicting relationships between various Chapters.

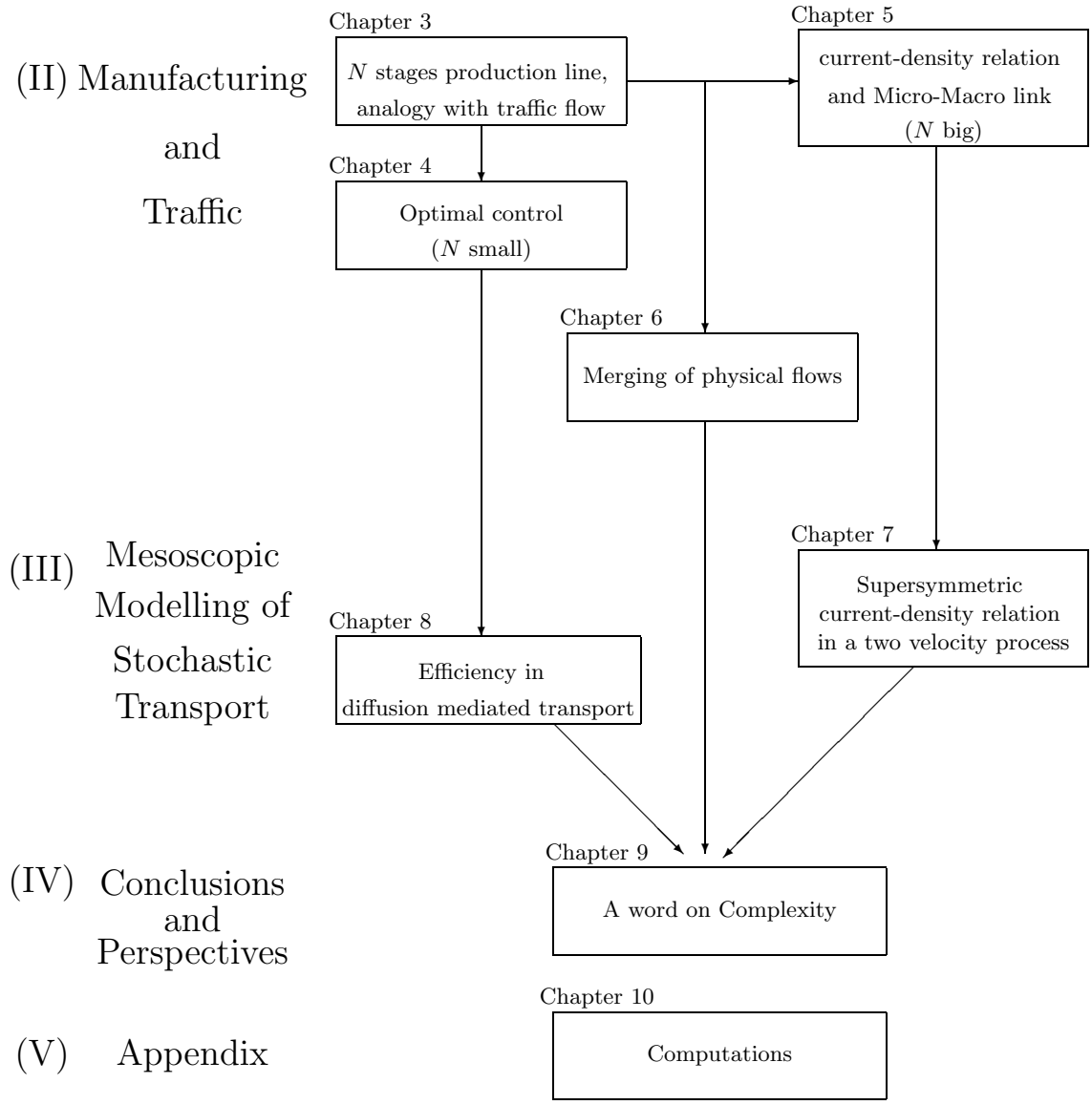

Fig. 1.3. Relationships between Chapters. Each Chapter is as self-contained as possible and contains an introductory part which is conceived as an entry point into different areas of the related literature.

2

A brief review of related literature

2.1 Introduction

In this Chapter the literature related to our subject is briefly reviewed. The references are classified into six topics. First we give a comprehensive review of the *literature that is directly related* to the main themes. We then review the related literature in the areas of:

- stochastic modelling and control of manufacturing systems,
- traffic theory,
- stochastic control,
- random evolution and
- diffusion mediated transport.

2.2 Directly related literature

The idea of using traffic theory to describe cooperative behaviors in production processes came up to my adviser in the fall of 1999 and was, to the best of my knowledge, at that time also new. However, we came aware by mid 2003 of works describing production processes using exactly the same idea. In my opinion, this is rather encouraging and invites to pursue this direction. Here I will briefly review these works.

- The first published work connecting supply chains and traffic theory is to our knowledge the Springer Lecture notes in Economics and Mathematical Systems "A theory of supply chain" by C.F Daganzo [25] (2003). He relates the occurrence of the bull-whip effect to stability conditions on the supply chain and discusses the stability of serial supply chains under several production scheduling policies.
- The first published work connecting supply chains and concepts of statistical mechanics is the paper "Kinetic and Fluid Model hierarchies for

supply chains" by D. Armbruster et al. [22] (2003). They present a model hierarchy for supply chains analogous to the scale hierarchy leading from the Newton-like description of the many body problem to the equations of gas dynamics. They discuss possible mean-field models for the supply chain and verify numerically their accuracies for serial supply chains. In our micro-meso-derivation we use the limit theorems for Markov processes established by W.A. Rosenkrantz and C.C.Y. Dorea [127]. On this work is based the diffusion approximation for a whole class of Markov processes exposed by W.A. Rosenkrantz and L.Z. Bing in [126] (1983). A variant of this approximation theorem including also our microscopic hopping model is given in Chapter 5.

- During 2003, Dirk Helbing, one of the leading traffic theorists, has generalized some ideas suggested by Daganzo and Armbruster et al. published in [65] (2003). The appealing title of this work declares a whole program: *"Modelling and Optimization of Production Processes: Lessons from Traffic Dynamics."* This transfer of knowledge contains besides the discussion of the "bull-whip effect" in the language of traffic theory also the connection with the"slower-is-faster effect" observed in pedestrian dynamics.
- The stochastic control paper [119] (1991) of P. Dai Pra and the paper "Generalized Efficiency and its Application to Microscopic Engines" [74] (1999) by I. Derényi et al. are directly relevant for Chapter 8 – the rigorous definition of an efficiency measure for diffusion mediated transport. The paper of Derényi et al. proposes an informal definition of a new efficiency measure for micro-devices transported with the aid of noise. The definition relies on the concept of "minimal energy cost of completing a task" which is basically an optimal control problem. It is at this level where the paper of Dai Pra gives a twist of rigor to Derényis definition by solving the stochastic optimal control problem.
- The merging of cars in multi-lane traffic into a one lane stream of cars is discussed in "On single-lane Roads", a work by A.J. Koning [86] (1989). Using the dictionary between production flows and cars in traffic, the paper constitutes the main source of inspiration for Chapter 6. The paper calculates the asymptotic behavior of the flow after the merge.
- Honglers' paper on "Supersymmetry and signal propagation in inhomogenous transmission lines" [68] made us discover supersymmetric relations in two-velocities jump processes (Chapter 7). An excellent introduction to Supersymmetry avoiding Grassmann-algebras and bra-cket notations which includes however many many enlightening examples is [21].

2.3 Related literature on Stochastic modelling and control of manufacturing systems

The modelling of stochastic manufacturing systems by means of queueing systems is very vast and excellent and comprehensive reviews are available

[14, 51, 111]. The nicely told story of "the evolution of manufacturing system models" [15] (2003) by J.A. Buzacott gives a personal view on the domain and motivates a reorientation of the field towards the understanding of competition and cooperation of supply chain partners.
A lot of control research on MSs is based on the model described by the inventory-production equation:

$$\dot{x}(t) = u(t) - d(t) \tag{2.1}$$

relating the change of inventory $\dot{x}$ with the production rate u and the demand rate d. With this model the discrete nature of parts is neglected and it is assumed that the material flows continuously between the components of the MS. The literature in continuous materials flow MSs is briefly reviewed.
Stationary Performance Measures. The first approach to our knowledge that treated a serial production line with a continuous flow model is due to B. Zimmern [154]. This original contribution has stimulated a strong research activity with the aim to calculate the average throughput and other performance measures for failure prone flow- and job-shop manufacturing systems (see [26] for a review). In particular J. Wijngaard [151] and similarly D. Dubois and J.P. Forestier [31] quantify the benefic (stationary) effect of interstage storage buffers on the output of two stage production lines. We make repeated use of these results in Chapter 4.
Control. Pioneering contributions in manufacturing flow control include the paper [5] by R. Akella and P.R. Kumar and the paper [13] by T. Bielecki and P.R. Kumar. Akella and Kumar showed the optimality of the Hedging point policy for the case of a *single machine* that produces one part type. They used a discounted type of performance index and the optimization was over an infinite time horizon. They also provided a closed form for the hedging point. Interestingly enough, they found that the hedging point could be zero, a result that is in compliance with the "just-in-time" manufacturing philosophy. Bielicki and Kumar solved the same problem using as performance measure the expected average cost. In order to find the hedging point, they derive the probability distribution of the inventory of finished parts. Then the hedging point is chosen to minimize the total expected cost of carrying the inventory of finished parts. The same strategy is applied in Chapter 4 to derive the optimal control of a two stage line for a specific cost structure.
Tandem two-machine MSs are studied by Ryzin et al. in [47], by Lou et al. in [140] and by Veatch and Wein in [144]. These works aim to minimize inventory holding and backorder costs and compare the performances of the optimal controls with the performances of simpler ones.
In his master thesis, M.N. Eleftheriu analysis hedging point policies for *multi-stage* MSs and finds hedging points for every buffer of the MS. The estimation is based on the failure rate that a buffer sees and depends on the failure of all the machines that are upstream with respect to the buffer [34].

However, when the production line consists of more than two machines together with internal buffers, the optimal production planning control becomes very complicated and optimal control policies cannot be described by hedging points. A promising approach to the almost optimal dynamic scheduling for production systems can be found in the PhD thesis of F. Dusonchet [33] where the (close to) optimal control of stochastic processes by means of switching indices is analyzed. Recognizing the complexity of the control problem, Sethi and Zhang [134] have developed a hierarchical approach for solving it approximately when the rate of change in machine states is much larger than the discount rate of the costs. In this case, they show that the original problem can be approximated by a deterministic problem and that the optimal solution of the deterministic problem is asymptotically optimal for the initial problem as the rate of change in machine state becomes large.

2.4 Related literature on Traffic theory

The works on traffic theory by D. Helbing form an important part of the actual body of traffic research literature. His recent review [64] (2001) together with the review of D. Chowdhury et al. [1] (2000) form an excellent overview on the subject and guides the reader through the vast body of available literature.

Micro and Macro Models. The microscopic optimal velocity car traffic model which inspires our dynamic description of the production line in Part II is discussed by Bando et al. [3]. How to suppress instabilities in this optimal velocity model by means of a delayed-feedback control is explained in [2] and is of practical relevance for the stability of production lines and supply chains. The related class of macroscopic traffic models, describing the collective vehicle dynamics in terms of the vehicle density $\rho(x,t)$ and the average flow $J(x,t)$, is the one introduced by Lighthill and Whitham in [95]. They assume the existence of an equilibrium current-density relation

$$J(x,t) = J(\rho(x,t)). \tag{2.2}$$

which together with the continuity equation (1.2) is the starting point of an elaborate shock wave theory. On the basis of experimental observations, Greenshields proposed in [55] an explicit choice for $J(\rho) \propto \rho(1-\rho)$ which we will derive from a mesoscopic level of description in Chapter 5.

Current-density relations. Obviously, traffic flow phenomena strongly depend on the occupancy of the road. Most important for traffic engineers are flow-density relations (also current-density relations) which can be measured on highways [45] and which show the generic form of an inverted V in the density-current diagram. The precise nature of this so-called fundamental diagram is still not clearly understood since the details of the complex experimental setup (such as the sample time between the monitoring of data) can strongly influence the empirical data. Theoretical works explaining several

features of the fundamental diagram include [98, 148, 90, 97, 9] and the fundamental diagram of an optimal velocity model is discussed e.g. in [139]. A rigorous treatment of current-density relations out of interacting particles systems is delivered by the vivant hydrodynamic scaling theory which is exposed in [84] (see also [94]).

Phase-transitions. The current-density relation already suggests the existence of at least two different dynamical phases of vehicular traffic on highways, namely a free-flow phase and a congested phase. Works debating different phases of traffic flow and the issues of phase transitions are [83, 138, 129]. The paper [105] by T. Nagatani investigate traffic jams induced by fluctuations of a leading car. This is of some interest for the stability of production lines facing a stochastic demand, where the fluctuating demands play the role of the fluctuating leading car.

Micro-Macro link. The different hierarchies of traffic modelling (micro-meso-macro) are explained e.g. in [85]. Derivations of macroscopic current-density relations from mesoscopic models (*i.e.* gas-kinetic-like models based on Boltzmann-like equations) start with a paper by I. Prigogine et al. [120]. The paper proposes a first gas-kinetic model for traffic dynamics. Several authors considerably improved this model (e.g. [150, 114, 107]). Probably the most advanced macroscopic, Navier-Stokes-like traffic model derived from a mesoscopic level of description is given in [63]. It withstand the general criticism of second-order models addressed by Daganzo [24]. A general outline of the micro-macro link can be found in [64] (Chapter E). In its more mathematical form, the micro-macro link is also known as hydrodynamic limit theory [84, 94, 125]. We mention in particular Derridas exact treatment of the asymmetric simple exclusion process [29]. The paper is an important source of inspiration for mathematical modelers trying to get full understanding of transport processes via exactly solvable models.

2.5 Related literature on Stochastic control

In stochastic control systems, the main objective is to find a control sequence that minimizes the expected value of a given performance functional. There are two approaches to accomplishing the minimization. The first approach is Pontryagin's minimum principle, which leads to a nonlinear two-point boundary value problem that must be solved to obtain an optimal control law [91]. The second method is Bellman's dynamic programming which leads to functional equations that are very amenable to solution by numerical methods [12]. Both approaches "converge" to the same functional equation, the Hamilton-Jacobi-Bellman (HJB) equation, which must be satisfied by an optimal controller and its trajectory. An excellent introduction to optimal stochastic control and HJB equations is the book by W.H. Fleming and H.M. Soner [46]. It contains in particular a chapter on logarithmic transformations which is the basis for a connection between non-linear HJB equations and linear evolution

equations for the associated Markov processes. P. Dai Pra uses this connection in [119] to solve an optimal transportation problem introduced by Schrödinger [131]. Recently the logarithmic transformation has been applied by Hongler et al. [103] to a simple class of jump Markov processes (*i.e.* random evolutions) which occur also in stochastic MS modelling.

2.6 Related literature on Random evolution

Random evolutions are stochastic linear dynamical systems where the randomness is in the equation of state. They are well adapted to the formalization of the random inventory-production equation 2.1. The ultimate starter for random evolutions is "the birth of random evolution" [66] (2003) by R. Hersh. It gives an up to date overview over the development of random evolutions. A comprehensive list of applications is e.g. [149] by G.H. Weiss (2002). To learn about random evolutions we propose Pinsky's "Lectures on Random Evolution" [117]. The lectures also include a stochastic treatment of the linearized Boltzmann equation which can be related (by a logarithmic transformation!) to the non linear Boltzmann model studied in Chapter 4.
Interesting applications for random evolutions concern transport in biological systems [59, 60]. Particularly worthwhile are the studies in [67, 109], where the authors apply the random evolution modelling to flagellated bacteria able to adapt their speed with the environment.

2.7 Related literature on Diffusion mediated transport

The most common illustrations for diffusion mediated transport –noisy transport far from equilibrum – are Brownian motors. A excellent comprehensive review on Brownian Motors is the aricle [123] by P. Reimann (2002). An overview on the energetics of Brownian Motors can be found in [112] by J.M.R. Parrondo and B. J. De Cisneros (2002). Both reviews contain an up to date list of important works done in the field. A connection with a variational principle, similar to the one we propose, is made in [96] (2003).

Part II

Flows in Manufacturing and Traffic systems

3

Cooperative Flow dynamics in production lines with buffer level dependent production rates

Summary. We study, in the fluid flow framework, the cooperative dynamics of a buffered production line in which the production rate of each work-cell does depend on the content of its adjacent buffers. Such state dependent fluid queueing networks are typical for people based manufacturing systems where human operators adapt their working rates to the observed environment. We unveil a close analogy between the flows delivered by such manufacturing lines and cars in highway traffic where the driving speed is naturally adapted to the actual headway. This close analogy is thoroughly explored. In particular, by investigating the dynamic response of small perturbations around free flow stationary regimes, we can draw a "phase diagram". This diagram exhibits two different flow patterns, namely the *free* and *jamming* production *regimes*. The transitions between these regimes are tuned by the production control parameters (i.e. the buffer capacities, the reaction sensitivity, the control sampling time, etc.). The parameters range defining the boundary between the two regions allow to extract a dimensionless dynamic flow-line-parameter $\mathcal{Z}$ which is directly relevant for design purposes. Similar to the Reynolds' number $\mathcal{R}$ in hydrodynamics, the value of $\mathcal{Z}$ indicates the flow-regime in which the production line is in.

3.1 Introduction

It is already half a century that B. Zimmern [154] wrote a pioneering paper devoted to the characterization of production flows in serial lines. This original contribution has stimulated a strong research activity with the aim to calculate the average throughput and other performance measures for failure prone flow- and job-shop manufacturing systems (see [26, 14] for comprehensive reviews devoted to this topic). Due to the tremendously growing role played by computers in the seventies and eighties of the XX$^{\text{th}}$ century, it has long been believed that the ultimate goal in manufacturing would consist in building complete production plants without any human presence. According to this "no-human presence" paradigm, most of the production flow research papers have been oriented towards the study of shop floors equipped with automated

machines with rigid behavior (i.e. either the machine is "on" and it delivers with maximal speed or it is "off" and nothing is produced). Today, this no-human factory is widely questioned and one indeed realizes that the inherent flexibility of human operators offers irreplaceable advantages at reasonable costs. In a very recent address, [15], Chap.3, J. A. Buzacott emphasized this point and delivers the view that the main challenge for future research in production systems should be oriented towards the study of models which incorporate key features like the people incentives and capabilities.
While cooperative dynamics does already occur in purely automated multi-stages lines (via the starving and blocking mechanisms), the presence of human operators introduces additional adaptability features. While in the purely automated case, the production rates of the work-cells are generically of the "bang-bang type" (*i.e.* produce at the maximal rate when "on" and no production when "off"), human operators usually behave in a much more flexible manner. It is for instance common for human operators to observe the content of their up- and down-stream buffers and then, based on these observations, to suitably regulate (*i.e.* increase or decrease) their processing rate in order to avoid blocking and/or starving of the flows. This greater flexibility in their dynamics behaviors obviously influences the overall production flows in either a positive or sometimes also a negative way [118]. An illustration is given by J.A. Buzacott ([15] Chap. 3.7) of an automated guided vehicles (AGV) based assembly line in which the operators freely decide when to launch their AGV. The key point here is the possibility for the operators to themselves freely control their idle time (and hence their production rate).
The aim of the present chapter is *i*) to study how the production flows depend on machines with flexible production rates typical in presence of human operators and *ii*) to show how a synergetic approach can be used to study the production flow dynamics. This is realized by means of a simple modelling framework. The modelling is based on the close analogy which exists between the production flows and the flow of cars in highway traffic (see [1, 64] for an up-to-date review of traffic theory). The analogy enables us to study analytically some features of the underlying cooperative dynamics. Cooperation gives rise to different flow regimes such as free-flows and jamming flows which are tuned according to the values of external control parameters. A given flow shop configuration, fixed by the content of the buffer levels and production rates of the machines, is thereby said to be in the free flow regime (resp. jamming flow regime) if time-localized perturbations of this configuration are damped out (resp. can propagate through the entire system). Applying the linear perturbation method to our simple production line, we are able to draw a flow diagram which exhibits transitions from a free to a jammed regime. The transitions are tuned by external control parameters such as the buffer contents the reactivity of the human operators or the sampling time at which the state of the system is monitored. The parameters range defining the boundary between these flow regimes follow analytically from our synergetic approach.

While the transitions from the free to the jammed flow regimes are well known in the car traffic domain, such transitions have so far received very little attention in the manufacturing literature. This is not surprising as, in manufacturing, one usually focuses on calculating *stationary* performance measures. A notable exception is the related *bullwhip effect* which is extensively discussed in supply chain theory. The bullwhip effect describes how "inaccurate information, a lack of transparency throughout the supply chain, and a disconnect between production and real-time supply chain information result in lost revenue, bad customer service, high inventory levels and unrealized profits" [20]. The main effect of these causes is to increase the demand variability as one moves up the supply chain away from the retail customer, and small changes in consumer demand can result in large variations in orders placed upstream. Similar to the buffer levels of a serial production line in the jammed flow regime, the supply network can eventually oscillate in large swings as each organization in the supply chain seeks to solve the problem from its own perspective.
The chapter is organized as follows: In section 2, we jointly present a production flow shop model and a single lane model for cars in traffic. A direct correspondence between the models is established and differences as well as similarities of the dynamics are discussed. The stability of the flows is analyzed in section 3 in the continuous and the discrete time framework. In the former case we construct a dimensionless stability parameter which is recognized to play a central role also in the calculation of the throughput via stationary probability measures. For discrete time, the dynamics is expressed as a coupled-map lattice for which a phase diagram for the flow is derived. Section 4 is devoted to conclusions.

3.2 Models

3.2.1 Buffered Flow Shop

Let us consider a flow shop producing a single final product. The flow shop is made up by N machines in tandem $\{M_k\}_{k=1..N}$ separated by $N-1$ buffers $\{B_k\}_{k=1..N-1}$ as showed in Fig. 3.1. We adopt here an hydrodynamic point of view and assume that the buffer population can be modelled by a continuous variable.
The buffer B_k is located between the machines M_k and M_{k+1}. The population level of B_k at time t is $y_k(t) \in \mathbb{R}$. Hence, we shall have $0 \leq y_k(t) \leq h_k$ where $h_k > 0$ stands for the capacity of the buffer B_k. We assume a degree of adaptability, to be defined below, of the production rate v_k of machine M_k. More specifically, we shall assume that v_k can vary continuously in the interval $[0, V_{\max,k}]$, where $V_{\max,k}$ is the maximal production rate of M_k.
The occasional breakdowns of random duration of the M_k's are modelled by independent Markov processes $I_1(t), ..., I_N(t)$, where $I_k(t)$ is an alternating

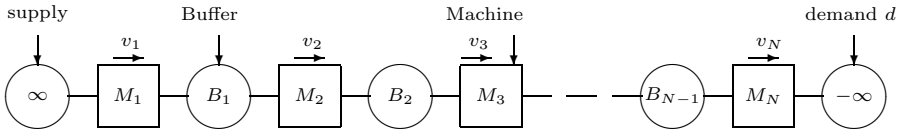

Fig. 3.1. Sketch of a flow shop composed of N machines and $N-1$ buffers. We suppose perfect supply such that M_1 is never starved (there is always enough raw materials stored in "$+\infty$") and a high demand rate such that M_N is never blocked (*i.e.* all the final goods are absorbed in "$-\infty$").

renewal process with exponential holding times in the two states $\{0,1\}$. We say that the machine M_k is up whenever $I_k(t)=1$ and M_k is down when $I_k(t)=0$. The I_k's are characterized by the mean up and the mean down times λ_k^{-1} respectively μ_k^{-1}.
For simplicity, the rate of demand $d(t)$ facing the system is from now on assumed to be large enough to systematically absorb the production. Accordingly and for notational ease, we set $v_{N+1}(t)=d(t)$ and $I_{N+1}(t)\equiv 1$. In addition the following assumptions are made:

A1) $y_k(t)=0 \Rightarrow v_{k+1}(t)\le v_k(t)$, $k=1,...,N-1$, which means that when the downstream buffer of M_k is empty, M_{k+1} is *starved*. In this case the production rate of M_{k+1} is slaved by the production rate of M_k.
A2) $y_k(t)=h_k \Rightarrow v_k(t)\le v_{k+1}(t)$, $k=1,...,N-1$, which means that when the upstream buffer of M_{k+1} is plain, M_k is *blocked*. In this case the production rate of M_k is slaved by the production rate of M_{k+1}.
A3) Transport time of items from M_k to B_k and from B_k to M_{k+1}, $k=1,...,N-1$, are assumed to be short and will be neglected.
A4) Machine M_1 is never starved (enough raw material) and M_N is not influenced by the market (enough demand).

The assumption **A**4 simplifies the "boundary" conditions and the assumptions **A**1-**A**3 can be summarised as follows: "while operating at time t and as long as M_k is neither starved nor blocked, M_k can produce continuously and independently of the other machines with the production rate $v_k(t)$ and its output is instantaneously stored in B_k." The evolution of the inventories can then be written as follows:

$$\frac{\mathrm{d}y_k(t)}{\mathrm{d}t} = v_k(t)I_k(t) - v_{k+1}(t)I_{k+1}(t), \;\; y_k(0)=y_k, \;\; k=1,...,N, \qquad (3.1)$$

where the y_k's are fixed initial conditions with $y_k\in[0,h_k]$. The inventories are naturally subject to the state constraints

$$\big(y_1(t),...,y_{N-1}(t),y_N(t)\big)\in[0,h_1]\times...\times[0,h_{N-1}]\times\mathbb{R}, \qquad (3.2)$$

which must be satisfied at every instant. To complete the dynamics of the flow shop model one has to specify the production rates v_k of the machines subject to the constraints:

$$\big(v_1(t), ..., v_N(t)\big) \in [0, V_{\max,1}] \times ... \times [0, V_{\max,N}]. \tag{3.3}$$

This is customarily done (at least in automated systems literature) by expressing the production rates as being the solutions of a convex production planning model which minimizes a specific cost functional (see e.g., [134]). This approach involves heavy algebra even when N is small and is indeed very unlikely to be explicitly solvable for $N > 3$. We will treat such a production planning problem for $N = 2$ in chapter 4. Here we are not dealing with such an optimization problem but we are interested in the dynamical response of a flow shop with state dependent production rates to a perturbation. Therefore we fix the dynamics (i.e. the production rates) by choosing a class of production rate functions which take into account (3.2) and (3.3). For this purpose we introduce below the so called "optimal-velocity" car traffic model first studied by M. Bando et al. [3] in analogy to which we will derive the "optimal" production rates. We stress here and at several occasions that in this chapter the adjective "optimal" does have a purely phenomenological meaning as it is not related to a cost functional of a production planing model.

3.2.2 Optimal-Velocity Car Traffic Model

We consider N cars $\{M_k\}_{k=1..N}$ travelling on a single lane as showed in Fig. 3.2. For $k = 1, ..., N-1$, denote by $x_k(t) > 0$ the headway between the cars

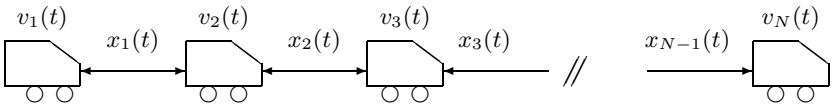

Fig. 3.2. N cars on a single-lane.

M_k, M_{k+1} and for $k = 1, ..., N$ denote by $v_k(t) \in [0, V_{\max,k}]$ the speed of M_k, where $V_{\max,k}$ is the maximal velocity of M_k.
The Optimal Velocity (OV) traffic model [3] states the existence of an optimal velocity function $\mathcal{V}_k$ which depends on the headways x_k, x_{k-1} and the presence of a response delay time τ_k, required for a driver of M_k to adjust its speed, such that:

$$\mathcal{V}_k(t) \overset{\text{not.}}{=} \mathcal{V}_k\big(x_{k-1}(t), x_k(t)\big) = v_k(t + \tau_k). \tag{3.4}$$

Expanding Eq.(3.4) up to first order, adding the corresponding headway variations and specifying the optimal velocity yields the following class of OV-models:

$$\begin{cases} \frac{\mathrm{d}x_k(t)}{\mathrm{d}t} = v_{k+1}(t) - v_k(t), \quad k = 1, \ldots, N, \\ \frac{\mathrm{d}v_k(t)}{\mathrm{d}t} = \alpha_k \Big(\mathcal{V}_k(t) - v_k(t) \Big), \quad k = 1, \ldots, N, \end{cases} \tag{3.5}$$

where $\alpha_k = \tau_k^{-1}$ and where the optimal velocity of M_k at time t is of the form:

$$\mathcal{V}_k(t) = V_{\max,k} \cdot F_k\big(x_{k-1}(t), x_k(t)\big). \tag{3.6}$$

In writing Eqs.(3.5) and (3.6), the following set of control parameters and functions are introduced:
a) The set of parameters $\alpha_k > 0$ which have the physical dimension of frequencies. They represent the *sensitivity* of the control mechanisms acting on the speed of the cars and are given by the inverse of the delay times τ_k introduced in (3.4) (i.e. $\alpha_k = \tau_k^{-1}$).
b) The set of functions F_k, associating to given up- and downstream headways x_{k-1} and x_k a dimensionless factor $F_k\big(x_{k-1}, x_k\big) \in [0, 1]$. When multiplied by the maximum speed $V_{\max,k}$ of M_k, F_k yields the optimal velocity of M_k. The functions F_k model directly the speed **adaptability** of M_k as a function of the headway to its adjacent neighbors. The type of controls that the F_k's introduce, are similar to those considered in [62] to describe the psychological effects of car drivers.
Note that the functions F_k are, and hence so are the OV-functions, of phenomenological nature and have to be chosen by the model builder. In particular, the OV-functions $\mathcal{V}_k$ are not directly related to an optimization problem and their generic features are based on common intuition. The functions $F_k(x, y)$ should certainly be non-increasing in the upstream variable x (no tendency to accelerate if the upstream headway increases) and non-decreasing in the downstream variable y (no tendency to brake down if the downstream headway increases). For calculation purposes we further assume from now on that the F_k's are at least twice continuously differentiable in x and y. Note that various explicit choices for OV-functions are used in traffic theory. They are guided by criteria like simplicity and existence of explicit solutions, low number of control parameters, existence of inflection points etc. (see e.g., [3, 62, 105]). They do all have their drawbacks and their advantages and common to all are the mentioned assumptions (monotonicity and differentiability). Here the generic setting is pursued and no explicit choice is made.

3.2.3 Correspondence between Flow Shops and Optimal-Velocity models

A glance at Figs. (3.1) and (3.2) and at Eqs. (3.1) and (3.5), suggests the following correspondence:

machines in a flow shop	$\leftrightarrow$	cars in a single lane,
free buffer space $h_k - y_k$	$\leftrightarrow$	headway x_k,
production rate	$\leftrightarrow$	car velocity,

from where we deduce, keeping failure prone machines, that an *optimal production rate flow shop model* can be written as:

$$\begin{cases} \frac{\mathrm{d}y_k(t)}{\mathrm{d}t} = v_k(t)I_k(t) - v_{k+1}(t)I_{k+1}(t), \quad k = 1, \ldots, N, \\ \frac{\mathrm{d}v_k(t)}{\mathrm{d}t} = \alpha_k \Big(V_{\max,k} \cdot \phi_k\big(y_{k-1}(t), y_k(t)\big) - v_k(t)I_k(t) \Big). \end{cases} \tag{3.7}$$

where the ϕ_k's are directly related to the F_k's by

$$\phi_k(x, y) := F_k\big(h_{k-1} - x, h_k - y\big) \tag{3.8}$$

thereby realizing the correspondence "free buffer space = headway".
In this setting, the functions $\phi_k\big(x, y\big)$ represent *the production control policy based on the adjacent buffer levels*. The function $y \mapsto \phi_k\big(x, y\big)$ indeed encodes for fixed x the influence of the free downstream buffer space on the production rate of M_k and similarly for fixed y, the function $x \mapsto \phi_k\big(x, y\big)$ describes the influence of the free upstream buffer space on the production rate of M_k. In particular, the starving and the blocking mechanisms of M_k are taken into account by imposing

$$\text{starving: } \phi_k(h_{k-1}, y) = F_k(0, h_k - y) = 0, \quad \forall y \tag{3.9}$$

and

$$\text{blocking: } \phi_k(x, 0) = F_k(h_{k-1} - x, h_k) = 0, \quad \forall x. \tag{3.10}$$

Indeed, when M_k is starved, the free upstream buffer space equals h_{k-1} and we have $\phi_k(h_{k-1}, y) = 0$ independently of the downstream buffer variable y. Similarly, when M_k is blocked, the free downstream buffer space equals 0 and we have $\phi_k(x_{k-1}, 0) = 0$ independently of the upstream buffer variable x. Eq. (3.7) therefore implies $v_k(t) = \exp(-\alpha_k t)$. Hence, in both cases (starved resp. blocked) the production rate of M_k decreases exponentially fast. For $\alpha \gg 1$, this behavior closely approaches the assumption **A**1: $v_k(t) \leq v_{k-1}(t)$ (resp. **A**2: $v_k(t) \leq v_{k+1}(t)$). In the limit when $\alpha_k \to \infty$ one effectively has a "bang-bang" type of reaction and the velocity is immediately adjusted to its "optimum". In this limiting case the assumptions made on F_k takes automatically into account the buffer level constraints expressed in Eq. (3.2) and Eq. (3.3). Note that **A**4 can be satisfied by imposing $\phi_1\big(x, x_1\big) = \phi_1\big(x_1\big)$ and $\phi_N\big(x_{N-1}, x_N\big) = \phi_N\big(x_{N-1}\big)$ which reflects the facts that M_1 is never starved (independent of the supply) and that M_N is never blocked (independent of the market).
Using the mentioned correspondence, the resulting *optimal production rate flow shop model* can be summarized as follows: to each machine M_k and at every time instant t, one can assign an "optimal" production rate $\mathcal{V}_k(t)$ of phenomenological character which depends on the up- and downstream buffers of M_k. This optimal production rate will be reached within a time interval of length τ_k thanks to the adaptability of the operators.
Remarks.

a) Depending only on x_{k-1} and x_k, the production rate of M_k is constantly adjusted by an operator who monitors the population levels in the up- and downstream buffers. It is better to produce with the "optimal" production rate $\mathcal{V}_k$ but deviations may exist between the optimal- and the real production rate. The operator tries to reduce the deviation $\Delta = \mathcal{V}_k - v_k$ by initiating an acceleration $\alpha_k \Delta$ of its production rate. This response mechanism replaces the state constraints given in Eqs. (3.2) and (3.3).
b) The "nearest neighbor-influence" on the production rates of the flow line is reminiscent from the interactions occurring in tandem supply chains. It is well known that unmanaged supply chains are not inherently stable (think e.g. of the bullwhip effect) and the objective of supply chain management is precisely to provide an uninterrupted and well timed flow of materials to customers. The often phenomenologically chosen countermeasures to instabilities include the shearing of production capacity and supply information. These approaches can be seen as practical caricatures of the "optimal production rate models" in the domain of supply chains (see also [65]).
c) The analogy between manufacturing- and traffic systems has its limits. In particular, to breakdowns of machines will correspond sudden stops of vehicles. Such "unitary crashes" are rather rare events on highways. In this sense the OV-traffic model (3.5) is a special case of the optimal production rate model (3.7). Indeed, setting $I_k = 1$ and removing the starving mechanism **A**1)– absent in real traffic – we obtain exactly the OV-model (3.5) of Bando et al.. At first sight, one could argue that focusing on $I_k = 1$ for production lines is not relevant. Indeed for fully reliable machines, one barely sees the need for introducing buffer places. This is however not so here. Indeed:

i) due to human presence, the production rates are not strictly constant but may fluctuate around their averages. The very presence of these fluctuations restore the importance of buffers as they increase the "compressibility" of the production flow. The transient response to a local fluctuation of the production rate will be given by our model.
ii) In presence of adaptable production rates, the ability of the system to respond to a non ideal production state which results after a failure is an essential dynamic performance factor. Hence the study of the transient response of the system to a state configuration out of the ideal one is essential.

d) The proposed correspondence

$$\text{free buffer space } h_k - y_k \quad \leftrightarrow \quad \text{headway } x_k,$$

between the free buffer space and the car headway identifies blocked machines $y_k = h_k$ (a situation taken into account by 3.10) with crashes of cars $x_k = 0$. The starving situation $y_k = 0$ (taken into account by 3.9) would correspond to an interaction between consecutive cars at the particular distance h_k. Such an interaction is of no direct interest in traffic theory and we therefore refrain

to interpret the eq. (3.9) in the traffic setting. This does however not influence the relevance of the model for production dynamics.
e) In the sense of remark **d)** one might prefer to realize a correspondence between the buffer content and the car headway by setting

$$\text{buffer content } y_k \quad \leftrightarrow \quad \text{headway } x_k.$$

Such a correspondence would identify starved machines $y_k = 0$ (a situation which is taken care of by 3.9) with crashes of cars $x_k = 0$. And this time it would be the blocking situation $y_k = h_k$ (taken into account by 3.10) which is of no direct interest in traffic theory. Once again, this does not influence the relevance of the model for production dynamics.

3.3 Linear stability analysis

Obviously, a steady state for cars in a line is given when all of them run orderly with the same constant optimal velocity $\mathcal{V}_k = v^e$ and with constant headway x_k^e, such that:

$$V_{\max,k} F_k\big(x_{k-1}^e, x_k^e\big) = v^e \quad k = 1, ..., N-1. \tag{3.11}$$

Here, we focus on the dynamic response of the flow shop to a single, time-localized perturbation of the free flow regime. We consider a time interval on which $I_k = 1$, $k = 1, \ldots, N$ i.e., on which all machines are operational. During such time intervals a steady state $(x_1^e, ..., x_{N-1}^e, v^e)$ satisfying Eq. (3.11), corresponds to a flow shop configuration where all stages have constant production rates v^e and where the buffers maintain the constant levels $(h_1 - x_1^e, ..., h_{N-1} - x_{N-1}^e)$ (recall that $x_i = h_i - y_i$ where y_i is the buffer level). We shall call this state a *free flow production regime* when localized perturbations are damped out. To formalize this definition we set

$$r_k(t) := \sum_{j=0}^{k-1} x_j(t) \quad k = 1, ..., N, \quad x_0 \equiv 0. \tag{3.12}$$

for the "absolute distance" of "car" M_k from the first car M_1 and undertake the stability analysis of (3.5) which reads now:

$$\begin{cases} \frac{\mathrm{d}r_k(t)}{\mathrm{d}t} = v_k(t), \ \text{k=1,...,N} \\ \frac{\mathrm{d}v_k(t)}{\mathrm{d}t} = \alpha_k\Big(V_{\max,k} F_k\big[r_k(t) - r_{k-1}(t), r_{k+1}(t) - r_k(t)\big] - v_k(t)\Big). \end{cases} \tag{3.13}$$

3.3.1 Time-continuous Analysis

Assume that M_N produces with a constant rate $v^e := \min\{V_{\max,k} \mid k = 1, ..., N\}$. The dynamics (3.13) has the following steady state:

$$\begin{cases} r_k^e(t) = \sum_{j=1}^{k-1} x_j^e + v^e t, \\ v_k^e(t) = \mathcal{V}_k(t) = v^e, \end{cases} \tag{3.14}$$

where the x_k^e's satisfy Eq. (3.11). To infer on the stability of the system we introduce a small perturbation $\delta r_k(t) \ll r_k^e(t)$:

$$\delta r_k(t) := r_k(t) - r_k^e(t).$$

Linearizing (3.13) around the steady state, we obtain the dynamical response equation:

$$\frac{\mathrm{d}^2 \delta r_k(t)}{\mathrm{d}t^2} = \alpha_k \Big[V_{\max,k} \Big(\delta r_{k+1} \partial_y F_k + \delta r_k \big(\partial_x F_k - \partial_y F_k \big) - \delta r_{k-1} \partial_x F_k \Big) - \frac{\mathrm{d}\delta r_k}{\mathrm{d}t} \Big] \tag{3.15}$$

where

$$\partial_x F_k := \frac{\partial F_k(x,y)}{\partial x}\Big|_{x=x_{k-1}^e} \quad \text{and} \quad \partial_y F_k := \frac{\partial F_k(x,y)}{\partial y}\Big|_{y=x_k^e}. \tag{3.16}$$

In expanding in a discrete Fourier series:

$$\delta r_k(t) := \frac{1}{N} \sum_{j=0}^{N-1} c_j e^{2\pi i \cdot j \frac{k}{N}} e^{\big(\lambda(j) - i\omega(j)\big)t}, \quad k \in \{1, ..., N\}, \tag{3.17}$$

where $i^2 = -1$, the set of dynamical equations (3.15) yields for every $j \in \{0, ..., N-1\}$ the characteristic relation:

$$P_k(\lambda - i\omega)\delta r_k + \alpha_k V_{\max,k} \Big(\partial_x F_k \delta r_{k-1} - \partial_y F_k \delta r_{k+1} \Big) = 0, \tag{3.18}$$

where we have omitted the j dependance of λ and ω and where

$$P_k(\lambda - i\omega) := (\lambda - i\omega)^2 + \alpha_k(\lambda - i\omega) + \alpha_k V_{\max,k}(\partial_y F_k - \partial_x F_k).$$

Any solution $\lambda(j) - i\omega(j)$ of (3.18) with $\lambda(j) > 0$ gives rise to a growing evolution of the perturbation and hence the initial state is not stable. The stability is given when $\lambda(j) < 0$, for $j = 1, ..., N-1$, ($j = 0$ corresponds to the neutral mode). This yields the condition (see also [62] and Chapt. III/A.2 in [64]):

$$\frac{V_{\max,k} \cdot (\partial_x F_k + \partial_y F_k)^2}{\alpha_k \cdot (\partial_y F_k - \partial_x F_k)} < \frac{1}{1 + \cos(\frac{2\pi j}{N})}. \tag{3.19}$$

Thus, the most unstable mode is realized for $\frac{j}{N} \to 0$. Accordingly stability will be guaranteed provided:

$$\frac{\alpha_k(\partial_y F_k - \partial_x F_k)}{V_{\max,k} \cdot (\partial_x F_k + \partial_y F_k)^2} > 2 \ \ \forall k \in \{1, ..., N\}. \tag{3.20}$$

We can now directly transfer this dimensionless stability condition to the flow shop model (note that $\partial_y \phi_k(x,y) = -\partial_y F_k(x,y)$ and $\partial_x \phi_k(x,y) = -\partial_x F_k(x,y)$):

$$\frac{\alpha_k(\partial_x \phi_k - \partial_y \phi_k)}{V_{\max,k} \cdot (\partial_x \phi_k + \partial_y \phi_k)^2} > 2 \ \ \forall k \in \{1, ..., N\}. \tag{3.21}$$

Remarks

1) When (3.21) is satisfied for all $k = 1, ..., N$, the variation of velocity of the upstream machine is damped out by the presence of the buffers and the flow shop is running in a soft regime. When (3.21) fails for some k, the regime of "jamming" or "chattering" may occur. This jamming flows are characterized by large fluctuations in the buffer population and hence the machines are likely to be found in a starved or blocked state.

2) The monotonicity assumptions on $F_k(x,y)$ go over to the production policies ϕ_k an read as $\partial_x \phi_k \geq 0$ and $\partial_y \phi_k \leq 0$. When the upward and downward influences of the buffer population onto the production rates are similar we can have $\partial_x \phi_k + \partial_y \phi_k = 0$. This situation will be coined "symmetric control".

3) For a symmetric control (i.e., $\partial_x \phi_k + \partial_y \phi_k = 0$) the fundamental inequality (3.21) is always satisfied and hence the steady state (3.14) of system (3.13) is unconditionally stable.

4) In close analogy with fluid mechanics where the Reynolds' number (determining whether a flow is laminar or turbulent) is used for design purpose, the dimensionless stability criterion given in eq.(3.21) suggests that the number:

$$\mathcal{Z} := \frac{\alpha(\partial_x \mathcal{V} - \partial_y \mathcal{V})}{(\partial_x \mathcal{V} + \partial_y \mathcal{V})^2} \tag{3.22}$$

is of direct interest for the modelling and design of serial production lines with environment dependent optimal production rates $\mathcal{V}(x,y) = V_{\max}\phi(x,y)$ and control sensitivity α.

5) The stability condition

$$\mathcal{Z}_k > 2, \ \ \forall k = 1, ..., N \tag{3.23}$$

depends implicitly on the buffer capacities via $\partial_x \phi_k$ and $\partial_y \phi_k$. To illustrate this point we give an example in the following section.

6) Using the flow-shop model eq. (3.13) for the dynamic description of tandem supply chains, the stability condition eq. (3.23) gives a practical guideline to take countermeasures in presence of instabilities. It establishes a condition between production adaptability and supply information and can be seen as the reactivity exigence on each supplier with respect to the changing (nearest neighbor) environment. The violation of this relation will finally lead to the occurrence of the bull whip effect. It is conjectured that such instabilities form the reason for the existence of business cycles [65].

3.3.2 A worked example; the stability of a production line following a pull production control.

Let us consider the case of a production line where in order to minimize work in process, the famous just in time philosophy is applied. Just in time advocates pull production control which says that inventories are not processed until there is adequate space in the next downstream buffer. Hence no upstream control is imposed (i.e. $\partial_x \phi_k = 0$). We further suppose that the ϕ_k's are independent of k and set:

$$\phi_k\big(x_{k-1}(t), x_k(t)\big) = \phi\big(x_k(t)\big) = \begin{cases} 1 & \text{if } x_k(t) = 0, \\ 1 - \frac{x_k(t)}{h_k} & \text{if } 0 < x_k(t) < h_k, \\ 0 & \text{if } x_k(t) \geq h_k. \end{cases} \tag{3.24}$$

Supposing such a linear influence of the downstream buffers on the production rates to hold, the relation (3.21) reduces to:

$$\mathcal{Z}_k := \frac{\alpha_k h_k}{V_{\max,k}} > 2 \ \ \forall k \in \{1, ..., N\}. \tag{3.25}$$

or equivalently

$$\frac{1}{2}\frac{h_k}{V_{\max,k}} > \frac{1}{\alpha_k} = \tau_k \ \ \forall k \in \{1, ..., N\}. \tag{3.26}$$

Hence for stability, the reaction time has to be shorter than the time required to empty a half filled buffer. Estimating the reaction time of the operators the simple and intuitive condition Eq. (3.26) can be used to determine the buffer capacities.
At this stage, it is worthwhile to bridge, at least partially, the conceptual gap between the stability relation (3.25) and the behavior of the stationary throughput $\langle t \rangle$ delivered by a production line. Remember that one method to estimate the average throughput of a flow shop relies on the aggregation methods based on the throughput delivered by two stage production lines (*i.e.* production dipoles). For a production dipole with identical and operation dependent failure prone machines the stationary measure analysis yields (see e.g., [69] p.71 and [19]):

$$\langle t \rangle = V_{\max} \frac{1}{1 + I_{\text{eff}}}, \quad \text{with } \ I := \frac{\mu}{\lambda} \leq I_{\text{eff}} := I\big[1 + \frac{2}{2 + \mathcal{F}(1 + I)}\big] \leq 2I,$$

where $V_{\max}$, λ and μ are respectively the common production rates, the mean times to failure and the mean times for reparation of the two machines, I the unavailability factor of the individual machines, I_{eff} the effective unavailability factor of the dipole, and where $\mathcal{F} = \frac{\mu h}{V_{\max}}$ is a dimensionless performance parameter introduced in [69]. Note that one can write:

$$1/\mathcal{F} = \frac{1 + I}{2}\big(I_{\text{eff}} - I\big)/\big(2I - I_{\text{eff}}\big), \tag{3.27}$$

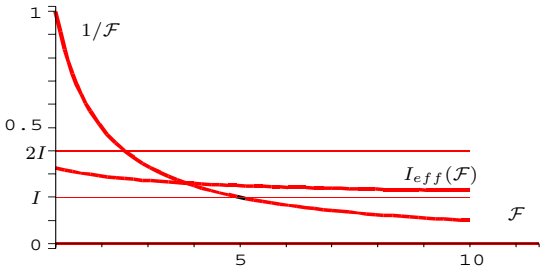

Fig. 3.3. Sketch of $1/\mathcal{F}$ and $I_{eff}(\mathcal{F})$ with $I = 0.2$. As $\mathcal{F} \propto h$, an increase of h reduces $I_{eff}(\mathcal{F})$ and hence enhances the average throughput $\langle t \rangle$. Note that the increase of $\langle t \rangle$, which is very rapid for small h, becomes very gradual for larger h and is therefore less rewarding. By identifying the role played by μ_k (reparation rate in the failure prone production lines) and α_k (sensitivity in the human based lines), the stability condition given in Eq. (3.28) shows that the significant gain in production throughput are achieved by avoiding the jamming regimes.

which is the expected effective unavailability decrease due to an increase of the buffer capacity h (see Figure 3.3). The dimensionless parameter $\mathcal{Z}_k$ given in (3.25) is directly related to $\mathcal{F}$ via:

$$\frac{1}{\mathcal{F}} = \frac{\alpha_k}{\mu_k}\frac{1}{\mathcal{Z}_k} < \frac{\alpha_k}{\mu_k}\frac{1}{2}. \tag{3.28}$$

Equation (3.28) relates the *stationary* (*i.e.* the expected) effective unavailability decrease $1/\mathcal{F}$ with the dimensionless number $\mathcal{Z}_k$ which is derived on the basis of a *dynamical* linear response analysis. Requiring stability for the transient response to a perturbation, the inequality in Eq. (3.28) implies a lower (upper) bound for the parameter $\mathcal{F}$, $(1/\mathcal{F})$. Therefore in view of Eq. (3.28), we see that the increase of the average throughput –which results when $\mathcal{F}$ is increased – can be interpreted as the ability of the production system to quickly absorb local perturbations (the characteristic time is given by the parameter α). Hence Eq. (3.28) establishes an enlightening connection between the properties of a single realization of the dynamics (transient performance measures) with those resulting from stationary statistical ensemble averages (stationary performance measure).
Taking $\mathcal{F} = 2$ is common practice at the shopfloor level and with Eq. (3.28) this leads to:

$$\frac{\alpha_k}{\mu} > 1 \;\; \forall k \in \{1, ..., N\}. \tag{3.29}$$

We therefore see that stability is ensured when the reaction time $1/\alpha$ is smaller than the mean time needed for machine reparation $1/\mu$.

3.3.3 Discrete time analysis

In practice it is likely that the state of the system will not be continuously monitored in time but rather on a discrete basis. Due to this time sampling, the production rate will itself be adapted only at discrete times. Let us now study this situation by considering the discrete analog of the above analysis. This is done by choosing a sampling time $T > 0$ and by updating the system (3.5) at time-instants $nT, \quad n \in \mathbb{N}$. The resulting model has the form of a coupled map lattice and reads for $k = 1, \ldots, N$:

$$\begin{cases} x_k(n+1) = x_k(n) + [v_{k+1}(n) - v_k(n)]\,T, \\ v_k(n+1) = v_k(n) + \alpha_k \left[V_{\max,k} \cdot F_k\big(x_{k-1}(n), x_k(n)\big) - v_k(n)\right] T, \end{cases} \tag{3.30}$$

where we write $f(n) := f(nT)$ with $n \in \mathbb{N}$ for an arbitrary function of time $f(t)$. As in the continuous case, we derive from Eqs. (3.30) a stationary regime:

$$x_k(n) = x_k^e \;\text{ and }\; v_k(n) = v^e \quad k = 1, ..., N,$$

provided that x_k^e and v^e satisfy the relations Eq. (3.11). Adding a perturbation term δx_k and linearizing around the steady state gives:

$$\delta x_k(n+1) = \delta x_k(n) + [\delta v_{k+1}(n) - \delta v_k(n)]\,T, \tag{3.31}$$

$$\delta v_k(n{+}1) = (1 - \alpha_k T)\,\delta v_k(n) + \alpha_k V_{\max,k} \left[\partial_x F_k(x_{k-1}^e)\delta x_{k-1} + \partial_y F_k(x_k^e)\delta x_k\right] T, \tag{3.32}$$

where $\partial_x F_k(x_{k-1}^e) =: \partial_x F_k$ and $\partial_y F_k(x_k^e) =: \partial_y F_k$ are defined as in Eq. (3.16). To simplify the analysis of the above equations, we suppose $\partial_x F_k \equiv 0$; i.e. there is no dependance of the production rate on the upstream buffer. Note that the inequalities

$$\frac{\alpha_k \cdot (\partial_y F_k - \partial_x F_k)}{V_{\max,k} \cdot (\partial_x F_k + \partial_y F_k)^2} \geq \frac{\alpha_k \cdot (\partial_y F_k - 0)}{V_{\max,k} \cdot (\partial_y F_k + 0)^2} \geq 2 \tag{3.33}$$

imply that systems which are stable without upstream controls ($\partial_x F_k \equiv 0$) remain stable when a monotone upstream control ($\partial_x F_k(x, x_k) \leq 0$) is added. Therefore, the subsequent calculations, performed with the auxiliary assumption $\partial_x F_k \equiv 0$, will still give relevant stability criterions.
Under this auxiliary assumption, Eqs. (3.31) and (3.32) take the canonical form of a discrete feedback system [2]:

$$\begin{pmatrix} \delta v_k(n+1) \\ \delta x_k(n+1) \end{pmatrix} = \begin{pmatrix} 1 - \alpha_k T & \alpha_k V_{\max,k} T \partial_y F_k \\ -T & 1 \end{pmatrix} \begin{pmatrix} \delta v_k(n) \\ \delta x_k(n) \end{pmatrix} + \begin{pmatrix} 0 \\ T \end{pmatrix} \delta v_{k+1}(n), \tag{3.34}$$

$$\delta v_k(n) = \begin{pmatrix} 1 & 0 \end{pmatrix} \begin{pmatrix} \delta v_k(n) \\ \delta x_k(n) \end{pmatrix}. \tag{3.35}$$

The behavior of the above discrete time linear system is analyzed via the transfer function $G_k(z)$ from $\delta v_{k+1}(n)$ to $\delta v_k(n)$:

$$G_k(z) = \begin{pmatrix} 1 & 0 \end{pmatrix} H_k(z)^{-1} \begin{pmatrix} 0 & T \end{pmatrix}^t, \tag{3.36}$$

with the definition

$$H_k(z) := \begin{pmatrix} \alpha_k T + z - 1 & -\alpha_k V_{\max,k} T \partial_y F_k \\ T & z - 1 \end{pmatrix}. \tag{3.37}$$

Stability condition. The stability of the steady state is achieved when the roots of the characteristic equation

$$\det\left(H_k(z)\right) = z^2 + z(\alpha_k T - 2) + \left[1 - \alpha_k T + \alpha_k V_{\max,k} T^2 \partial_y F_k\right] = 0 \tag{3.38}$$

lie inside the unit circle. The use of the Schur-Cohn criterion for Eq. (3.38) (stating equivalent conditions that the roots of the characteristic equation all have magnitude less than unity, see e.g., pp. 56 in [75]) directly implies:

$$\text{Stability} \;\Leftrightarrow\; \begin{cases} 0 < V_{\max,k} |\partial_y F_k| T < 1 \\ 0 < \alpha_k T < \frac{4}{2 - V_{\max,k} T |\partial_y F_k|} \end{cases} \;\Leftrightarrow\; \begin{cases} 0 < V_{\max,k} |\partial_y F_k| < 1/T \\ 0 < \alpha_k < 4/T. \end{cases} \tag{3.39}$$

No-jamming condition. The global criterion attenuating velocity disturbances along the production line uses the so-called H_∞-norm of the transfer matrixes G_k and is given by:

$$\max_{|z|=1} |G_k(z)| \leq 1 \quad \forall\, k \in \{1, \ldots, N-1\}. \tag{3.40}$$

Using Eqs. (3.36) and (3.39) together with lengthy algebra, the no-jamming condition (3.40) can be rewritten as (see also, [2]):

$$\max\left(0, \frac{1}{T} \frac{8 + \alpha_k T(\alpha_k T - 8)}{\alpha_k T(\alpha_k T - 6)}\right) \leq V_{\max,k} |\partial_y F_k| \leq \frac{\alpha_k}{2 + \alpha_k T}. \tag{3.41}$$

Using $|\partial_y \phi_k(x, y)| = |\partial_y F_k(x, y)|$, we can reformulate the no-jamming condition for the flow shop model (3.7):

$$\max\left(0, \frac{1}{T} \frac{8 + \alpha_k T(\alpha_k T - 8)}{\alpha_k T(\alpha_k T - 6)}\right) \leq V_{\max,k} |\partial_y \phi_k| \leq \frac{\alpha_k}{2 + \alpha_k T} \tag{3.42}$$

or equivalently in terms of the dimensionless stability parameters $X_k = \alpha_k T$ and $\mathcal{Z}_k := -\frac{\alpha_k}{V_{\max,k} \partial_y \phi_k} = \frac{\alpha_k}{V_{\max,k} |\partial_y \phi_k|}$:

$$\max\left(0, \frac{1}{X_k} \frac{8 + X_k(X_k - 8)}{X_k(X_k - 6)}\right) \leq \frac{1}{\mathcal{Z}_k} \leq \frac{1}{2 + X_k}. \tag{3.43}$$

The region for a soft-running regime (i.e. a free-flow traffic) defined by condition (3.42) is sketched in the flow diagram Fig. 3.4 for different sampling times $T = 4$, $T = 2$ and $T = 1.5$. The x- and y- axes are resp. spanned by

the control parameters α and $V_{\max,k}|\partial_y \phi_k|$. The Figure (3.4) shows the influence of an increasing sampling time T on the soft-running regime given by (3.42). It clearly exhibits that when the state of the system is less frequently monitored the control parameters must be chosen more carefully to guarantee a soft-running production flow (homogeneous flow). Note that for $T \to 0$ (*i.e.* continuous monitoring of the system states) condition (3.42) consistently coincides with the time continuous stability relation (3.21) (remember that by assumption, $\partial_x \phi_k = 0$). A dimensionless interpretation of the soft-running

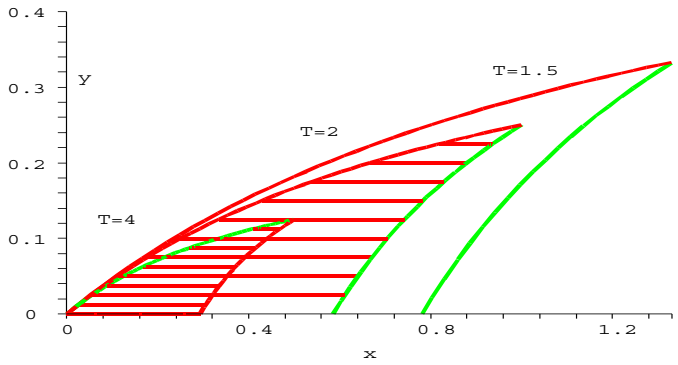

Fig. 3.4. Sketch of the free flow production regions enclosed by the x-axes and: $\frac{2/T+x(Tx-8)}{Tx(Tx-6)} \leq y \leq \frac{x}{2+Tx}$, for $T = 4, 2$ and $T = 1.5$. The x- and y-axis represent respectively the sensitivity $x = \alpha$ and the parameter $y = V_{\max,k}|\partial_y \phi_k|$. The free-flow regions decrease with increasing sampling times T and vanish for $T \to \infty$.

regime is sketched in the flow diagram Fig.(3.5) which is based on the condition (3.43). Here the x- and y- axes are resp. spanned by the *dimensionless* parameters αT and $1/\mathcal{Z}$. The figure (3.5) illustrates that above a critical value for αT no homogeneous production flow can be expected.

3.4 Concluding remarks

Among the numerous performance characteristics that modern production systems have to fulfill, the ability to quickly react to sudden and often unexpected changes of the environment is nowadays considered to be the most crucial. It has been realized that this time dependent flexibility requirement can often be achieved only at the expense of introducing human operators in the production process. The presence of human operators together with changing environments into a production line strongly complexifies the modelling of the production flows. In particular, stationary performance measures alone are not enough to suitably characterize the production flows and the

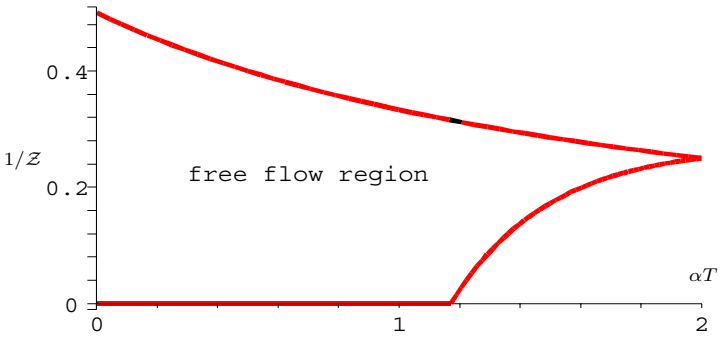

Fig. 3.5. Sketch of the free flow production region using the dimensionless quantities αT (x-axis) and $1/\mathcal{Z}$ (y-axis) delimited by the x-axis and the Eq. (3.43). Note that no free-flow can be expected if $\alpha T > 2$. For $\alpha T = 0$ the free-flow condition equals the time continuous stability condition $\mathcal{Z} > 2$.

knowledge of the transient response of the system to fluctuations becomes mandatory. The central role played by transient phenomena is obviously not restricted to production. Indeed, since about a half of century, the ubiquitous presence of transient regimes in vehicular traffic has stimulated an important research activity which produces a wealth of methods and results developed for their understanding. These methods were hardly so far being used in the production flow and supply chain context. In this chapter, we have adopted a synergetic view to explore some of the analogies between simple car traffic models and production lines in which the production rates depend on the contents of adjacent buffers. Thanks to a suitable dictionary, we are able to identify production flow regimes which are realized for definite ranges of external control parameters. The present study offers a view complementary to the stationary performance measures analysis and is based on specific realizations of the dynamics. Such an approach is mandatory for the study of the time dependent response to perturbations around the "laminar" production flow regimes and other transient behaviors such as the bullwhip effect encountered in supply chains.

3.5 Contributions of Chapter 3

- We introduce a class of models describing the cooperative dynamics of buffered production lines. Their mathematical form for a N stage tandem line is:

$$\begin{cases} \frac{\mathrm{d}y_k(t)}{\mathrm{d}t} = v_k(t) - v_{k+1}(t), \quad k = 1, \ldots, N, \\ \frac{\mathrm{d}v_k(t)}{\mathrm{d}t} = \alpha_k \Big(\mathcal{V}_k\big(y_{k-1}(t), y_k(t)\big) - v_k(t) \Big). \end{cases} \tag{3.44}$$

The "optimal" production rates $\mathcal{V}_k$ depend on the contents of adjacent buffers y_{k-1}, y_k according to which the real production rates v_k are adjusted proportionally to the sensitivity α_k.

- We identify two production flow patterns for the model: the free-flow and the jamming flow regimes.
- We extract the relevant dimensionless parameter $\mathcal{Z}$ governing the transitions from free to jammed production flows:

$$\mathcal{Z}_k := \frac{\alpha_k(\partial_x \mathcal{V}_k - \partial_y \mathcal{V}_k)}{(\partial_x \mathcal{V}_k + \partial_y \mathcal{V}_k)^2}. \tag{3.45}$$

The no-jam condition reads

$$\mathcal{Z}_k > 2, \quad \forall k = 1, ..., N. \tag{3.46}$$

The dynamical parameter is closely related to the stationary efficiency gain due to an increase of the buffer capacity. The increase of the average throughput –which results when the buffer capacity is increased – can be interpreted as the ability of the production system to quickly absorb local perturbations. The trade off between efficiency gain and stability is quantified in case of a two stage line.

- Interpreting the model (3.44) as a the dynamic description of tandem supply chains, the above stability condition gives a practical guideline to take countermeasures in presence of instabilities. It establishes a condition between production adaptability and supply information and can be seen as the reactivity exigence on each supplier with respect to the changing (nearest neighbor) environment. The violation of this relation will finally lead to the occurrence of the bull whip effect.
- We draw an explicit "phase diagram" in terms of the control parameters such as the buffer capacity, the reaction time inherent to the presence of human operators or the choice of the sampling time when a discrete monitoring is performed. The diagram differentiate between free flow and jamming flow regimes and offers a new quantitative understanding of the role played by the control parameters.

4

Optimal thresholds control for failure prone two stage tandem production systems

Summary. We consider the flow dynamics of a tandem production system formed by two failure prone machines separated by a buffer stock. The production rates of the machines are regulated by a feedback mechanism which solves an associated optimal control problem with an average cost criterion. The cost structure penalizes both the entrance into and the sojourn on the buffer boundaries. The generic structure of the optimal control involves four buffer content thresholds. When the buffer content crosses these thresholds, the production rates are tuned to reduce the tendency to enter into the buffer boundaries. Using the fluid modelling framework, we obtain analytical results for the stationary buffer level distribution in case an operating machine can produce with, either a "nominal" or a "reduced" rate. In the stationary regime, the optimal positions of the buffer thresholds, the throughput and the average buffer content are given.

4.1 Introduction

The presence of a buffer stock between two failure prone machines M_1 and M_2 – a situation encountered in Chapter 3 for $N = 2$ – enhances the global throughput of the installation and its quantitative effect is calculated for example in [14, 51, 77, 99, 151]. A buffer does however not eliminate all interruptions of the production flow even when both machines are potentially able to produce. Indeed starving interruptions of M_2 which arise when the buffer is empty and blocking interruptions of M_1 occurring when the buffer is filled up can occur. Besides reducing the overall throughput, the blocking and starving interruptions do, in certain circumstances, generate additional nuisances with strongly penalizing consequences. Typical examples arise in fluid installations, the Internet or people based manufacturing and will be discussed below.

To reduce the probability of occurrences of starving or blocking states, one obviously can increase the buffer capacity (called H thereafter). This solution is however often not feasible as it may lead to prohibitive costs (presence of large size installations incompatible with the available layout and creation of large work-in process). If one is limited to a fixed buffer capacity, one can

try to explore alternative solutions. One of these is to introduce a feedback control mechanism based on both the buffer content $X(t) \in [0, H]$ and the operating states ("on" and "off") of the machines. This feedback mechanism is devised to reduce the sojourn times spent in and/or to reduce the entrance frequency into the filled or empty buffer states. In this Chapter, we shall use analytical methods to find the *optimal feedback control* in the simple case where the possible production rates $v_k(t) \stackrel{\text{not.}}{=} v_k(X(t))$ of M_k, $k = 1, 2$ can achieve either a nominal value or a reduced one. Note that in contrast to Chapter 3 where the term "optimal" refers to a phenomenological and hence to an ad-hoc satisfaction measure, it will have a well defined meaning in this Chapter.
Typical situations where buffer content dependent regulations of the production rates can actually occur are:

i) *Fluid installations.* To prevent overflow losses or dry states in fluid installations involving pumps one introduces backoffs "replacing" the hard constraints (here full or empty tank) by soft constraints (tank content high or low). When the tank content violates the soft constraints, the inflow resp. outflow rates of the tank are regulated in order to keep its content away from the hard constraints.
ii) *The Internet.* Overflows of a buffer in the Internet may produce unacceptable information losses. To cope with this situation, a Transmission Control Protocol TCP is introduced. The TCP regulates the traffic rates of the sources. It controls the transfer rates as follows: during overflows, the buffer sends negative feedback signals to the sources in order to reduce its sending rates. Otherwise the buffer sends positive feedback signals to the sources to augment the sending rates [104].
iii) *High production flows.* When high production flows are involved, the rise to the nominal production regime of the machines may not be instantaneous. Examples are paper wrapping installations where the paper tension depends on the dynamics of adjacent machines. Sudden accelerations of the installation scratch the paper. In such cases, reaching a buffer boundary with maximal rate has therefore to be avoided. A solution is to reduce the production rate when approaching the full or empty buffer states. Such policy is also relevant when uncertainties concerning the actual physical population level of the buffer exist.
iv) *People based manufacturing.* Tunings of the production rate occur naturally when the flexible behavior of human operators influences the workforce of the machines. In case of flexible workers, the problem of different worker speed may be handled adopting an adaptative (*i.e.* state dependent) production strategy. A simple workforce allocation policy prescribes to operators to move from production cells with highly populated upstream buffers to cells with low populated downstream buffers and vice versa. This production policy is effectively equivalent to a buffer dependent control dynamics. Hence the feedback control problem considered

here, can be viewed as a caricature of elementary allocation problems arising in people based manufacturing (see e.g., [58] and especially [118] where the benefic influence on the line efficiency of such state dependent policies is studied).

From now on, we shall construct a control policy $u(t) = (v_1(t), v_2(t))$ which optimally solves the production planning problem with a cost criterion exhibiting the following features:

i) a cost term $g(v_2)$ depending on the production rate of the second machine which penalizes slow production rates,
ii) a term penalizing large work-in-process,
iii) a term penalizing full and empty buffer states,
iv) a term penalizing the entrance rates into the full and empty buffer states.

Quantitatively, the above features are summarized into the performance measures of the form:

$$L\big[X(t), v_2(X(t))\big] := g\big(v_2(X(t))\big) + h\big(X(t)\big), \tag{4.1}$$

with g a positive function such that $g(0) \geq g(v_2 = \text{reduced}) \geq g(v_2 = \text{nominal})$ and where the function h, defined on $[0, H]$, does take into account *ii*), *iii*) and *iv*) by specifically choosing:

$$\begin{aligned} h(X) = \delta_0 1_{\{X=0\}} + \gamma_0 1_{\{\text{transition from } X>0 \text{ to } X=0\}} + \tilde{h}(X) 1_{\{0<X<H\}} \\ + \delta_H 1_{\{X=H\}} + \gamma_H 1_{\{\text{transition from } X<H \text{ to } X=H\}}, \end{aligned} \tag{4.2}$$

with $\tilde{h}$ being a strictly convex function and δ_0 resp. δ_H being the extra costs incurred when the buffer is empty resp. full (corresponding to the spots in Figure 4.1). Finally γ_0 resp. γ_H are the costs incurred each time the buffer content enters the empty resp. the full state (corresponding to the arrows in Figure 4.1 (A)).
Using the cost criterion Eq. (4.1), the following points will be addressed in this Chapter:

1) use the associated Hamilton-Jacobi-Bellmann equation characterizing the optimal control problem and, following the lines given in [5] and [13], show that the optimal policy has a generic form involving four buffer thresholds z^*, Z^*, y^* and Y^*. Specifically, when both machines are operating, the control imposes the following dynamics:
   - M_1 and M_2 produce with the nominal rates when $X(t) \in [z^*, Z^*]$.
   - M_1 produces with the nominal and M_2 with the reduced production rate when $X(t) < z^*$.
   - M_2 produces with the nominal and M_1 with the reduced production rate when $X(t) > Z^*$.

   When only one machine is operational, the thresholds control imposes the following dynamics:

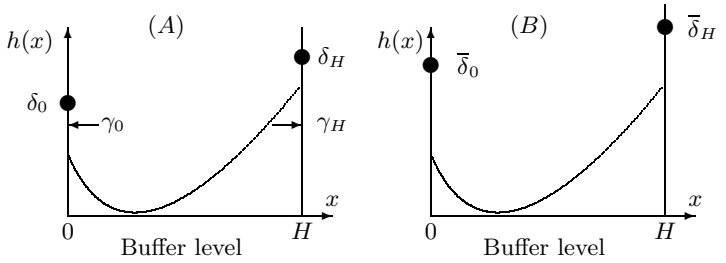

Fig. 4.1. (A): Sketch of the generic cost structure h considered in this Chapter. h is strictly convex and penalizes *ii*) large work-in-process, *iii*) states *at* the buffer boundaries (indicated by the spots) and *iv*) transitions *into* the buffer boundaries (indicated by the arrows). (B): The costs due to transitions into boundary states can be adequately removed by attributing higher values to δ_0 and δ_H (see Eq. (4.27) below).

- in case M_2 is under repair, M_1 produces with the nominal rate when $X(t) \leq Y^*$ and otherwise with the reduced rate.
- in case M_1 is under repair, M_2 produces with the nominal rate when $X(t) \geq y^*$ and otherwise with the reduced rate.

2) study the production flow dynamics resulting when the system operates under the thresholds policy and derive the stationary probability distribution of the buffer content.
3) calculate the long-run average costs associated with Eq. (4.1), namely:

$$V(z,Z,y,Y) = \lim_{T\to\infty} \frac{1}{T}\mathbb{E}\Big[\int_0^T \Big(L\big[X(s), v_2(X(s))\big]\Big)\mathrm{d}s\Big] = \mathbb{E}_S\Big(L\big[X, v_2(X)\big]\Big), \tag{4.3}$$

where $\mathbb{E}_S$ is the stationary expectation and then obtain the optimal thresholds z^*, Z^*, y^* and Y^* by minimizing $V(z,Z,y,Y)$.

To derive analytical results, we shall use a fluid modelling approach. A continuous state representation indeed avoids the combinatorial complexity inherent to Markov chain models with large state spaces. For fluid queues, the problem reduces to solve five coupled systems of linear partial differential equations (the Chapman-Kolmogorov equations) together with appropriate boundary conditions.

Related articles in the manufacturing flow control literature include [5] and [13] for one stage lines and [47, 140, 144] for two stages. These contributions aim to minimize the inventory holding and backorder costs. Here, the focus is on the costs incurred when starvation and blocking occur. Such optimization problems are less discussed (an exception being the decomposition method of Hu in [73] where starving costs naturally enter into the cost structure). For larger systems, the controls rely on heuristic policies. For example, Fuzzy controllers related to two thresholds policies are investigated in [106].

The chapter is organized as follows: In section 2, we introduce the tandem system and the production planning problem and derive the optimality of

the four-thresholds feedback control. In section 3, we write the resulting Chapman-Kolmogorov equation governing the buffer population dynamics. The stationary probability measures solving the Chapman-Kolmogorov equations are derived in section 4. Performance measures and numerical examples are given in section 5. Finally, section 6 is devoted to perspectives and conclusions.

4.2 The Model

Consider a single product transfer-line composed of two machines M_1 and M_2 separated by a buffer B with fixed finite capacity $H > 0$ (see Figure 4.2).

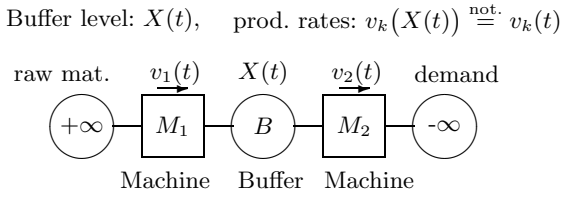

Fig. 4.2. Sketch of a two-stages transfer-line with a permanent supply of raw material and a permanent absorbing demand.

The machines M_1 and M_2 are failure prone, thus giving rise to breakdowns and repairs with random durations. These random events will be modelled by two Markovian renewal processes $I_1(t)$ and $I_2(t)$ which take on values in $\{0, 1\}$ ("0 =off", "1 =on") and which are defined on a common probability space $(\Omega, \mathcal{F}, \mathbb{P})$. They are characterized by the first moments λ_i^{-1} resp. μ_i^{-1} of their exponentially distributed holding times in the states $\{1\}$ resp. $\{0\}$. These failure processes are supposed to be *operation dependent* rather than time dependent. This means that machines can fail only while processing workpieces.
The processed material is assumed to behave as a (continuous) fluid and the flow of products is from the upstream-buffer of M_1 (which is permanently supplied with raw material) to the downstream-buffer of M_2 (which can always absorb the stream of finished goods). The transfer times from M_1 to B and from B to M_2 are supposed to be negligible. The buffer content at time t is denoted by $X(t)$ and is subject to the state constraint $X(t) \in [0, H]$. With these assumptions, the state of the tandem system is represented by the vector valued process $(X(t), I_1(t), I_2(t)) \in \mathcal{S} := [0, H] \times \{0, 1\}^2$. The state constraint is realized by requiring that the production rates $v_1(\cdot)$ and $v_2(\cdot)$ satisfy the boundary constraints:

$$v_2\big(X(t)=0\big)I_2(t) \le v_1\big(X(t)=0\big)I_1(t), \tag{4.4}$$
$$v_1\big(X(t)=H\big)I_1(t) \le v_2\big(X(t)=H\big)I_2(t). \tag{4.5}$$

The boundary constraints express the fact that the production rate of M_2 (resp. of M_1) is slaved by the production rate of M_1 (resp. of M_2) in case the storage buffer is empty (resp. full). We assume that the machine M_1 (resp. M_2) can produce either with a nominal rate v_1^+ (resp. v_2^+) or with a reduced rate $v_1^- < v_1^+$ (resp. $v_2^- < v_2^+$). The production rates are imposed a priori and fulfill $v_1^- < v_2^+$ and $v_2^- < v_1^+$ in order to potentially respect the constraints Eqs. (4.4) and (4.5). The buffer content process $X(t)$ then reads:

$$X(t) = X(0) + \int_0^t \big(I_1(s)v_1(X(s)) - I_2(s)v_2(X(s))\big)\mathrm{d}s. \tag{4.6}$$

4.2.1 The production planning problem

For a given state $(x, i_1, i_2) \in \mathcal{S}$, the dynamics of $X(t)$ given by Eq. (4.6) is controlled by the process of possible production rates $u(x, i_1, i_2) \in U(x, i_1, i_2)$ where for $x \neq 0, H$, the state dependent control space $U(x, i_1, i_2)$ is:

$$U(x, i_1, i_2) := \{(v_1, v_2) \mid v_1 \in \{i_1 v_1^+, i_1 v_1^-\}, v_2 \in \{i_2 v_2^+, i_2 v_2^-\}\}. \tag{4.7}$$

For $x = 0$ or $x = H$ we include in addition the boundary constraints expressed in Eqs. (4.4) and (4.5). Note that when both machines are under repair, the control does not enter into the dynamics and we have $U(x, 0, 0) = \{(0, 0)\}$. Our goal is now to find a feedback policy $u(X(t), I_1(t), I_2(t)) \in U(X(t), I_1(t), I_2(t))$ which minimizes the long run average expected cost incurred per unit time

$$\lim_{T\to\infty} \frac{1}{T}\mathbb{E}\Big[\int_0^T \Big(L\big[X(s), v_2(X(s))\big]\Big)\mathrm{d}s\Big], \tag{4.8}$$

where $\mathbb{E}$ denotes the expectation and $L = g + h$ stands for the running costs. The assumptions on g (positive and monotone) and h (strictly convex) are the usual ones (see [134] p.35). More specifically, h is of the form (see Figure 4.1 (B)):

$$h(x) = \overline{\delta}_0 1_{\{x=0\}} + \tilde{h}(x)1_{\{0<X<H\}} + \overline{\delta}_H 1_{\{X=H\}}, \tag{4.9}$$

with $\tilde{h}$, strictly convex satisfying $\tilde{h}(0^+) \le \overline{\delta}_0$ and $\tilde{h}(H^-) \le \overline{\delta}_H$ (hence, h also is strictly convex).

To find the optimal policy minimizing Eq. (4.8), we follow the idea developed in [13] and view the average cost criterion as being the limit of an associated discounted cost criterion involving a discount factor β. As the structure of the optimal control of the latter problem is independent of β, its generic structure will be preserved for the average optimization criterion resulting in the $\beta \to 0$ limit.

Let us therefore introduce the discounted cost functional $J(x_0, i_1, i_2)$ with $x_0 \in [0, H]$ and $(i_1, i_2) \in \{0, 1\}^2$, associated to the running costs L given in Eq. (4.1):

$$J(x_0, i_1, i_2) = \mathbb{E}_{x_0, i_1, i_2}\Big[\int_0^\infty \Big(L\big[X(s), v_2(X(s))\big]\Big)\mathrm{e}^{-\beta s}\mathrm{d}s\Big], \tag{4.10}$$

with $\beta > 0$ a discount parameter and where $\mathbb{E}_{x_0, i_1, i_2}$ is the conditional expectation operator subject to the initial conditions $X(0) = x_0$ and $(I_1(0), I_2(0)) = (i_1, i_2)$. To simplify notations, we write $l = 1, 2, 3, 4$ for the four possible operating states $(i_1, i_2) = (0, 0), (0, 1), (1, 0), (1, 1)$ and define for $x \in [0, H]$ and $l \in \{1, 2, 3, 4\}$ the value function minimizing the discounted costs:

$$x \mapsto \phi(x, l) = \min_{(v_1, v_2) \in U(x,l)} J(x, l). \tag{4.11}$$

Then $x \mapsto \phi(x, l)$ is the unique viscosity solution of the HJB dynamic programming equation (see e.g., [46] Chapt. III Eq. (9.4)):

$$\beta \begin{pmatrix} \phi(x,1) \\ \phi(x,2) \\ \phi(x,3) \\ \phi(x,4) \end{pmatrix} = \begin{pmatrix} \min_{x,1}\, g(v_2) \\ \min_{x,2}\, g(v_2) - v_2\phi_x(x,2) \\ \min_{x,3}\, g(v_2) + v_1\phi_x(x,3) \\ \min_{x,4}\, g(v_2) + (v_1 - v_2)\phi_x(x,4) \end{pmatrix} + A \begin{pmatrix} \phi(x,1) \\ \phi(x,2) \\ \phi(x,3) \\ \phi(x,4) \end{pmatrix} + h(x) \begin{pmatrix} 1 \\ 1 \\ 1 \\ 1 \end{pmatrix}, \tag{4.12}$$

where the minimum "$\min_{x,l}$" is taken over the couples $(v_1, v_2) \in U(x, l)$, where ϕ_x is the derivative of ϕ with respect to x and where the matrix A is given by:

$$A = \begin{pmatrix} -\mu_1 - \mu_2 & +\mu_2 & +\mu_1 & 0 \\ +\lambda_2 & -\mu_1 - \lambda_2 & 0 & +\mu_1 \\ +\lambda_1 & 0 & -\mu_2 - \lambda_1 & +\mu_2 \\ 0 & +\lambda_1 & +\lambda_2 & -\lambda_1 - \lambda_2 \end{pmatrix}.$$

As we are mainly interested in the optimal feedback policy (v_1, v_2) holding when both machines are operational (*i.e.* $l = 4 = (1, 1)$), let us focus on the following minimum in more detail:

$$\min_{(v_1, v_2) \in U(x,4)} g(v_2) + (v_1 - v_2)\phi_x(x, 4). \tag{4.13}$$

The strict convexity of $\phi(x, l)$ (see [46] p.149 and also [134] p.380) guarantees the existence of a level $Z \in [0, H]$ such that:

$$\phi_x(x, 4) \begin{cases} \geq 0 \text{ for } x \geq Z, \\ \leq 0 \text{ for } x \leq Z. \end{cases}$$

Setting $C(v_1, v_2) := g(v_2) + (v_1 - v_2)\phi_x(x, 4)$, we have to compare the four values $\{C(v_1^{\pm}, v_2^{\pm})\}$ separately for $x \geq Z$ and for $x < Z$. For $x \geq Z$ we have $\phi_x(x, 4) \geq 0$ and therefore $C(v_1^-, v_2^+) = \min_{x,4} C(v_1, v_2)$. For $x < Z$ we have

$\phi_x(x,4) \leq 0$ and therefore $C(v_1^+, v_2) \leq C(v_1, v_2)$ for all $(v_1, v_2) \in U(x,4)$ (*i.e.* the minimum is realized with $v_1 = v_1^+$). Comparison of the two values $\{C(v_1^+, v_2^\pm)\}$ yield:

$$C(v_1^+, v_2^+) \leq C(v_1^+, v_2^-) \Leftrightarrow \phi_x(x,4) \geq \frac{g(v_2^+) - g(v_2^-)}{v_2^+ - v_2^-} =: c. \tag{4.14}$$

Note that by the assumptions made on g, the constant c is negative. Define now the storage level $z \in [0, H]$ such that:

$$\phi_x(x,4) \begin{cases} \geq c \text{ for } x \geq z, \\ \leq c \text{ for } x \leq z. \end{cases} \tag{4.15}$$

The existence of z follows directly from the strict convexity of $\phi(x,l)$. The convexity of $\phi(x,l)$ together with the fact that $c < 0$ imply $z < Z$. The policy minimizing Eq. (4.13) then reads:

$$u(x,1,1) = \big(v_1(x), v_2(x)\big) = \begin{cases} (v_1^+, v_2^-) \text{ for } x < z, \\ (v_1^+, v_2^+) \text{ for } z \leq x \leq Z, \\ (v_1^-, v_2^+) \text{ for } x > Z. \end{cases} \tag{4.16}$$

Following similar arguments when one of the two machines is under repair we find:

(a) the policy realizing the minimum $\min_{x,3} g(0) + v_1 \phi_x(x,3)$:

$$u(x,1,0) = \big(v_1(x), 0\big) = \begin{cases} (v_1^+, 0) \text{ for } 0 \leq x < Y, \\ (v_1^-, 0) \text{ for } Y \leq x < H, \\ (0,0) \quad \text{for } x = H, \end{cases} \tag{4.17}$$

where $Y \in [0, H]$ is the smallest buffer level such that $\phi_x(x,3) \geq 0$ for all $x \in]Y, H]$.

(b) the policy realizing the minimum $\min_{x,2} g(v_2) - v_2 \phi_x(x,2)$:

$$u(x,0,1) = \big(0, v_2(x)\big) = \begin{cases} (0,0) \quad \text{for } x = 0, \\ (0, v_2^-) \text{ for } 0 < x < y, \\ (0, v_2^+) \text{ for } y \leq x \leq H, \end{cases} \tag{4.18}$$

where $y \in [0, H]$ is the smallest buffer level such that $\phi_x(x,2) \geq c$ for all $x \in]y, H]$ with c as defined in Eq. (4.14).

Remarks.

1) When both machines are on, the optimal control is defined via two thresholds z and Z. When only one machine is operational, the optimal control is determined via one threshold (Y if M_1 is "on" and y if M_2 is "on").

2) A priori, the four thresholds z, y, Y, Z are different. However, in the limit $v_1^+ \to 0$ resp. $v_2^+ \to 0$ we have $Z = Y$ resp. $z = y$. In these limiting cases, the drifts $v_1^+ - v_2$ resp. $v_2^+ - v_1$, resulting when both machines are

operational, coincide with the drifts $0 - v_2$ resp. $0 - v_1$ arising when one of the machines is under repair.
For $v_1^+ > 0$ we have $z \leq y$ and for $v_2^+ > 0$ we have $Y \leq Z$. In fact, if $v_1^+ > 0$ and if both machines are "on", the drift $v_2 - v_1^+$ directed toward the boundary is strictly smaller than the drift $v_2 - 0$ resulting when M_1 is under repair. Therefore, if both machines are "on" and if the optimal control imposes to switch from v_2^+ to v_2^- in order to reduce the drift $v_1^+ - v_2^+$ *toward* the $\{0\}$ boundary, it will, a fortiori, impose to switch from v_2^+ to v_2^- when M_1 is under repair, hence $z \leq y$. A similar reasoning shows that for $v_2^+ > 0$ we have $Y \leq Z$.

3) The optimal control is compatible with the boundary constraints expressed in Eqs. (4.4) and (4.5).

4) The derivation of the optimal control is independent of the ordering relations among the possible production rates v_1 and v_2. This means that for all four possible order relations (1) $v_1^- \leq v_2^- \leq v_1^+ \leq v_2^+$, (2) $v_1^- \leq v_2^- \leq v_2^+ \leq v_1^+$, (3) $v_2^- \leq v_1^- \leq v_1^+ \leq v_2^+$, (4) $v_2^- \leq v_1^- \leq v_2^+ \leq v_1^+$ the optimal control is of the form given by Eqs. (4.16-4.18) (recall that by assumption, $v_i^- < v_i^+$, $i = 1, 2$ and $v_i^- < v_k^+$, $i \neq k$). The average cost criterion can therefore be minimized with respect to (v_1^-, v_2^-) without changing the structural form of the optimal control. This offers the possibility to optimally choose the reduced rates by a simple optimization of the average costs in case (v_1^-, v_2^-) are not fixed a priori.

5) Suppose that the rates v_i $i = 1, 2$ can vary continuously within $[v_i^-, v_i^+]$ and that g is twice continuously differentiable and strictly convex. Then the structure of the optimal control still involves four thresholds as given by Eqs. (4.16-4.18) provided the following modifications are introduced:

- replace in Eq. (4.16) the constant v_2^- by

$$v_2(x) = \max\big(0, v_2^+ - \frac{g'(v_2^+) - \phi_x(x,4)}{g''(\xi_x)}\big)$$

  with $\xi_x \in (v_2(x), v_2^+)$ such that

$$g(v_2(x)) = g(v_2^+) + g'(v_2^+)(v_2(x) - v_2^+) + g''(\xi_x)(v_2(x) - v_2^+)^2.$$

  The threshold z is replaced by the lowest buffer level $x \in [0, H]$ such that $g'(v_2^+) = \phi_x(x, 4)$.
- replace in Eq. (4.18) the constant v_2^- by

$$v_2(x) = \max\big(0, v_2^+ - \frac{g'(v_2^+) - \phi_x(x,2)}{g''(\xi_x)}\big)$$

  with $\xi_x \in (v_2(x), v_2^+)$ such that

$$g(v_2(x)) = g(v_2^+) + g'(v_2^+)(v_2(x) - v_2^+) + g''(\xi_x)(v_2(x) - v_2^+)^2.$$

  The threshold y is replaced by the lowest buffer level $x \in [0, H]$ such that $g'(v_2^+) = \phi_x(x, 2)$.

Note that the optimal control $(v_1(x), v_2(x))$ is of bang-bang type in the first argument v_1 (switch between the minimum and the maximum speed) as given in the discrete case Eqs. (4.16-4.18). In the second argument v_2, the optimal control increases with the gradient of the value function from v_2^- to v_2^+.

6) Employing the analogy with cars in traffic (see Chapter 3) the optimal velocity function $\mathcal{V}$ minimizing the amount of crash-scenarios between two cars is of the form discussed in 5). In particular, the car which follows the leading car tries to keep a safety distance by "switching" between two velocities. This behavior is clearly caricatural as instantaneous velocity switches demand for infinite acceleration forces. Nevertheless we will use this observation in Chapter 5 to discuss analytically the dynamics of N cars following each other on a one lane road admitting only two possible velocity states (fast and slow).

4.3 Chapman-Kolmogorov-equations

According to remark 2) above, the optimal production rates are defined by four thresholds z, y, Z, Y verifying $z \leq y$, $Y \leq Z$ and $z < Z$. It follows that in order to exhaust the possible thresholds arrangements, five relevant configurations for the control thresholds have to be treated, namely: (1) $z < y < Y < Z$, (2) $z < Y < y < Z$, (3) $Y < z < y < Z$, (4) $Y < z < Z < y$, and (5) $z < Y < Z < y$. Let us focus on configuration (1). The four alternative configurations are discussed in the appendix.
Fix four thresholds $z, Z, y, Y \in (0, H)$ with $z < y < Y < Z$ and assume that the production rates are regulated by the Eqs. (4.16-4.18). The resulting state dependent production rates are listed in table 4.1. According to the ordering

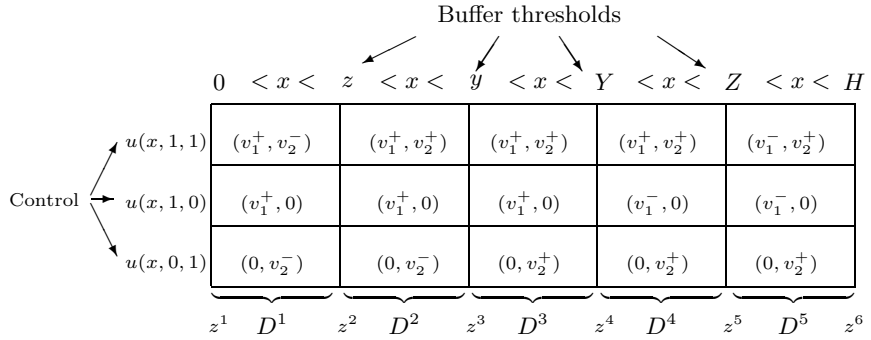

Table 4.1. The production rates given by the control Eqs. (4.16-4.18) for fixed thresholds $z, Z, y, Y \in (0, H)$ with $z < y < Y < Z$. The thresholds divide the buffer into five domains $D^1, ..., D^5$. We denote by z^k the lower boundary of D^k and set $z^6 = H$.

$z < y < Y < Z$ we set $D^1 = (0, z)$, $D^2 = (z, y)$, $D^3 = (y, Y)$, $D^4 = (Y, Z)$ and $D^5 = (Z, H)$. For a given state $(x, i, j) \in \mathcal{S}$ with $x \in D^k$ we denote by

$v^k_{n;(i,j)}$ the rate of M_n, $n = 1, 2$ prescribed by the control Eqs. (4.16-4.18). We now introduce the probabilities:

$$\begin{aligned}
L_{i,j}(t) &= \mathbb{P}\big(X(t) = 0, I_1(t) = i, I_2(t) = j\big), \;\; i, j \in \{0, 1\},\\
z_{i,j}(t) &= \mathbb{P}\big(X(t) = z, I_1(t) = i, I_2(t) = j\big), \;\; i, j \in \{0, 1\},\\
y_{i,j}(t) &= \mathbb{P}\big(X(t) = y, I_1(t) = i, I_2(t) = j\big), \;\; i, j \in \{0, 1\},\\
Y_{i,j}(t) &= \mathbb{P}\big(X(t) = Y, I_1(t) = i, I_2(t) = j\big), \;\; i, j \in \{0, 1\},\\
Z_{i,j}(t) &= \mathbb{P}\big(X(t) = Z, I_1(t) = i, I_2(t) = j\big), \;\; i, j \in \{0, 1\},\\
H_{i,j}(t) &= \mathbb{P}\big(X(t) = H, I_1(t) = i, I_2(t) = j\big), \; i, j \in \{0, 1\},
\end{aligned} \tag{4.19}$$

and for $k = 1, ..., 5$ and for $x \in D^k$:

$$F^k_{i,j}(x, t) = \mathbb{P}\big(X(t) \in (z^k, x], I_1(t) = i, I_2(t) = j\big), \; i, j \in \{0, 1\}. \tag{4.20}$$

The existence of the $t \to \infty$ limits of Eqs. (4.19) and (4.20) (referred from now on as the stationary distribution of the buffer level) follows from the ergodicity of the process $X(t)$ which is a direct consequence of the compactness of $\mathcal{S}$ and the irreducibility of $(X(t), I_1(t), I_2(t))$. The notations for the stationary distributions will be those given in Eqs. (4.19) and (4.20) with "t" being omitted (e.g., $L_{i,j} := \lim_{t\to\infty} L_{i,j}(t)$, $F^k_{i,j}(x) := \lim_{t\to\infty} F^k_{i,j}(x, t)$ and so on). Following the lines of [19, 51] and [31], let us now write the stationary Chapman-Kolmogorov (C-K) equation which governs the buffer population under the assumption $z < y < Y < Z$.

4.3.1 The absolutely continuous part of the C-K equations

For $x \in D^k$, the stationary distribution function solves the following system:

$$(\mu_1 + \mu_2)F^k_{0,0}(x) - \lambda_1 F^k_{1,0}(x) - \lambda_2 F^k_{0,1}(x) = 0 \tag{4.21}$$

$$(\lambda_1 + \lambda_2)F^k_{1,1}(x) - \mu_2 F^k_{1,0}(x) - \mu_1 F^k_{0,1}(x) = \big(f^k_{1,1}(x) - f^k_{1,1}(z^k)\big)(v^k_{2;(1,1)} - v^k_{1;(1,1)}) \tag{4.22}$$

$$(\lambda_1 + \mu_2)F^k_{1,0}(x) - \mu_1 F^k_{0,0}(x) - \lambda_2 F^k_{1,1}(x) = -\big(f^k_{1,0}(x) - f^k_{1,0}(z^k)\big)v^k_{1;(1,0)} \tag{4.23}$$

$$(\lambda_2 + \mu_1)F^k_{0,1}(x) - \mu_2 F^k_{0,0}(x) - \lambda_1 F^k_{1,1}(x) = \big(f^k_{0,1}(x) - f^k_{0,1}(z^k)\big)v^k_{2;(0,1)}, \tag{4.24}$$

where $f^k_{i,j}$ denotes the derivative of $F^k_{i,j}$.

4.3.2 The C-K equations at the boundaries 0 and H

For $x \in D^1$ we have $v^1_{1;(1,1)} > v^1_{2;(1,1)}$ and the storage level tends to increase when both machines are on. The lower buffer boundary is reached only if M_2 is operational and M_1 has failed long enough. We then have [19]:

$$L_{0,0} = L_{1,0} = L_{1,1} = 0, \;\; L_{0,1} = \frac{v_2^-}{\mu_1} f^1_{0,1}(0^+). \tag{4.25}$$

Similarly for $x \in D^5$ with $v_1^- < v_2^+$, the storage level tends to decrease. The upper buffer boundary is reached only when M_1 is operational and M_2 has failed long enough and we have:

$$H_{0,0} = H_{0,1} = H_{1,1} = 0, \;\; H_{1,0} = \frac{v_1^-}{\mu_2} f_{1,0}^5(H^-). \tag{4.26}$$

Note that Eqs. (4.25) and (4.26) directly connect the stationary probabilities to enter into boundary states to those which stay on the boundary. Therefore, under the assumption $v_1^+ > v_2^-$ and $v_1^- < v_2^+$, the cost functional Eq. (4.2) can be rewritten in the equivalent form:

$$h(X) = (\delta_0 + \frac{v_2^-}{\mu_1}\gamma_0)1_{\{X=0\}} + \tilde{h}(X)1_{\{0<X<H\}} + (\delta_H + \frac{v_1^-}{\mu_2}\gamma_H)1_{\{X=H\}} \tag{4.27}$$

4.3.3 The C-K equations at the thresholds y and Y

According to the optimal control, the rate of M_2 (resp. M_1) changes at y (resp. at Y) only if M_1 (resp. M_2) is under repair. The resulting drift $v_2 - 0$ (resp. $0 - v_1$) at y (resp. Y) does not vanish and no probability mass exists at these points. Therefore the C-K equations at y and Y are trivial:

$$y_{i,j} = Y_{i,j} = 0, \;\; i,j \in \{0,1\}. \tag{4.28}$$

4.3.4 The C-K equations at the thresholds z and Z

When $v_1^+ \neq v_2^+$ the drift $v_2(x) - v_1(x)$ at $x = z$ and $x = Z$ does not vanish and we have:

$$z_{i,j} = Z_{i,j} = 0, \;\; i,j \in \{0,1\}. \tag{4.29}$$

When $v_1^+ = v_2^+$ and when both machines are on, an increasing inventory $X(t) \leq z$ sticks at z (unless a machine failure occurs) and similarly, a decreasing inventory $X(t) \geq Z$ sticks at Z yielding non trivial C-K equations. Let us investigate the probability $z_{1,1}$ in detail (the upper threshold Z requires a similar treatment).
Fix an infinitesimal $h > 0$. The probability $z_{1,1}(t+h)$ depends, up to order $\mathcal{O}(h)$, on the following contributions:

state at time t	transition rate	state at time $t+h$
$\big(X(t) = z, 1, 1\big)$	$1 - (\lambda_1 + \lambda_2)h + \mathcal{O}(h^2)$	$\big(X(t+h) = z, 1, 1\big)$
$\big(X(t) \in [z - (v_1^+ - v_2^-)h, z[, 1, 1\big)$	$1 - (\lambda_1 + \lambda_2)h + \mathcal{O}(h^2)$	$\big(X(t+h) = z, 1, 1\big)$
$\big(X(t) \in [z - v_1^+ h, z[, 1, 0\big)$	$\mu_2 h + \mathcal{O}(h^2)$	$\big(X(t+h) = z, 1, 1\big)$
$\big(X(t) \in]z, z + v_2^- h], 0, 1\big)$	$\mu_1 h + \mathcal{O}(h^2)$	$\big(X(t+h) = z, 1, 1\big)$.

Up to first order in h, the probabilities for $\big(X(t), I_1(t), I_2(t)\big)$ to be at time t in one of these 4 states are respectively:

$$z_{1,1}(t); \quad (v_1^+ - v_2^-) f_{1,1}^1(z^-, t)h; \quad v_1^+ f_{1,0}^1(z^-, t)h; \quad v_2^- f_{0,1}^2(z^+, t)h.$$

Summing up the probabilities weighted with their associated transition rates (and neglecting terms of order h^2), we obtain in the $h \to 0$ limit:

$$\dot{z}_{1,1}(t) := \frac{\mathrm{d}}{\mathrm{d}t} z_{1,1}(t) = -(\lambda_1 + \lambda_2) z_{1,1}(t) + (v_1^+ - v_2^-) f_{1,1}^1(z^-, t). \tag{4.30}$$

Therefore, the stationary probability $z_{1,1}$ is:

$$z_{1,1} = \frac{(v_1^+ - v_2^-)}{(\lambda_1 + \lambda_2)} f_{1,1}^1(z^-). \tag{4.31}$$

Similarly for all t and all $h > 0$, one finds:

$$\begin{aligned}
\dot{z}_{0,0}(t) \qquad &= -(\mu_1 + \mu_2) z_{0,0}(t), \\
z_{0,1}(t+h) &= h\big(\lambda_1 z_{1,1}(t) + \mu_2 z_{0,0}(t) + v_2 f_{0,1}^2(z^+, t)\big), \\
z_{1,0}(t+h) &= h\big(\lambda_2 z_{1,1}(t) + \mu_1 z_{0,0}(t) + v_1 f_{1,0}^1(z^-, t)\big).
\end{aligned}$$

The stationary $C-K$ equations follow in the limit $h \to 0$ and $t \to \infty$ and read as:

$$z_{0,0} = z_{0,1} = z_{1,0} = 0, \;\; z_{1,1} = \frac{(v_1^+ - v_2^-)}{(\lambda_1 + \lambda_2)} f_{1,1}^1(z^-). \tag{4.32}$$

Similarly, the stationary $C-K$ equations at the level Z read as:

$$Z_{0,0} = Z_{1,0} = Z_{0,1} = 0, \;\; Z_{1,1} = \frac{(v_2^+ - v_1^-)}{(\lambda_1 + \lambda_2)} f_{1,1}^5(Z^+). \tag{4.33}$$

4.3.5 Constants of integration

We distinguish between two cases:

(i) Case where $v_1^+ = v_2^+$ (Figure 4.3 (A)). For $k = 1$ and $k = 5$, the Eqs. (4.21 - 4.24) form an ordinary linear differential system of order 3 and for $k = 2, 3, 4$, they form a system of order 2 (the RHS of Eq. (4.22) vanishes). The linear system is readily solved for the five regions D^k, $k = 1, ..., 5$ and the solution is specified by determining 12 constants of integration. Two constants can be extracted from the relations:

$$F_{i,j}^k(z^k) = 0, \;\; i, j \in \{0, 1\} \tag{4.34}$$

for $k = 1$ and $k = 5$. Two further constants are found by the boundary constraints at 0 and H (see e.g., Eqs. (14) and (17) in [19]):

$$f^1_{1,0}(0^+) = f^5_{0,1}(H^-) = 0. \tag{4.35}$$

Similar to the above boundary constraints we have for $k = 2, 3, 4$ (Eq. (15) in [19]):

$$v^k_{1;(1,0)} f^k_{1,0}(z^k) = v^k_{2;(0,1)} f^k_{0,1}(z^k) \tag{4.36}$$

which fixes 3 further constants of integration. A flow balance argument at the thresholds y, Y, z and Z (*i.e.* equating the flow rate of leaving a threshold with the flow rate of entering it) gives four further constants (see section 4, "matching at the thresholds"). The last integration constant comes from the probability normalization:

$$L_{0,1} + \sum_{k=1}^{5} \sum_{i,j=0}^{1} F^k_{i,j}(z^{k+1}) + z_{1,1} + Z_{1,1} + H_{1,0} = 1. \tag{4.37}$$

(ii) Case where $v_1^+ \neq v_2^+$ (Figure 4.3 (B)). The Eqs. (4.21)–(4.24) form an ordinary linear differential system of order 3 which can be solved for the five regions D^k, $k = 1, ..., 5$. Hence, 15 constants of integration must be determined. Five constants can be extracted from the relations:

$$F^k_{i,j}(z^k) = 0, \quad i, j \in \{0, 1\} \tag{4.38}$$

for $k = 1, ..., 5$. Two further constants are given by the boundary constraints at 0 and H:

$$f^1_{1,0}(0^+) = f^5_{0,1}(H^-) = 0. \tag{4.39}$$

Similar to the above boundary constraints we have for $k = 2, 3, 4$:

$$f^k_{1,0}(z^k) = 0, \quad \text{if } v_1^+ > v_2^+, \tag{4.40}$$

$$f^k_{0,1}(z^{k+1}) = 0, \quad \text{if } v_1^+ < v_2^+, \tag{4.41}$$

which fixes 3 constants. A flow balance argument at the four thresholds z, y, Y, Z, given in section 4, will determine 4 further constants of integration. The remaining constant is given by the probability normalization Eq. (4.37).

4.4 Stationary probability distribution

Here we recall from [19] the solutions of the stationary C-K equations and match them together at the thresholds by using the conservation of probability flow.

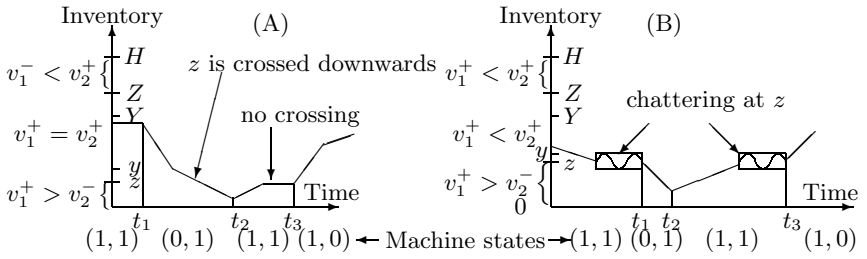

Fig. 4.3. Sketch of two possible sample paths of $X(t)$ with random switches of machine states at t_1, t_2, t_3. (A): $v_1^+ = v_2^+$. The feedback control imposes the thresholds z and Z to behave as semipermeable membranes. Indeed for operating machines $(I_1, I_2) = (1, 1)$, an increasing inventory gets trapped at z, while a decreasing inventory crosses z (similar behavior at Z). (B): $v_1^+ < v_2^+$. In principle, the thresholds z and Z are both "permeable" for all machine states. Note that chattering at z occurs because $v_2 - v_1$ changes its sign at z.

4.4.1 Solutions for the absolutely continuous part

We distinguish between two cases.

(i) Case where $v_1^+ = v_2^+$. Integrating the linear system (4.23), (4.24), taking into account the constraints (4.34) and using Eqs. (4.21), (4.22), we get for $x \in D^k$, $k = 1, 5$:

$$\begin{aligned} F^k_{0,0}(x) &= \tfrac{1}{\mu_1+\mu_2}\Big[\lambda_1\big(F^k_{1,0}(x) + \lambda_2 F^k_{0,1}(x)\big)\Big], \\ F^k_{1,1}(x) &= \tfrac{1}{(v^k_{2;(1,1)} - v^k_{1;(1,1)})}\Big[v^k_{1;(1,0)} F^k_{1,0}(x) - v^k_{2;(0,1)} F^k_{0,1}(x)\Big], \end{aligned} \tag{4.42}$$

which in case

$$v^k_{1;(1,0)} \frac{\mu_1}{\mu_1 + \lambda_1} = v^k_{2;(0,1)} \frac{\mu_2}{\mu_2 + \lambda_2} \tag{4.43}$$

(i.e. both machines have the same productivity) are completed by:

$$\begin{aligned} F^k_{1,0}(x) &= \tfrac{B}{D} K_k (e^{(A+D)(x-z^k)} - 1) + S_k \tfrac{D}{A+D} x, \\ F^k_{0,1}(x) &= K_k (e^{(A+D)(x-z^k)} - 1) - S_k \tfrac{E}{A+D} x, \end{aligned} \tag{4.44}$$

and which in case $v^k_{1;(1,0)} \frac{\mu_1}{\mu_1+\lambda_1} \neq v^k_{2;(0,1)} \frac{\mu_2}{\mu_2+\lambda_2}$ are completed by:

$$\begin{aligned} F^k_{1,0}(x) &= K_k (e^{k_1(x-z^k)} - 1) + S_k (e^{k_2(x-z^k)} - 1), \\ F^k_{0,1}(x) &= K_k (e^{k_1(x-z^k)} - 1) \tfrac{k_1 - A}{B} + S_k (e^{k_2(x-z^k)} - 1) \tfrac{k_2 - A}{B}. \end{aligned} \tag{4.45}$$

In both cases, the Eqs. (4.35) relate the K_k's with the constants S_k for $k = 1, 5$. The S_k's remain to be determined and $k_1 < k_2$ are the roots of:

$$\xi^2 - \big(A + D\big)\xi + AD - EB = 0, \tag{4.46}$$

with

$$A = \frac{\lambda_2}{v^k_{2;(1,1)} - v^k_{1;(1,1)}} - \frac{\mu_2(\mu_1+\mu_2+\lambda_1)}{v^k_{1;(1,0)}(\mu_1+\mu_2)},\ B = \frac{\lambda_2}{v^k_{1;(1,0)}}\big(\frac{\mu_1}{\mu_1+\mu_2} - \frac{v^k_{2;(0,1)}}{v^k_{2;(1,1)} - v^k_{1;(1,1)}}\big),$$

$$D = \frac{\lambda_1}{v^k_{2;(1,1)} - v^k_{1;(1,1)}} + \frac{\mu_1(\mu_1+\mu_2+\lambda_2)}{v^k_{2;(0,1)}(\mu_1+\mu_2)},\ E = -\frac{\lambda_1}{v^k_{2;(0,1)}}\big(\frac{\mu_2}{\mu_1+\mu_2} + \frac{v^k_{1;(1,0)}}{v^k_{2;(1,1)} - v^k_{1;(1,1)}}\big).$$

For $x \in D^k$, $k = 2, 3, 4$ we integrate the system Eqs. (4.23), (4.24). Taking into account the Eqs. (4.36) and using Eqs. (4.21), (4.22), we get (see e.g., [19] Eqs. (2.1), (7.1), (8.1), (9.1)):

$$\begin{aligned} F^k_{0,0}(x) &= \tfrac{1}{\mu_1+\mu_2}\Big(\lambda_1 F^k_{1,0}(x) + \lambda_2 F^k_{0,1}(x)\Big), \\ F^k_{1,1}(x) &= \tfrac{1}{\lambda_1+\lambda_2}\Big(\mu_2 F^k_{1,0}(x) + \mu_1 F^k_{0,1}(x)\Big), \\ F^k_{1,0}(x) &= \tfrac{v^k_{2;(0,1)}}{v^k_{1;(1,0)}} F^k_{0,1}(x). \end{aligned} \tag{4.47}$$

Two cases are to be considered:

- $\lambda_2\mu_1 v^k_{1;(1,0)} \neq \lambda_1\mu_2 v^k_{2;(0,1)}$. In this case $F^k_{0,1}(x)$ is given by:

$$F^k_{0,1}(x) = S_k\big\{\exp\big[U(\frac{\lambda_2\mu_1}{v^k_{2;(0,1)}} - \frac{\lambda_1\mu_2}{v^k_{1;(1,0)}})(x - z^k)\big] - 1\big\}, \tag{4.48}$$

  with $S_k \in \mathbb{R}$ a constant and

$$U = \frac{\lambda_2 + \lambda_1 + \mu_1 + \mu_2}{(\mu_1+\mu_2)(\lambda_1+\lambda_2)}. \tag{4.49}$$

- $\lambda_2\mu_1 v^k_{1;(1,0)} = \lambda_1\mu_2 v^k_{2;(0,1)}$. In this case $F^k_{0,1}(x)$ is given by:

$$F^k_{0,1}(x) = S_k(x - z^k), \tag{4.50}$$

  with $S_k \in \mathbb{R}$ a constant, implying that the distributions $F^k_{i,j}$ on D^k are uniform.

(ii) Case where $v_1^+ \neq v_2^+$. When Eq. (4.43) is satisfied the $F^k_{i,j}$'s $k = 1, ..., 5$, are given by Eqs. (4.42) and (4.44). Otherwise they are given by Eqs. (4.42) and (4.45). The constants K_k are related to the S_k's by using the constraints (4.39) for $k = 1, 5$ and the constraints (4.40) or (4.41) for $k = 2, 3, 4$ depending on whether $v_1^+ > v_2^+$ or $v_1^+ < v_2^+$. The parameters k_1, k_2, A, B, D and E are related as above and the solutions are fully determined once the remaining constants S_k, $k = 1, ..., 5$ are fixed.

4.4.2 Solutions at 0 and H

Due to the presence of a drift term (directed away from the nearest boundary), the stationary boundary equations are decoupled. The solutions which are identical for $v_2^+ \neq v_1^+$ and for $v_2^+ = v_1^+$ are directly given by the Eqs. (4.25) and (4.26).

4.4.3 Solutions at z and Z

When $v_2^+ \neq v_1^+$ no probability masses accumulate and the stationary solution is trivial:

$$z_{i,j} = Z_{i,j} = 0, \quad i,j = 0,1. \tag{4.51}$$

When $v_2^+ = v_1^+$ the stationary solutions Eqs. (4.32) and (4.33) can be summarized for $k = 2$ by:

$$z_{0,0} = z_{1,0} = z_{0,1} = 0, \;\; z_{1,1} = \frac{(v_{1;(1,1)}^{k-1} - v_{2;(1,1)}^{k-1})}{(\lambda_1 + \lambda_2)} f_{1,1}^k(z^k). \tag{4.52}$$

and for $k = 5$ by:

$$Z_{0,0} = Z_{1,0} = Z_{0,1} = 0, \;\; Z_{1,1} = \frac{(v_{2;(1,1)}^{k} - v_{1;(1,1)}^{k})}{(\lambda_1 + \lambda_2)} f_{1,1}^k(z^k). \tag{4.53}$$

4.4.4 Solutions at y and Y

The C-K equations at y and Y are trivial and so are their solutions given by Eqs. (4.28).

4.4.5 Matching at z and Z

The constants S_1 and S_2 resp. S_4 and S_5 are connected via a flow conservation argument at z and Z. We distinguish between two cases.

(i) The case $v_1^+ = v_2^+$. At z (and similarly at Z), four possible sample-path configurations occur (Figure 4.4).

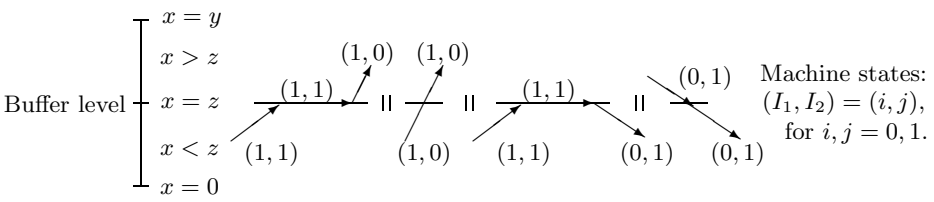

Fig. 4.4. Sketch of the four possible sample paths "visiting" the lower boundary z. The slope of the arrows are proportional to $v_1 - v_2$. The leftmost path, for example, represents a change of buffer level due to a flow from the domain "$< z$" to domain "$> z$" with velocity $v_1^+ - v_2^-$ in the region "$< z$", with velocity zero at "z" and, after failure of machine M_2, with velocity v_1^+ in the region "$> z$".

Through the threshold z, it exists a probability flow connecting the regions $0 < x < z$ and $z < x < Z$. The flow "permeability" at z depends on the specific

sample path (*i.e.* on the machine states). In particular no probability current crosses z when both machines are operational. This allows the formation of a finite probability mass $z_{1,1}$ which splits up into a downward and upward probability flow. The detailed balance equations for the upward and downward flows at z and Z (*i.e.* at z^k for $k = 2$ and $k = 5$) are:

$$v^k_{1;(1,0)} f^k_{1,0}(z^k) - v^{k-1}_{1;(1,0)} f^{k-1}_{1,0}(z^k) = z^k_{11}\lambda_2 \tag{4.54}$$

$$v^{k-1}_{2;(0,1)} f^{k-1}_{0,1}(z^k) - v^k_{2;(0,1)} f^k_{0,1}(z^k) = z^k_{11}\lambda_1, \tag{4.55}$$

Eq. (4.54) relates S_1 with S_2 for $k = 2$ and S_4 with S_5 for $k = 5$ (Eq. (4.55) contains the same information).

(ii) The case $v_2^+ \neq v_1^+$. For $x \in (0, z) \cup (Z, H)$, the buffer content evolves towards the buffer bulk $[z, Z]$. For $z \leq x \leq Z$, and when both machines are on, the inventory approaches one of the two thresholds, say z (*i.e.* $v_2^+ > v_1^+$). Due to the chattering at z no stationary probability mass can accumulate at this point (the state $(z, 1, 1)$ is transient). At Z the drift changes its value but not its sign. No chattering occurs and no stationary probability mass can accumulate at Z. Hence the three absolutely continuous parts must fit continuously at z and Z. One actually fits the solutions at z and Z using the flow balance at these thresholds (see Figure 4.5). For $v_1^+ < v_2^+$ (chattering at z) the flow balance reads:

$$v^k_{1;(1,0)} f^k_{1,0}(z^k) = v^{k-1}_{2;(0,1)} f^{k-1}_{0,1}(z^k), \quad k = 2 \tag{4.56}$$

$$(v^{k-1}_{2;(1,1)} - v^{k-1}_{1;(1,1)}) f^{k-1}_{1,1}(z^k) + v^{k-1}_{1;(1,0)} f^{k-1}_{1,0}(z^k) = v^k_{2;(0,1)} f^k_{0,1}(z^k), \quad k = 5. \tag{4.57}$$

Similarly for $v_1^+ > v_2^+$ (chattering at Z), the flow balance is:

$$v^k_{1;(1,0)} f^k_{1,0}(z^k) = v^{k-1}_{2;(0,1)} f^{k-1}_{0,1}(z^k), \quad k = 5 \tag{4.58}$$

$$(v^k_{1;(1,1)} - v^k_{2;(1,1)}) f^k_{1,1}(z^k) + v^k_{1;(1,0)} f^k_{1,0}(z^k) = v^{k-1}_{2;(0,1)} f^{k-1}_{0,1}(z^k), \quad k = 2. \tag{4.59}$$

4.4.6 Matching at y and Y

(i) The case $v_1^+ = v_2^+$. Equating the upward and downward flows at $z^3 = y$ and $z^4 = Y$ yields (see figure 4.6):

$$v^k_{1;(1,0)} f^k_{1,0}(z^k) = v^{k-1}_{2;(0,1)} f^{k-1}_{0,1}(z^k), \tag{4.60}$$

which relates S_2 with S_3 for $k = 3$ and S_3 with S_4 for $k = 4$.

(ii) The case $v_2^+ \neq v_1^+$. Equating the upward and downward flows at z^k, $k = 3, 4$ (see figure 4.7) yields in case $v_2^+ > v_1^+$:

$$(v^{k-1}_{2;(1,1)} - v^{k-1}_{1;(1,1)}) f^{k-1}_{1,1}(z^k) + v^{k-1}_{2;(0,1)} f^{k-1}_{0,1}(z^k) = v^k_{1;(1,0)} f^k_{1,0}(z^k) \tag{4.61}$$

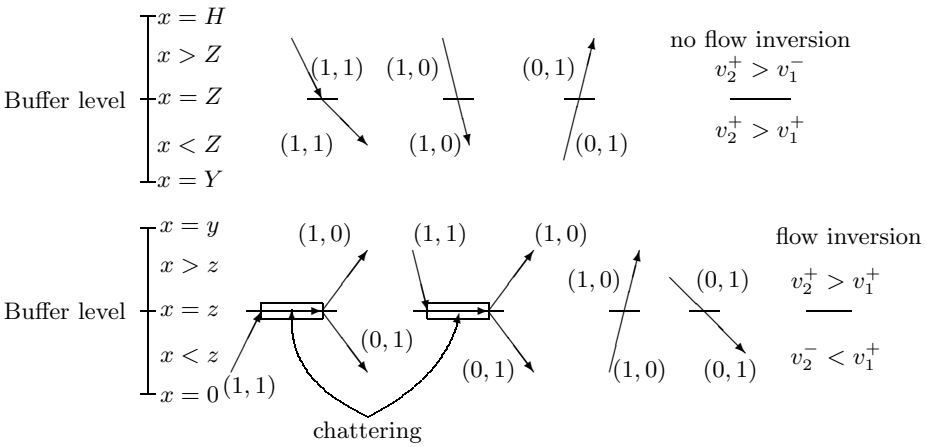

Fig. 4.5. Sketch of the possible sample paths "visiting" the buffer levels Z (on top) and z (bottom) in case $v_1^+ < v_2^+$ (flow inversion at z). The slope of the arrows are proportional to $v_1 - v_2$. The machine state $(1, 1)$ drives X toward z. The buffer level gets trapped at z and chatters around it unless a machine failure occurs. The probability flow trapped at z splits into an upward and downward flow.

Fig. 4.6. Sketch of the possible sample paths crossing the buffer levels y (left) and Y (right) in case $v_1^+ = v_2^+$. The slope of the arrows are proportional to $v_1 - v_2$. In the stationary regime, the upward flow equals the downward flow.

and in case $v_2^+ < v_1^+$:

$$(v^k_{1;(1,1)} - v^k_{2;(1,1)}) f^k_{1,1}(z^k) + v^k_{1;(1,0)} f^k_{1,0}(z^k) = v^{k-1}_{2;(0,1)} f^{k-1}_{0,1}(z^k). \quad (4.62)$$

This relates S_2 with S_3 for $k = 3$ and S_3 with S_4 for $k = 4$.

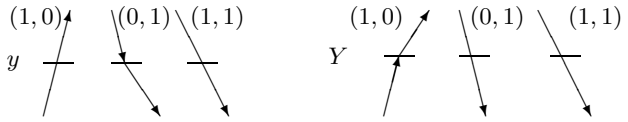

Fig. 4.7. Sketch of the possible sample paths crossing the buffer levels y (left) and Y (right) for $v_2^+ > v_1^+$. The slope of the arrows are proportional to $v_1 - v_2$. In the stationary regime, the upward flow equals the downward flow.

4.4.7 The cumulative distribution function

The normalization of probability given by Eq. (4.37) ultimately fixes the constants S_k, $k = 1, ..., 5$. This fully characterizes the stationary distributions for fixed thresholds $z < y < Y < Z$. The resulting marginal cumulative distribution function (CDF) F of the buffer population reads:

(i) in case $v_2^+ = v_1^+$:

$$F(y) = L_{0,1}1_{\{y\geq 0\}} + H_{1,0}1_{\{y=H\}} + z_{1,1}1_{\{y\geq z\}} + Z_{1,1}1_{\{y\geq Z\}} + \\ + \sum_{k=1}^{5}\sum_{i,j=0}^{1} F_{i,j}^k(\min(z^{k+1}, y))1_{\{y>z^k\}}, \tag{4.63}$$

where for $k = 1, 5$, the $F_{i,j}^k$'s are given by Eqs. (4.42) and (4.44) when Eq. (4.43) is satisfied and by Eqs. (4.42) and (4.45) otherwise. For $k = 2, 3, 4$ the $F_{i,j}^k$'s are given by Eqs. (4.47) and (4.48) in case $\lambda_2\mu_1 v_{1;(1,0)}^k \neq \lambda_1\mu_2 v_{2;(0,1)}^k$ and by Eqs. (4.47) and (4.50) in case $\lambda_2\mu_1 v_{1;(1,0)}^k = \lambda_1\mu_2 v_{2;(0,1)}^k$. The constants S_k are fixed according to the Eqs. (4.37), (4.54) and Eq. (4.60). The resulting CDF is sketched in Figure (4.8) for different values of v_1^- and λ_2.

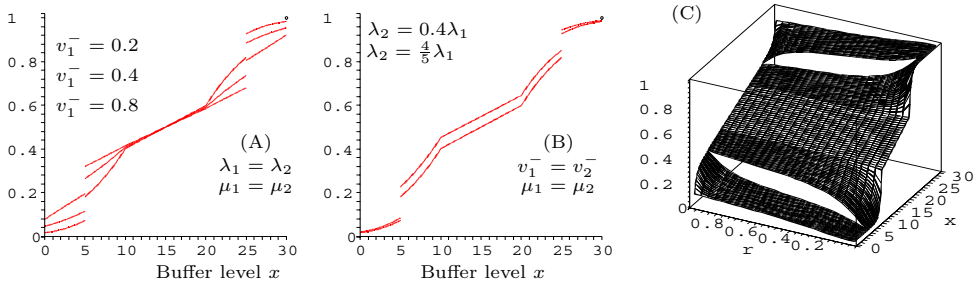

Fig. 4.8. Graph of the marginal distribution F for fixed thresholds $z = 5$, $y = 10$, $Y = 20$, $Z = 25$ in case $v_1^+ = v_2^+$. **(A)**: The reduced speed v_1^- is varied and increases from 0.2 (highest curve) over 0.4 to 0.8 (lowest curve). The fixed parameters are $\lambda_1 = \lambda_2 = 1/80$, $\mu_1 = \mu_2 = 1/20$, $v_1^+ = v_2^+ = 1$, $v_2^- = 0.6$ and $H = 30$. **(B)**: The unavailability parameter $I_2 = \lambda_2/\mu_2$ of M_2 is varied ($I_2 = 0.2$ and $I_2 = 0.25$) by changing λ_2. The fixed parameters are $\lambda_1 = 1/80$, $\mu_1 = \mu_2 = 1/20$, $v_1^+ = v_2^+ = 1$, $v_1^- = v_2^- = 0.6$ and $H = 30$. The discontinuities at z resp. Z are more pronounced for $I_2 = 0.2$ (upper curve) than for $I_2 = 0.25$ (lower curve). This is due to an increase of $z_{1,1}$ resp. $Z_{1,1}$ occurring when the machines are more likely to be (both) operational. **(C)**: The marginal distribution for a fully symmetric case (identical machines). The reduced production rates $v_1^- = v_2^- =: r$ are varied from 0 to 1.

(ii) in case $v_2^+ \neq v_1^+$:

$$F(y)=L_{0,1}1_{\{y\geq 0\}}+H_{1,0}1_{\{y=H\}}+\sum_{k=1}^{5}\sum_{i,j=0}^{1}F_{i,j}^{k}(\min(z^{k+1},y))1_{\{y>z^{k}\}}(4.64)$$

For $k=1,...,5$, the $F_{i,j}^{k}$'s are given by Eqs. (4.42) and (4.44) in case Eq. (4.43) is satisfied and by Eqs. (4.42) and (4.45) if it is not. The constants S_k are fixed according to the Eqs. (4.37), (4.56), (4.57) and Eq. (4.61) if $v_2^+ > v_1^+$ and otherwise according to the Eqs. (4.37), (4.58), (4.59) and Eq. (4.62). The resulting CDF is sketched in Figure (4.9) for different values of v_2^- and λ_2.

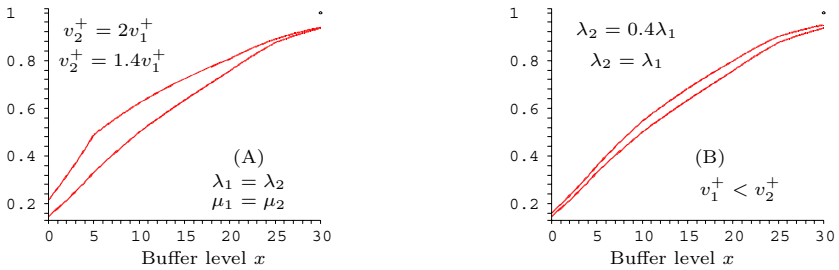

Fig. 4.9. The marginal distributions of the buffer level for fixed thresholds $z=5$, $y=10$, $Y=20$, $Z=25$ in case $v_1^+ < v_2^+$ (*i.e.* flow inversion at z). Fixed Parameters: $v_1^- = v_2^- = 0.6$, $v_1^+ = 1$, $\lambda_1 = 1/80$, $\mu_1 = \mu_2 = 1/20$ and $H=30$. **(A)**: Upper curve: $v_2^+ = 2v_1^+$; Lower curve: $v_2^+ = 1.4v_1^+$. In both cases we have $\lambda_1 = \lambda_2$. The chattering at z is visibly less pronounced in case v_2^+ is close to v_1^+. **(B)**: Upper curve, $\lambda_2 = 0.4\lambda_1$. Lower curve $\lambda_2 = \lambda_1$. In both cases we have $v_2^+ = 1.4v_1^+$.

Remark. The function $F^1 \overset{\text{not.}}{=} F$ is the CDF of the buffer population conditioned on the ordering relations $z<y<Y<Z$. In exactly the same way one computes the CDF's for the ordering relations (2) $z<Y<y<Z$, (3) $Y<z<y<Z$, (4) $Y<z<Z<y$, and (5) $z<Y<Z<y$ (see appendix). The corresponding stationary CDF's are denoted by F^i, $i=2,...,5$.

4.5 The optimal thresholds

The stationary distribution can now be used to calculate the optimal positions of the thresholds z, y, Y and Z conditioned on the relations $z \leq y \leq Y \leq Z$. The long-run average cost reads:

$$
\begin{aligned}
V_1(z,y,Y,Z) = \mathbb{E}_S^1(g(v_2)+h(X)) &= \int_0^H (g(v_2)+h(X))\mathrm{d}F^1(x) \qquad (4.65)\\
&= \big(g(v_2^-)+\delta_0+\frac{\mu_1}{v_2^-}\gamma_0\big)L_{0,1} + \big(g(0)+\delta_H+\frac{\mu_2}{v_1^-}\gamma_H\big)H_{1,0}\\
&\quad +\big(g(v_2^+)+h(z)\big)z_{1,1} + \big(g(v_2^+)+h(Z)\big)Z_{1,1}\\
&\quad +\sum_{k=1}^{5}\sum_{i,j=0}^{1}\int_{z^k}^{z^{k+1}} (g(v^k_{2;(i,j)})+h(x))\mathrm{d}F^k_{i,j}(x),
\end{aligned}
$$

where $\mathbb{E}_S^1$ is the stationary expectation of the buffer population conditioned on $z \le y \le Y \le Z$. Minimizing V_1 yields (at least one set of) optimal thresholds z_1^*, y_1^*, Y_1^* and Z_1^* satisfying $z_1^* \le y_1^* \le Y_1^* \le Z_1^*$. Similarly, for $i = 2, ..., 5$ one finds a set of thresholds $z_i^{2*} \le z_i^{3*} \le z_i^{4*} \le z_i^{5*}$ minimizing the expected costs

$$
V_i(z_i^2, z_i^3, z_i^4, z_i^5) = \mathbb{E}_S^i(g(v_2)+h(X)) = \int_0^H (g(v_2)+h(X))\mathrm{d}F^i(x). \qquad (4.66)
$$

Here, F^i is the stationary buffer level distribution conditioned on the threshold ordering i, where for $i = 2$ we have $z_2^2 = z$, $z_2^3 = Y$, $z_2^4 = y$, $z_2^5 = Z$, for $i = 3$ we have $z_3^2 = Y$, $z_3^3 = z$, $z_3^4 = y$, $z_3^5 = Z$, for $i = 4$ we have $z_4^2 = Y$, $z_4^3 = z$, $z_4^4 = Z$, $z_4^5 = y$ and for $i = 5$ we have $z_5^2 = z$, $z_5^3 = Y$, $z_5^4 = Z$, $z_5^5 = y$. The optimal thresholds $z_j^{2*}, z_j^{3*}, z_j^{4*}$ and z_j^{5*} are the ones satisfying:

$$
V_j(z_j^{2*}, z_j^{3*}, z_j^{4*}, z_j^{5*}) = \min_{i=1,\dots,5} V_i(z_i^{2*}, z_i^{3*}, z_i^{4*}, z_i^{5*}). \qquad (4.67)
$$

Numerical example. A full discussion of the value functions V_i as a function of the thresholds z, y, Y and Z for general parameters $H, \lambda_1, \lambda_2, \mu_1, \mu_2$ and v_1, v_2 obviously involves heavy algebra. We therefore refrain here from writing down explicit expressions but we rather sketch their behaviors for the specific choice $\lambda_1 = \lambda_2 = 1/80$, $\mu_1 = \mu_2 = 1/20$, $v_1^+ = v_2^+ = 1$, $v_1^- = v_2^- = 0.6$ and $H = 30$ (Figure 4.10). The Maple file generating the solutions is available in [37]. In addition, we give the average inventory and the mean throughput of the system.

The optimal thresholds z_j^*, y_j^*, Y_j^* and Z_j^*. We impose the following cost structure (in cost units per production unit):

$$
\begin{aligned}
&\gamma_0 = \gamma_H = 100,\\
&\delta_0 = \delta_H = 100,\\
&\tilde{h}(x) = (x - H/2)^2.
\end{aligned}
$$

Numerical computations performed on a PC using Maple yield (see [37]):

$$
\min_{i=1,\dots,5} V_i(z_i^{2,*}, z_i^{3,*}, z_i^{4,*}, z_i^{5,*}) = V_2(Y_2^*, z_2^*, y_2^*, Z_2^*). = 296,2. \qquad (4.68)
$$

The optimal thresholds ordering is (2) with $Y_2^* = 12 \le z_2^* = 12 \le y_2^* = 16.6 \le Z_2^* = 19.6$. The cost function $V_2(12, z, 16.6, Z)$ is sketched in Figure (4.10).

The average inventory $\mathbb{E}(X)$**.** The average inventory $\mathbb{E}(X)$ is given by:

$$\mathbb{E}(X) = \mathbb{E}_2(X) = \int_0^H x \mathrm{d}F^2(x)$$

which for our numerical example yields $\mathbb{E}(X) = 14.6$. Fixing the thresholds y and Y, the corresponding graph in figure (4.10) indicates that $\mathbb{E}(X)$ varies almost linearly in both variables z and Z.

The mean throughput $\mathbb{E}(T)$**.** The throughput of the controlled system is:

$$\begin{aligned} T \stackrel{\text{def.}}{=} & \left(v_2^- 1_{\{0<X<y\}} + v_2^+ 1_{\{y\leq X\leq H\}}\right) 1_{\{(I_1,I_2)=(0,1)\}} + \\ & \left(v_2^- 1_{\{0<X<z\}} + v_2^+ 1_{\{z\leq X\leq H\}}\right) 1_{\{(I_1,I_2)=(1,1)\}}. \end{aligned}$$

Using the optimal thresholds ordering $Y < z < y < Z$, the average throughput is:

$$\begin{aligned} \mathbb{E}_2(T) = & v_2^+ \left(F_{0,1}^4(Z) + F_{0,1}^5(H) + z_{1,1} + F_{1,1}^3(y) + F_{1,1}^4(Z) + Z_{1,1} + F_{1,1}^5(H)\right) \\ & + v_2^- \left(F_{0,1}^1(Y) + F_{0,1}^2(z) + F_{0,1}^3(y) + F_{1,1}^1(Y) + F_{1,1}^2(z)\right). \end{aligned}$$

The numerical example yields $\mathbb{E}(T) = 0.70$, a value close to the maximum mean throughput 0.72 which is reached for $y \to 0$ and $Y \to H$ (*i.e.* in case operating machines produce at rate v_i^+ and no threshold control is applied). Fixing the thresholds y and Y, the corresponding graph in figure (4.10) indicates that $\mathbb{E}(T)$ is increasing in Z and decreasing in z. Increasing Z or decreasing z does indeed enlarge the region where the control assigns the nominal speed to M_2.

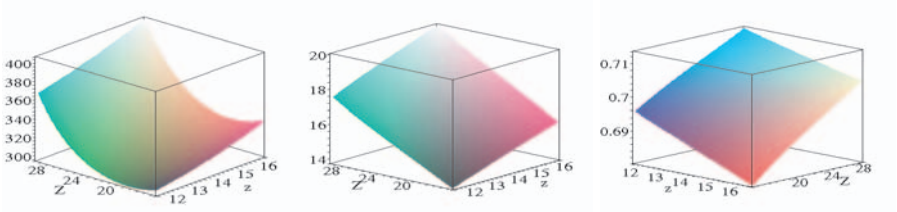

Fig. 4.10. Left: The stationary average costs $V_2(12, z, 16.6, Z)$ for $12 < z < 16.6$ and $16.6 < Z < 30$. **Middle**: The expected inventory $\mathbb{E}_2(X)(12, z, 16.6, Z)$ for $12 < z < 16.6$ and $16.6 < Z < 30$. **Right**: The expected throughput $\mathbb{E}_2(T)(12, z, 16.6, Z)$ for $12 < z < 16.6$ and $16.6 < Z < 30$. Parameters: $\mu_1 = \mu_2 = 1/20$, $\lambda_1 = \lambda_2 = 1/80$, $v_1^+ = v_2^+ = 1$, $v_1^- = v_2^- = 0.6$ and $H = 30$.

4.6 Concluding remarks

Usually in manufacturing systems, the production flow dynamics is governed by machines operating either with their nominal production rates or being

stopped due to failures, blocking or starving mechanisms. For lines with relatively low buffer capacities, this strict on-off machine operating mode do generate frequent and impulsive interruptions of the production flows. In a wide class of inventory processes (e.g. fluid installations, data transfer in the Internet, production installations involving high production flows as those arising in food industries), the entrance into and the stay on the buffer boundaries can be strongly penalizing. This penalty can be modelled by an ad-hoc cost function and the benefits of any modification of either the line configuration (the buffers contents in particular) or its operating mode can be evaluated by solving an associated optimization problem. This is completely discussed for a two speed tandem production system.
It is interesting to appreciate the resulting optimal production rate control in the light of the analogy "traffic flow versus production flow" as studied in Chapter 3. Transporting the formal structure of the optimal production rate into the realm of traffic theory, we recover an optimal velocity function $\mathcal{V}$ minimizing the amount of crash-scenarios between two cars according to a well defined optimization problem.

4.7 Contributions of Chapter 4

- Using as performance measure the expected average cost induced by a specific cost function, we derive the structural form of the optimal production rates $u^*(x, i_1, i_2)$ of a two speed tandem production system. Here x indicates the buffer content and i_1, i_2 are the two possible machine states of the two failure prone machines composing the production system. The cost function includes the following features:
  i) a cost term $g(v_2)$ depending on the production rate of the second machine which penalizes slow production rates,
  ii) a term penalizing large work-in-process,
  iii) a term penalizing full and empty buffer states,
  iv) a term penalizing the entrance rates into the full and empty buffer states.

  The resulting optimal feedback control is characterized by four threshold levels z, Z, y, Y for the buffer content (see Eqs. 4.16-4.18). When these levels are crossed, the rates are adjusted to reduce the probability to enter into or to stay on the boundaries.
- Exact stationary probability measures are derived which enable exact calculations for the expected average costs as a function of the thresholds:

$$V(z, Z, y, Y) = \lim_{T\to\infty} \frac{1}{T}\mathbb{E}\Big[\int_0^T \Big(L\big[X(s), v_2(X(s))\big]\Big)\mathrm{d}s\Big]. \tag{4.69}$$

  From this we deduce the optimal control u^* by a simple optimization of the expected average costs $V(z, Z, y, Y)$ over the thresholds.

5

Multi-scale analysis for a simple traffic model

Summary. We apply the micro-macro program of statistical mechanics to a simple one-dimensional interacting particle system with interactions joining on a minimum level of detailed knowledge the kinetic features of migration, reaction and collision. The application includes a micro-meso-macro link for cars in one-lane traffic where the three mentioned kinetic features model respectively *i*) transport, *ii*) spontaneous accelerations and decelerations and *iii*) anisotropic decelerations of cars due to slow front-cars.
Starting from the space-discrete particle hopping model, we establish in a first step its convergence to a space-continuous Boltzmann-like model which constitutes the mesoscopic level of description. In a second step we derive the functional relation between the vehicular density (*i.e.* the particles density) $\rho(x,t)$ and the flux $J(x,t)$ which occurs also in a popular ad-hoc traffic model proposed by Greenshields.

5.1 Introduction

The understanding of the collective dynamics of coupled elementary cells forming a complex physical, biological and/or socio-ecological system is a formidable interdisciplinary task and the ubiquity of such cooperative mechanisms in various fields generate a strong ongoing research activity in the basic sciences [142, 84], the applied sciences [64, 57, 35] and in between (complexity research [11, 136, 141]).
The origin of complex behavior is located in the interplay of the "microscopic" (elementary) components of the system which give rise to new collective properties, qualitatively different from the microscopic properties. The main steps toward a formal understanding of the collective dynamics are contained in the micro-to-macro paradigm behavior formulated in analogy to the kinetic theory of dilute gases. On the *microscopic* level of description the elementary cells evolve under Newton-like dynamics. A reduced description is given by the *mesoscopic* Boltzmann-like equation which describes the evolution of the probability distribution of the components in the phase space [143]. When the mean free path between the elementary cells goes to zero, the solution to

the Boltzmann equation relaxes to a Maxwellian distribution and the process yields a *macroscopic* description via fluid-dynamic-like equations. This ambitious program of statistical physics has contributed to the understanding of micro and macro properties of systems with great practical interest such as granular and self driven many particle systems [52, 64].
In this chapter we like to pursue this generic program in a very simple one-dimensional context. The main kinetics of the interacting particles defining the space discrete stochastic hopping model derives from a dramatically simplified view on cars in traffic including only migration, reaction and collision terms. This view is simple enough such that the necessary mathematics can still be handled, yet sharp enough to capture some of the basic mechanisms of interacting cars in one-lane traffic. The micro-meso link is realized by a discrete-space approximation of a Boltzmann-type equation introduced by Ruijgrok and Wu which describes the mesoscopic regime. The meso-macro link then involves a classical central limit procedure.
That our choice for the minimal model (reduction to migration, reaction and collision terms) is not too simple is convincingly demonstrated by the micro-macro link which unveils in the macro regime an experimentally founded traffic model which is still used in traffic theory.
The chapter is organized as follows: In section 2 we establish the space discrete microscopic model in a general setting, present the mesoscopic (space continuous) model and derive the convergence of the former to the latter (*i.e.* the micro-meso link). In section 3 we briefly recall a few concept of traffic modelling and apply the result of section 2. In section 4, we derive the fundamental diagram defining the macroscopic limit model. In section 5, we discuss the probabilistic background of the meso-macro derivation and the last section is devoted to some conclusions.

5.2 Discrete derivation of Ruijgrok's and Wu's non-linear two velocity Boltzmann model [1]

5.2.1 Space discrete stochastic hopping model

We consider interacting particles which are spatially distributed over equally spaced cells $C(j) = [jh, (j+1)h[\subset \mathbb{R}$ of length h. Particles can move to the left and to the right with constant velocities $v^{\pm} = \pm 1$. We denote the number of particles in $C(j)$ with speed 1, resp., -1, at time t by $N_h^+(jh,t)$, resp., $N_h^-(jh,t)$.
The particles with speed 1 *migrate* from $C(j)$ to $C(j+1)$ and those with speed -1 from $C(j)$ to $C(j-1)$ both at rate $|v^{\pm}|/h = 1/h$. Other migration rates are zero. More precisely, we assume that for a time interval of length $\Delta t < h$ the (nonzero) migration probabilities are

[1] The presentation of this section follows closely section 1 of Rosenkrantz and Bings paper [126].

$$\begin{aligned}\tfrac{\Delta t}{h} + o(\Delta t) &= \text{probability that a single particle with speed 1 moves}\\ &\quad \text{within } \Delta t \text{ from } C(j) \text{ to } C(j+1)\\ &= \text{probability that a single particle with speed } -1 \text{ moves}\\ &\quad \text{within } \Delta t \text{ from } C(j) \text{ to } C(j-1),\end{aligned}$$

where $o(\Delta t)$ is a quantity verifying $\lim_{\Delta t \downarrow 0} o(\Delta t)/\Delta t = 0$. Without interaction, each particle travels on the set $\{C(j) \mid j \in \mathbb{Z}\}$, which we identify with

$$I_h = \{jh \in \mathbb{R} \mid 0, \pm 1, \pm 2, \dots\},$$

according to a continuous time Markov chain with infinitesimal generator matrix $Q_h^i = (Q_h^i(j,k))_{j,k\in\mathbb{Z}}$, $i = \pm$, given by

$$Q_h^-(j,k) = \begin{cases} 0 & \text{for } |j-k| > 1,\\ 0 & \text{for } k = j+1,\\ 1/h & \text{for } k = j-1,\\ -1/h & \text{for } j = k,\end{cases} \qquad Q_h^+(j,k) = \begin{cases} 0 & \text{for } |j-k| > 1,\\ 1/h & \text{for } k = j+1,\\ 0 & \text{for } k = j-1,\\ -1/h & \text{for } j = k.\end{cases}$$

The quantities $N_h^i(jh,t)$ satisfy the Kolmogorov forward equations:

$$\begin{cases} \partial_t N_h^-(jh,t) = \sum_k N_h^-(kh,t) Q_h^-(k,j) = A_h N_h^-(jh,t),\\ \partial_t N_h^+(jh,t) = \sum_k N_h^+(kh,t) Q_h^+(k,j) = -A_h N_h^+((j-1)h,t),\\ N_h^\pm(jh,0) \quad = \text{initial distribution of particles with speed } \pm 1,\end{cases} \tag{5.1}$$

where $A_h f(jh) := \frac{1}{h}[f(jh+h) - f(jh)]$ is the difference operator acting on the Banach space $X_h := \mathcal{C}_0(I_h)$ of all functions $f : I_h \to \mathbb{R}$ with $\lim_{|jh|\to\infty} f(jh) = 0$ and which is endowed with the sup norm $\|f\|_h := \sup_j |f(jh)|$.
In addition to the migration rules we assume that particles *react* as follows: in the small interval of time $[t, t+\Delta t[$ the number of particles in $C(j)$ with speed $+1$ increases due to spontaneous transitions of -1 particles in $C(j)$ to $+1$ particles at rate $\alpha > 0$ by the amount

$$\alpha N_h^-(jh,t)\Delta t + o(\Delta t) \tag{5.2}$$

and decreases by the amount

$$\beta N_h^+(jh,t)\Delta t + o(\Delta t) \tag{5.3}$$

due to spontaneous transitions of $+1$ particles in $C(j)$ to -1 particles at rate $\beta > 0$. Similarly, the number of particles in $C(j)$ with speed -1 decreases by the amount $\alpha N_h^-(jh,t)\Delta t + o(\Delta t)$ and increases by $\beta N_h^+(jh,t)\Delta t + o(\Delta t)$. Moreover, particles in $C(j)$ of different speeds can *collide*, thereby giving rise to -1 particles in $C(j)$. This collision rule decreases the number of $+1$ particles and increases the number of -1 particles in $C(j)$ according to

$$\frac{\mu}{h} N_h^-(jh,t) N_h^+(jh,t) \Delta t + o(\Delta t). \tag{5.4}$$

The term $\frac{\mu}{h}$ reflects the fact that the rate of interactions depends not only on the number of particles in each cell but also on its length; *i.e.*, the same number of particles crowded into an interval of smaller length will interact at a proportionally higher rate.
Denoting -1 particles by $(-)$ and $+1$ particles by $(+)$, the migration and the interaction (reaction and collision) mechanisms can be summarized as follows:

$$\begin{array}{ll} \text{migration: } (-) \longrightarrow C(j-1), & (+) \longrightarrow C(j+1), \\ \text{reaction: } \quad (-) \longrightarrow (+), & (+) \longrightarrow (-), \\ \text{collision: } \quad (+,-) \longrightarrow (-,-), & \end{array}$$

and the interactions are taken to be of mass action type. This means that the rate of each interaction is proportional to the concentration of each type of particle entering the interaction. Under this assumption and when $\Delta t \to 0$, the functions $N_h^{\pm}(jh,t)$ satisfy the nonlinear forward equation:

$$\begin{aligned} \partial_t N_h^-(jh,t) = &\quad A_h N_h^-(jh,t) - \alpha N_h^-(jh,t) + \beta N_h^+(jh,t) + \tfrac{\mu}{h} N_h^-(jh,t) N_h^+(jh,t), \\ \partial_t N_h^+(jh,t) = &-A_h N_h^+((j-1)h,t) + \alpha N_h^-(jh,t) - \beta N_h^+(jh,t) - \tfrac{\mu}{h} N_h^-(jh,t) N_h^+(jh,t), \\ N_h^{\pm}(jh,0) \;\; = &\quad g_h^{\pm}(jh), \end{aligned} \tag{5.5}$$

with $g_h^{\pm} \in X_h$ some given (positive) initial distribution of the interacting particles.
If, in addition, we assume the existence of functions $g^{\pm} \in \mathcal{C}_0^1(\mathbb{R})$ and $\rho^{\pm} \in \mathcal{C}_0^{2,1}(\mathbb{R} \times \mathbb{R}^+)$ satisfying for all $j \in \mathbb{Z}$ and all $h > 0$

$$g_h^{\pm}(jh) = g^{\pm}(jh) + o(h), \tag{5.6}$$

$$\frac{1}{h} N_h^{\pm}(jh,t) = \rho^{\pm}(jh,t), \tag{5.7}$$

then $\rho^-(x,t)$and $\rho^+(x,t)$ satisfy the nonlinear two-velocity Boltzmann equation of Ruijgrok and Wu introduced in [128]:

$$\begin{cases} \partial_t \rho^-(x,t) = A\rho^-(x,t) - \alpha\rho^-(x,t) + \beta\rho^+(x,t) + \mu\rho^-(x,t)\rho^+(x,t), \\ \partial_t \rho^+(x,t) = -A\rho^+(x,t) + \alpha\rho^-(x,t) - \beta\rho^+(x,t) - \mu\rho^-(x,t)\rho^+(x,t), \\ \rho^{\pm}(x,0) \quad = g^{\pm}(x), \end{cases} \tag{5.8}$$

where $A = \frac{\partial}{\partial_x}$ is the differential operator on the Banach space $X := \mathcal{C}_0(\mathbb{R})$ (endowed with the supremum norm $\|f\| := \sup_x |f(x)|$) with domain

$$\mathcal{D}(A) = \{f \in X \mid f \text{ absolutely continuous}, \; f' \in X\}. \tag{5.9}$$

The physical content of the system (5.8) is briefly stated in the remark section below. For the mathematical discussion of the explicit solutions which

we recall in the next paragraph, we refer to [128]. Our concern is to derive the "mesoscopic equations" (5.8) from the discrete equations (5.5) without assumption (5.7) by showing that for all $x \in \mathbb{R}$ and uniformly for t in compact subsets of $\mathbb{R}^+$ the limit

$$\lim_{h\searrow 0,\ jh\to x} \frac{1}{h} N_h^{\pm}(jh,t) \tag{5.10}$$

exists and that the pointwise defined functions

$$\rho^{\pm}(x,t) := \lim_{h\searrow 0,\ jh\to x} \frac{1}{h} N_h^{\pm}(jh,t) \tag{5.11}$$

solve equations (5.8). This is done in the next paragraph.

Remark.

The RW model (5.8) was originally motivated by practical considerations in connection with controlled thermonuclear fusion. The interesting feature for applications is that (5.8) can be solved explicitly for a large class of initial conditions in terms of modified Bessel functions. Consequently, shock waves and approach to equilibrium can be investigated analytically. In this chapter we extend the fields of applications to a nonlinear transport phenomenon encountered in vehicular traffic flow. At the proposed level of description, the main ingredients for nonlinearity in traffic flows come from a certain anisotropic collision behavior (a fast driver behind a slow one has to slow down or to overtake if he can). This is taken into account by the RW model. Indeed, it is seen from section 1 that there is one binary collision of the form $(+,-) \to (-,-)$. The presence of this collision mechanism, together with the absence of the inverse collision $(-,-) \to (+,-)$, means the violation of the detailed balance of momentum which is the mentioned desired anisotropic collision feature encountered in vehicular traffic flow.

5.2.2 Micro-meso link

Before we derive (5.11) recall that the RW model (5.8) can be linearized by means of the logarithmic transformation:

$$\begin{cases} \rho^+(x,t) = \frac{2}{\mu}(\partial_t - A)\Big(\ln\big(u(x,t)\big) + \frac{\beta+\alpha}{2}t - \frac{\beta-\alpha}{2}x\Big), \\ \rho^-(x,t) = -\frac{2}{\mu}(\partial_t + A)\Big(\ln\big(u(x,t)\big) + \frac{\beta+\alpha}{2}t + \frac{\beta-\alpha}{2}x\Big), \end{cases} \tag{5.12}$$

where the strictly positive function $u := u(x,t) > 0$ satisfies the hyperbolic equation:

$$\partial_t^2 u(x,t) = \big(A^2 + \alpha\beta I\big)u(x,t), \tag{5.13}$$

with I the identity operator. The above linear PDE, equivalent to the telegraphist equation, has to be solved with the initial conditions:

$$u^0(y) = u(y,0) = \exp\left\{\frac{1}{2}\int_{-\infty}^{y} [\mu(g^-(x) + g^+(x)) + \alpha - \beta]\mathrm{d}x\right\}, \quad (5.14)$$

$$u_t^0(y) = u_t(y,0) = \frac{1}{2}u(y,0)\big(\mu(g^-(y) - g^+(y)) + \beta + \alpha\big). \quad (5.15)$$

It is well known [53, Chap. 2.8] that the solution to the above Cauchy problem (5.13), (5.14), (5.15) is formally given by

$$u(x,t) := C(t)u^0(x) + \int_0^t C(s)u_t^0(x)\mathrm{d}s, \quad (5.16)$$

where $C(t)$ is the strongly continuous cosine operator function associated with the infinitesimal generator $B = A^2 + \alpha\beta I$ with domain

$$\mathcal{D}(B) := \{f \in X \mid C(\cdot)f \in \mathcal{C}^2(\mathbb{R}, X)\}. \quad (5.17)$$

The (strong) solution to (5.13) is explicitly given by (5.16) via the representation formula (see, e.g., [53, p. 121]):

$$C(t)f = \frac{1}{2}\big[T(t) + T(-t)\big]f + \frac{\alpha\beta}{2}t\int_0^t (t^2 - s^2)^{-1/2} I_1\big((t^2 - s^2)^{1/2}\big)\big[T(t) + T(-t)\big]f\mathrm{d}s \quad (5.18)$$

for $f \in X$. Therein I_1 is the modified Bessel function, and $T = \{T(t) \mid t \in \mathbb{R}\}$ is the $(\mathcal{C}_0)$ group of isometries on X associated with the generator $A = \frac{\partial}{\partial_x}$ given by

$$\big[T(t)f\big](x) = f(x + t). \quad (5.19)$$

The fact that the (strong) solution to (5.13) is given by a strongly continuous cosine operator function $C(t)$ gives us—besides existence, uniqueness, and continuous dependence on the initial data—the continuous dependence on A. It is this bonus—exploited in a version of the Trotter–Kato approximation theorem [89]—together with the obvious regularity properties of the explicit solution (5.16) which enables the rigorous derivation of the limit (5.11). To this end we rewrite (5.12) as an abstract inhomogeneous Cauchy problem in the Banach space

$$Y := X \times X = \mathcal{C}_0(\mathbb{R}) \times \mathcal{C}_0(\mathbb{R}),$$

equipped with the norm $\|(f_1, f_2)\| = \|f_1\| + \|f_2\|$ and set

$$\rho(x,t) := \big(\rho^-(x,t), \rho^+(x,t)\big), \quad (5.20)$$

$$\dot{\rho}(t) := \big(\partial_t\rho^-(x,t), \partial_t\rho^+(x,t)\big), \quad (5.21)$$

$$F\big(\rho(x,t)\big) := \big(-\alpha\rho^-(x,t) + \beta\rho^+(x,t) + \mu\rho^-(x,t)\rho^+(x,t), \quad (5.22)$$
$$\alpha\rho^-(x,t) - \beta\rho^+(x,t) - \mu\rho^-(x,t)\rho^+(x,t)\big),$$

$$\mathbf{A}\rho(x,t) := \big(A\rho^-(x,t), -A\rho^+(x,t)\big). \quad (5.23)$$

Clearly, $F(Y) \subset Y$, but F is otherwise nonlinear and unbounded. An elementary estimation for arbitrary $\rho, \xi \in Y$ yields

$$\|F\big(\rho(x,t)\big) - F\big(\xi(x,t)\big)\| \le \big(2\max(\beta,\alpha) + 2\mu\max(\|\xi^+\|,\|\rho^-\|)\big)\|\rho-\xi\|, \tag{5.24}$$

establishing that F is locally Lipschitz continuous in the sense that for all ρ, ξ in the set $\{\rho \in Y \mid \|\rho\| \le M\}$, where $M > 0$ is fixed, we have

$$\|F\big(\rho(x,t)\big) - F\big(\xi(x,t)\big)\| \le \big(2\max(\beta,\alpha) + 2\mu M\big)\|\rho-\xi\| =: \tilde{M}\|\rho-\xi\|. \tag{5.25}$$

Using this notation, (5.12) takes the form of an abstract semi-linear Cauchy problem, namely,

$$\dot{\rho}(t) = \mathbf{A}\rho(t) + F\big(\rho(t)\big), \tag{5.26}$$

$$\rho(0) = g(0) = \big(g^-, g^+\big). \tag{5.27}$$

It is clear from (5.12), (5.16), and the representation formula (5.18) that the initial value problem (5.26), (5.27) has a strong solution $\rho \in \mathcal{D}(A) \times \mathcal{D}(A)$ whenever g^- and g^+ are sufficiently regular; typically, $g^\pm \in \mathcal{C}^2(\mathbb{R})$. Indeed, using the representation formula (5.18) it is immediate to check that for all fixed $T > 0$ the following implications hold:

$$(g^-, g^+) \in \mathcal{C}^2(\mathbb{R}) \times \mathcal{C}^2(\mathbb{R}) \Rightarrow (\rho^-(t), \rho^+(t)) \in \mathcal{C}^1(\mathbb{R}) \times \mathcal{C}^1(\mathbb{R}), \quad t \in [0,T],$$
$$\text{and} \quad \sup_{0\le t\le T} \left| \frac{\partial \rho^\pm(x,t)}{\partial x} \right| < \infty. \tag{5.28}$$

Clearly, the strong solution u is also a mild one; i.e., u is continuous and satisfies the integral equation (see, e.g., [116, p. 183]):

$$\rho(t) = G(t)\rho(0) + \int_0^t G(t-s)F(\rho(s))\mathrm{d}s, \tag{5.29}$$

where the (C_0) contraction semigroup $G(t)$ is given by

$$G(t)\big(f_1(x), f_2(x)\big) = \big(T(t)f_1(x), T(t)f_2(x)\big) = \big(f_1(x+t), f_2(x+t)\big).$$

Similarly, the space discrete RW model eqs.(5.5) takes the form

$$\dot{\rho}_h(t) = \mathbf{A}_h\rho_h(t) + F\big(\rho_h(t)\big), \tag{5.30}$$

$$\rho_h(0) = g_h(0), \tag{5.31}$$

where

$$\rho_h(jh,t) := \big(h^{-1}N_h^-(jh,t), h^{-1}N_h^+(jh,t)\big),$$
$$\mathbf{A}_h\rho_h(t) := \big(A_h h^{-1}N_h^-(jh,t), -A_h h^{-1}N_h^+(jh,t)\big).$$

Note that the Cauchy problem (5.30), (5.31) has to be solved in the Banach space

$$Y_h := X_h \times X_h = \mathcal{C}_0(I_h) \times \mathcal{C}_0(I_h),$$

equipped with the norm $\|(f_1,f_2)\|_h = \|f_1\|_h + \|f_2\|_h$. The existence of a unique mild solution ρ_h of (5.30), (5.31) (defined on some maximal interval $[0, T[$,

where $T = T(\tilde{M}, g^{\pm}))$ relies on the local Lipschitz property established in (5.25) (see, e.g., Theorem 1.4 in [116]). For $t \in [0, T[$ this solution satisfies

$$\rho_h(t) = G_h(t)\rho_h(0) + \int_0^t G_h(t-s)F(\rho_h(s))\mathrm{d}s, \tag{5.32}$$

where $G_h(t)$ is the (C_0) contraction semigroup on Y_h given by

$$G_h(t)\big(f_1(jh), f_2(jh)\big) = \big(T_h(t)f_1(jh), T_h(t)f_2(jh)\big).$$

Here $T_h(t) = \exp(tA_h)$ means the (C_0) contraction semigroup generated by the finite difference operator A_h (with domain $\mathcal{D}(A_h) = X_h$) explicitly given by (see, e.g., [53, p. 23])

$$T_h(t)f(j) = e^{-t/h}\sum_{k=0}^{\infty}\frac{(t/h)^k}{k!}f(j+hk). \tag{5.33}$$

Following [126] we define the bounded linear mappings

$$\begin{aligned} P_h : Y &\to Y_h, \\ (\rho^-, \rho^+) &\mapsto P_h(\rho^-, \rho^+) : \mathbb{R} \to \mathbb{R}\times\mathbb{R}, \\ &\qquad x \mapsto (\rho^-(jh), \rho^+(jh)) \ \text{ for } \ jh \le x < (j+1)h \end{aligned}$$

joining the evident properties:

(1) $\|P_h f\|_h \le \|f\|$;
(2) $\lim_{h\to 0}\|P_h f\|_h = \|f\|$;
(3) for any $f_h \in Y_h$ there exists a $f \in Y$ such that $f_h = P_h f$ and $\|f_h\|_h \le \|f\|$.

It follows (by definition) that the sequence of Banach spaces Y_h with the sequence of bounded linear maps P_h approximate the Banach space Y for $h \to 0$.
The convergence of the "linear" part $G_h(t)\rho_h(0)$ of ρ_h given in the integral representation (5.32) to $G(t)\rho(0)$ follows from a variant of the Trotter–Kato approximation theorem due to Kurtz (see, e.g., [127, Thm. 2.6]). The theorem ensures that for every fixed $s \in [0, \infty[$ and for every $\rho \in \mathcal{D}(A)\times\mathcal{D}(A) \subset \mathcal{C}_0^2(\mathbb{R})\times\mathcal{C}_0^2(\mathbb{R})$ we have

$$\lim_{h\searrow 0}\sup_{0\le t\le s}\|G_h(t)P_h\rho - P_h G(t)\rho\|_h = 0. \tag{5.34}$$

In particular, for the initial condition $\rho(0)$ we have

$$P_h G(t)\rho(0) = G_h(t)P_h\rho(0) + o(h). \tag{5.35}$$

To treat the inhomogeneous part within the time horizon $T > 0$, we apply P_h to the integral representation (5.29) and use (5.35) to obtain

$$
\begin{aligned}
P_h\rho(t) &= P_hG(t)\rho(0) + \int_0^t P_hG(t-s)F(\rho(s))\mathrm{d}s \qquad (5.36)\\
&= G_h(t)P_h\rho(0) + o(h) + \int_0^t \big(G_h(t-s)P_hF(\rho(s)) + o(h)\big)\mathrm{d}s\\
&= G_h(t)P_h\rho(0) + \int_0^t G_h(t-s)F(P_h\rho(s))\mathrm{d}s + o(h)
\end{aligned}
$$

for $t \in [0,T]$. Therefore,

$$
\begin{aligned}
P_h\rho(t) - \rho_h(t) &= G_h(t)\big(P_h\rho(0) - \rho_h(0)\big) + o(h) \qquad (5.37)\\
&\quad + \int_0^t G_h(t-s)\big(F(P_h\rho(s)) - F(\rho_h(s))\big)\mathrm{d}s.
\end{aligned}
$$

Set

$$\phi_h(t) := \|P_h\rho(t) - \rho_h(t)\|_h \qquad (5.38)$$

and note that by assumption (5.6) we have

$$\phi_h(0) = o(h). \qquad (5.39)$$

Applying the local Lipschitz property established in (5.25) and using the fact that $\|G_h(t)f\|_h \le \|f\|_h$ one concludes on the existence of a constant K depending on T (and M) such that

$$\phi_h(t) \le Kh + K\int_0^t \phi_h(s)\mathrm{d}s. \qquad (5.40)$$

Using Gronwall's inequality, the above directly implies that $\phi_h(t) \le Kh\exp(Kt)$ for $t \in [0,T]$, and therefore

$$\lim_{h\searrow 0}\phi_h(t) = \lim_{h\searrow 0}\|P_h\rho(t) - \rho_h(t)\|_h = 0 \ \text{ for } \ t \in [0,T], \qquad (5.41)$$

which proves (5.10) and (5.11).
To conclude this technical section we resume that the proof establishes the convergence of a space-discrete hopping model including migration, reaction and collision mechanisms to the nonlinear two-velocity Boltzmann model of Ruijgrok and Wu. The next paragraph aims to apply this convergence to car traffic modelling.

5.3 Application to Traffic modelling

A traffic system composed of drivers, vehicles, and roadways, exhibits extremely complex behavior including congestion formation, stop-and-go traffic, and hysteresis due to the heterogeneous drivers' behavior, the highly nonlinear group dynamics, and large system dimensions. Traffic theory proposes mathematical descriptions of the processes in order to understand the dynamics of traffic flow. Two complementary approaches have dominated traffic-flow modelling:

(i) a purely *microscopic* approach in which the individual vehicular interactions are taken into account (see [1, 105] and the references therein) and
(ii) a *macroscopic* approach which is based on fluid dynamical equations describing the behavior of a compressible fluid (see [64, 95, 115] and the references therein).

Even within the microscopic approach there are different types of mathematical descriptions. The so-called car-following theory, for example, provides a deterministic, Newton-like description of the motion of individual vehicles. In contrast, particle hopping modelling and stochastic microscopic modelling describe traffic in terms of the stochastic dynamics of individual vehicles and will be the point of view adopted in this application.
The macroscopic description is always based on a continuity equation,

$$\partial_t \rho(x,t) + \partial_x J(x,t) = 0, \tag{5.42}$$

and completed by a relation between the current $J(x,t)$ and the vehicle density $\rho(x,t)$, which is known in traffic engineering as the *fundamental diagram*. This relation contains all the dynamic information specific to a particular macroscopic model. Among the various fundamental diagrams which have been explored, a very simple and popular one is the Lighthill–Whitham (LW) equation [95], assuming that there exists an equilibrium flow-density relationship of the form

$$J(x,t) = j(\rho(x,t)) - D\partial_x \rho(x,t), \tag{5.43}$$

where $D > 0$ is a diffusion constant. Moreover, on the basis of experimental observations, Greenshields [55] proposed the choice

$$j(\rho(x,t)) = V_{\max}\rho(x,t)\big(1 - \rho(x,t)\big), \tag{5.44}$$

where the phenomenological parameter $V_{\max}$ is the maximum average speed for $\rho \to 0$. Eq.(5.43) together with Eq.(5.44) is known as the *improved Greenshields traffic model*.
For $D \to 0$, the nonlinear model can explain the formations of shock waves which correspond to congestion formation in traffic flow [95]. Indeed, the improved Greenshields model together with Eq. (5.42) is reduced, via the linear transformation $(x,t) \mapsto (y,\tau) := (x - V_{\max}t, t)$, to

$$\partial_\tau \rho(y,\tau) - 2V_{\max}\rho(y,\tau)\partial_y \rho(y,\tau) = D\partial_y^2 \rho(y,\tau) \tag{5.45}$$

which is directly recognized as the viscous form of the famous Burgers' equation. For $D \to 0$, solutions to the above equation, specified by some initial condition ρ_0, are known to develop discontinuities in finite time even in case the initial data ρ_0 is smooth.
Despite this success in describing congestion formation in traffic flow the LW theory fails in describing more complicated traffic-flow phenomena such as

stop-and-go traffic or hysteresis (see, e.g., [87]). This is due to the unrealistic assumption that the traffic flow is always in equilibrium. In reality, the dynamics is a result of the retarded response of drivers to various (mostly) frontal stimuli [93]. Among different non-equilibrium models [115, 93, 64] we propose here (see also [39]) the exactly solvable two-velocity RW model (5.8) which takes into account acceleration behavior and anisotropic interactions of vehicles with different speeds in the most simple manner. Despite its simplicity, it will be remarked below that the RW model can partially explain hysteresis and we will show in the next section that the model relaxes in a diffusive limit to the improved Greenshields traffic model. This meso-macro link explains the importance of the empirical density-flux relation (5.44) and, reciprocally, corroborates the relevance of the RW model in traffic theoretical contexts.

Remark.

The RW model shows the signature of hysteretic behavior for a specific range of parameters. Indeed, for $\alpha > \beta$ there exists a class of spatially inhomogeneous equilibrium distributions of the RW model eqs. (5.8) indexed by two continuous real parameters $x_0 \in \mathbb{R}$ and C, $0 \leq C \leq (\sqrt{\alpha} - \sqrt{\beta})^2$, given by (see [128, sect. 5]):

$$\rho^+(x) = \frac{\mu C + \alpha - \beta}{2\mu} + \frac{r}{2\mu} \tanh((x - x_0)r/2),$$
$$\rho^-(x) = \frac{-\mu C + \alpha - \beta}{2\mu} + \frac{r}{2\mu} \tanh((x - x_0)r/2),$$

with r depending on the parameters α, β, μ, and C only. The parameter C corresponds to the equilibrium flow $C = \rho^+(x) - \rho^-(x)$ and is determined by the initial conditions $g^\pm$ given in (5.8). The equilibrium density ρ at x_0 is simply $\rho(x_0) = \rho^+(x_0) + \rho^+(x_0) = \frac{\alpha-\beta}{\mu}$ and hence independent of the flow C. Therefore, without changing the equilibrium density $\rho(x_0)$, different initial conditions lead to different equilibrium flow states at x_0 which is a typical signature for hysteresis (see e.g., [1, p. 264]).

Let us now apply the limit result of section 2 in order to realize the micro-meso link. We start with the description of the stochastic microscopic model (i.e., the particle hopping model).

We observe cars on a long highway without on/off ramps. We further suppose that at any instant of time t the heterogeneous drivers' behavior can be classified into "slow" resp., "fast" drivers corresponding to cars with speed v_1 (slow) resp. cars with speed v_2 (fast). Informally, the basic modelling assumptions are the following:

(A1) The fairly diverse driving habits of the people are modelled by spontaneous (Markovian) transitions from one behavior to the other.

(A2) The interactions are typically short ranged in the sense that only consecutive cars (with different speeds) can interact. The rate of interactions

within a short region is proportional to the number of drivers of each type in this region.

(A3) The anisotropic character of traffic flow is taken into account by saying that vehicles from behind should not influence the actions of their leading vehicles.

(A1) implies transitions of the form $v_1 \to v_2$ and $v_2 \to v_1$. (A2), together with (A3), states that (only) consecutive cars can interact in the following way, $(v_2, v_1) \to (v_1, v_1)$, or $(v_1, v_2) \to (v_2, v_2)$, where (x, y) means an ordered couple of consecutive cars with velocities x and y, respectively. The former interaction is quite natural for highway traffic, saying that a fast car behind a slow one has to slow down (or to overtake if it can). The latter interaction is somewhat special (nevertheless not completely lacking in real traffic), and we will neglect it. Hence we extend the assumptions by the following:

(A4) Slow cars behind fast ones do not interact.

With assumptions (A1)–(A4), which form our stochastic microscopic traffic model, we are able to apply the convergence result of section 2. Indeed, describing the cars in a moving framework which links the coordinates to the center of inertia,

$$(x,t) \mapsto (y,\tau) := \Big(x - \frac{v_1+v_2}{2}t, t\Big), \tag{5.46}$$

the velocities of the vehicles are transformed as

$$v_1 \mapsto -v_0, \quad v_2 \mapsto v_0, \tag{5.47}$$

where $v_0 := (v_2 - v_1)/2$. Partitioning the y-axes into equally spaced cells $C(j) = [jh, (j+1)h[$ of length h we see that in the moving coordinates cars migrate from $C(j)$ to $C(j-1)$ or $C(j+1)$ at the rate v_0/h.
(A1) implies that within a time interval $[t, t+\Delta t[$ the number of particles $N_h^+(jh,t)$ (resp., $N_h^-(jh,t)$) in $C(j)$ with speed v_0 (resp., $-v_0$) at time t increases by an amount proportional to $N_h^-(jh,t)\Delta t + o(\Delta t)$ (resp., $N_h^+(jh,t)\Delta t + o(\Delta t)$) and decreases by an amount proportional to $N_h^+(jh,t)\Delta t + o(\Delta t)$ (resp., $N_h^-(jh,t)\Delta t + o(\Delta t)$).
From (A2)–(A4) we infer the local collision rule $(v_0, -v_0) \to (-v_0, -v_0)$. By the second part of assumption (A2), this will increase (decrease) the number of slow (fast) cars within the time interval $[t, t+\Delta t[$ by the amount

$$\frac{\mu}{h} N_h^+(jh,t) N_h^-(jh,t)\Delta t + o(\Delta t).$$

Hence, using the convergence result of section 2, we see that under the stochastic microscopic assumptions (A1)–(A4), the resulting mesoscopic description of the cars in traffic is given by the RW model:

$$\begin{cases} \partial_t \rho^-(x,t) - v_0 \rho_x^-(x,t) = -\alpha \rho^-(x,t) + \beta \rho^+(x,t) + \mu \rho^-(x,t)\rho^+(x,t), \\ \partial_t \rho^+(x,t) + v_0 \rho_x^+(x,t) = +\alpha \rho^-(x,t) - \beta \rho^+(x,t) - \mu \rho^-(x,t)\rho^+(x,t). \end{cases} \tag{5.48}$$

It describes in a moving coordinate system the evolution of the distribution functions of fast cars ρ^+ and slow cars ρ^-. An explicit solution of the traffic density $\rho = \rho^- + \rho^+$ is sketched in Figure 5.1. The initial conditions reflect a situation where a platoon of fast cars is behind a platoon of slow cars. When the fast cars catch up with the slow ones the collision mechanism $(+,-) \longrightarrow (-,-)$ increases (decreases) the concentration of slow (fast) cars, and only a few fast cars pass the train of slow cars without undergoing collisions.

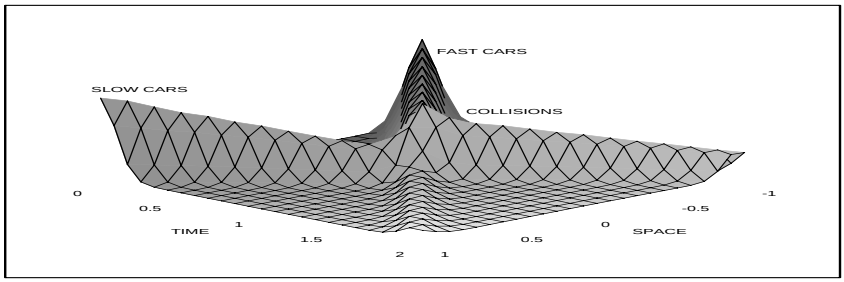

Fig. 5.1. Sketch of the density profiles in a moving coordinate system for Gaussian initial conditions. When the platoons meet (fast cars catch up with the slow ones), the collision term will become important and decrease the amount of fast cars and increase the amount of slow cars. The parameters are $\alpha = 50$, $\beta = 10$, $\mu = 80$, and $v_0 = 1$.

5.4 The Mesoscopic derivation of Greenshields fundamental diagram

In this section we show that the RW model relaxes in a diffusive limit to the improved Greenshields model. We indeed derive Greenshields flux relation Eq. (5.44) starting from the mesoscopic RW model. This completes together with the above microscopic description the micro-meso-macro link.

To underline the applicability of the two-velocities model to arbitrary speeds (not only $\pm v_0$) let us rewrite the one-dimensional, nonlinear RW model Eq. (5.48) in the form:

$$\begin{cases} (\partial_t + v_1 \partial_x)\hat{\rho}^- = \mu \hat{\rho}^- \hat{\rho}^+ - \alpha \hat{\rho}^- + \beta \hat{\rho}^+ \\ (\partial_t + v_2 \partial_x)\hat{\rho}^+ = -\mu \hat{\rho}^- \hat{\rho}^+ + \alpha \hat{\rho}^- - \beta \hat{\rho}^+, \end{cases} \tag{5.49}$$

where $(x,t) \in \mathbb{R} \times \mathbb{R}^+$, $\hat{\rho}^- := \hat{\rho}^-(x,t)$ and $\hat{\rho}^+ := \hat{\rho}^+(x,t)$ are the distribution functions of vehicles with velocities v_1 and v_2 respectively and where α, β and μ are positive constants. As clear from the microscopic derivation, the model takes into account three velocity exchange mechanisms contained on the right hand side of Eqs. (5.49), namely:

(a) a binary collision of the form $(v_1, v_2) \xrightarrow{\mu} (v_1, v_1)$, modelling a transition from (v_1, v_2) to (v_1, v_1) with intensity μ,
(b) a spontaneous transition of the form $(v_1) \xrightarrow{\alpha} (v_2)$, with transition rate α, and
(c) a spontaneous transition of the form $(v_2) \xrightarrow{\beta} (v_1)$, with transition rate β.

Recall from the microscopic model that the absence of the inverse collision of type (a) indicates violation of the detailed balance, which is an intrinsic feature of vehicular traffic [29].
Suppose now (without loss of generality) that $v_1 = -v_2 =: \gamma$ and that the densities are given by a logarithmic transformation of the form:

$$\begin{cases} \hat{\rho}^-(x,t) = \frac{1}{\mu}(\partial_t + \gamma\partial_x)\Big(\ln\big(u(x,t)\big) + ax + bt\Big) \\ \hat{\rho}^+(x,t) = -\frac{1}{\mu}(\partial_t - \gamma\partial_x)\Big(\ln\big(u(x,t)\big) + ax + bt\Big) \end{cases} \tag{5.50}$$

for a strictly positive function $u := u(x,t) > 0$ and two constants a and b.
With these assumptions Eqs. (5.49) simplify to the linear hyperbolic PDE

$$\partial_t^2 u + (\alpha+\beta+2b)\partial_t u = \gamma^2\partial_x^2 u + \gamma\big(\alpha-\beta+2\gamma a\big)\partial_x u + u\cdot\big((\gamma a)^2 + \gamma a(\alpha-\beta) - b^2 - b(\alpha+\beta)\big). \tag{5.51}$$

By the ad-hoc choice of the constants $a := \frac{\beta-\alpha}{2\gamma}$ and $b := -\frac{\alpha+\beta}{2} + \sqrt{\frac{\alpha^2+\beta^2}{2}}$, Eq. (5.51) reduces to the famous telegraphist equation:

$$\partial_t^2 u + \sqrt{2(\alpha^2+\beta^2)}\partial_t u = \gamma^2\partial_x^2 u. \tag{5.52}$$

The logarithmic transform (L-T) which reduces the non-linear Eqs. (5.49) to the linear telegraphist equation (5.52) plays a role similar to the well-known Hopf-Cole transformation (H-C), reducing the Burgers' equation to the (linear) heat equation. This observation, thoroughly discussed in [70], and the central role of the Burgers' equation in traffic modelling (see e.g. [29]), leads us to emphasize the importance of the RW-model in the traffic context.

5.4.1 Derivation of Greenshields' Model

Let us now show how the Greenshields' flux relation:

$$J(x,t) = V_{\max} \cdot \rho(x,t)(1 - \rho(x,t)) - D\partial_x\rho(x,t) \tag{5.53}$$

can be mesoscopically derived. To this aim we link as in section 3 the car coordinates to the center of inertia:

$$\big(x,t\big) \mapsto \Big(x - \bar{v}t, t\Big), \;\; \bar{v} := \frac{v_1 + v_2}{2}. \tag{5.54}$$

In this coordinates, the velocities of the vehicles are transformed as

$$v_1 \mapsto -v_0, \;\; v_2 \mapsto v_0, \tag{5.55}$$

where

$$v_0 := \frac{v_2 - v_1}{2}. \tag{5.56}$$

The second step is a diffusive re-scaling of the coordinates of the form

$$y := c(x - \bar{v}t), \;\; \tau := c^2 t, \tag{5.57}$$

which is accompanied by the normalization transformation

$$\hat{\rho}^- \mapsto \rho^- := \hat{\rho}^-/c, \tag{5.58}$$

$$\hat{\rho}^+ \mapsto \rho^+ := \hat{\rho}^+/c, \tag{5.59}$$

where c is a dimensionless scaling parameter. The diffusive limit $c \to 0$ (see e.g., [143]) corresponds to the transition from a kinetic to a macroscopic description of the traffic. With the coordinates given by (5.55) and the diffusive re-scaling (5.57), (5.59), the system (5.49) reads:

$$\begin{cases} (\partial_\tau - \frac{v_0}{c}\partial_y)\rho^- = \frac{\mu}{c}\rho^-\rho^+ - \frac{\alpha}{c^2}\rho^- + \frac{\beta}{c^2}\rho^+ \\ (\partial_\tau + \frac{v_0}{c}\partial_y)\rho^+ = -\frac{\mu}{c}\rho^-\rho^+ + \frac{\alpha}{c^2}\rho^- - \frac{\beta}{c^2}\rho^+. \end{cases} \tag{5.60}$$

The macroscopic variables for the system (5.60) are the vehicle density $\rho := \rho(y,\tau)$ and the flux $J := J(y,\tau)$ respectively given by:

$$\begin{aligned} \rho(y,\tau) &= \rho^-\big(x(y,\tau),t(y,\tau)\big) + \rho^+\big(x(y,\tau),t(y,\tau)\big) \\ &= \tfrac{1}{c}\Big(\hat{\rho}^-\big(x(y,\tau),t(y,\tau)\big) + \hat{\rho}^+\big(x(y,\tau),t(y,\tau)\big)\Big), \end{aligned} \tag{5.61}$$

$$\begin{aligned} J(y,\tau) &= \tfrac{v_0}{c}\Big(\rho^+\big(x(y,\tau),t(y,\tau)\big) - \rho^-\big(x(y,\tau),t(y,\tau)\big)\Big) \\ &= \tfrac{v_0}{c^2}\Big(\hat{\rho}^+\big(x(y,\tau),t(y,\tau)\big) - \hat{\rho}^-\big(x(y,\tau),t(y,\tau)\big)\Big). \end{aligned} \tag{5.62}$$

By addition of both equations in (5.60), we immediately have the continuity equation

$$\partial_\tau \rho + \partial_y J = 0. \tag{5.63}$$

From Eqs. (5.61) and (5.62), we have:

$$\begin{cases} \rho^- = \frac{1}{2v_0}\big(v_0\rho - cJ\big) \\ \rho^+ = \frac{1}{2v_0}\big(v_0\rho + cJ\big). \end{cases} \tag{5.64}$$

Introducing the linear combination of the two equations in the system (5.60):

$$-v_0\cdot(\partial_\tau-\frac{v_0}{c}\partial_y)\rho^-+v_0\cdot(\partial_\tau+\frac{v_0}{c}\partial_y)\rho^+ = 2v_0\Big(-\frac{\mu}{c}\rho^-\rho^+ + \frac{\alpha}{c^2}\rho^- - \frac{\beta}{c^2}\rho^+\Big) \quad (5.65)$$

and performing a few elementary manipulations of Eqs. (5.64), we end up with:

$$\frac{c^2}{v_0^2}\partial_\tau J + \partial_y\rho = \rho\Big(\frac{\alpha-\beta}{cv_0} - \frac{\mu}{2v_0}\rho\Big) + J\Big(\frac{\mu c^2}{2v_0^3}J - \frac{\alpha+\beta}{v_0^2}\Big). \quad (5.66)$$

To explicitly connect the RW-model with Greenshields equation (5.53) we introduce the relation:

$$\alpha = \beta + \frac{\mu}{2}c, \quad (5.67)$$

and the definitions

$$D := \frac{v_0^2}{\alpha+\beta}, \;\; V_{\max} := \frac{\mu}{2(\alpha+\beta)}v_0. \quad (5.68)$$

With these definitions which we discuss below, Eq. (5.66) reduces in the diffusive limit, $c \to 0$, to Greenshields' flux relation:

$$J = V_{\max}\cdot\rho(1-\rho) - D\partial_y\rho. \quad (5.69)$$

5.4.2 Discussion

At this point, it is worth-while to comment the physical content of Eq. (5.67). First we see from the fact that the collisions $(v_1, v_2) \xrightarrow{\mu} (v_1, v_1)$ steadily increases the density of particles having velocity v_1, the only possibility to reach an equilibrium is to have a transition imbalance $\alpha > \beta$. The derivation of (5.67) shows that for an equilibrium to exist, the difference of transition rats $\alpha - \beta$ should read as $c\mu/2$. Note that the constant D as given in (5.68) is consistent with the diffusion constant $\overline{D}$ of the telegraphist equation. In fact, when replacing in (5.52) α by $\frac{\alpha}{c^2}$, β by $\frac{\beta}{c^2}$, and γ by $\frac{v_0}{c}$ one finds the telegraphist equation associated to (5.60):

$$\partial_t u = \underbrace{\frac{v_0^2}{\sqrt{2(\alpha^2+\beta^2)}}}_{=:\overline{D}}\partial_x^2 u - \frac{c^2}{\sqrt{2(\alpha^2+\beta^2)}}\partial_t^2 u, \quad (5.70)$$

and using (5.67), we see that $\lim_{c\to 0}\overline{D} = \lim_{c\to 0} D = v_o^2/(2\alpha)$.
Let us now also examine the diffusive limit $c \to 0$. For this, consider the piecewise deterministic process solving the stochastic differential equation:

$$\mathrm{d}X_\gamma(t) := \gamma I(\gamma^2 t)\mathrm{d}t \quad (5.71)$$

where $\gamma := \frac{v_0}{c}$ and $\gamma I(\gamma^2 t)$ is a random telegraph process (i.e. a continuous time two states Markov chain) which takes on values in $\{-\gamma, +\gamma\}$ and whose transition rate is given by $\sqrt{2(\alpha^2+\beta^2)}/(2c^2)$. The Master equation that can be associated with the Markov process $\big(X_\gamma(t), \gamma I(\gamma^2 t)\big)$ has the form

$$\frac{\mathrm{d}T_t\phi}{\mathrm{d}t} = GT_t\phi, \tag{5.72}$$

where the operator T_t is the stochastic semigroup associated with the Markov process $\big(X_\gamma(t), \gamma I(\gamma^2 t)\big)$ acting on locally bounded and measurable functions ϕ defined on $\mathbb{R} \times \{-\gamma, \gamma\}$. It is defined as

$$T_t\phi(x,y) = \mathbb{E}_{x,y}\big[\phi\big(X_\gamma(t), \gamma I(\gamma^2 t)\big)\big], \;\; (x,y) \in \mathbb{R} \times \{-\gamma, \gamma\}, \tag{5.73}$$

where $\mathbb{E}_{x,y}$ is the expectation conditioned on the initial values $\big(X_\gamma(0), \gamma I(0)\big) = (x,y)$. The infinitesimal generator $G = \frac{\mathrm{d}T_t}{\mathrm{d}t}\big|_{t=0}$ of the semigroup T_t is given by:

$$G = \begin{pmatrix} -\gamma\partial_x & 0 \\ 0 & \gamma\partial_x \end{pmatrix} + \sqrt{2(\alpha^2+\beta^2)}/(2c^2) \begin{pmatrix} -1 & 1 \\ 1 & -1 \end{pmatrix}. \tag{5.74}$$

These facts discussed in [117], can be used to determine the system of backward equations describing the Markov process which reads:

$$\frac{\partial}{\partial_t} \begin{pmatrix} u_-(x,t) \\ u_+(x,t) \end{pmatrix} = G \begin{pmatrix} u_-(x,t) \\ u_+(x,t) \end{pmatrix} \tag{5.75}$$

where $u_-(x,t) := T_t\phi(x,-\gamma)$ and $u_+(x,t) := T_t\phi(x,\gamma)$ for ϕ of class $\mathcal{C}^1$. Applying the operators ∂_x, ∂_t to (5.75), it is seen that both field components u_- and u_+ satisfy the telegraphist equation (5.70). This probabilistic connection between Eq.(5.70) and stochastic processes was first noticed by [54] and [82]. Due to the central limit theorem (CLT), the random telegraph process defined in (5.71) converges for $c \to 0$ to a Gaussian white noise and in this limit we can write (5.71) as:

$$\mathrm{d}X_t := \sqrt{D}\mathrm{d}W_t \tag{5.76}$$

with W_t being the standard Brownian motion (see e.g., [48] p. 210).
The Chapman-Kolmogorov equation associated with the process (5.76) is the heat equation. Moreover, both the heat equation and the telegraphist equation are equivalent, up to nonlinear transformations (L-T) and (H-C), to the

Burgers' and the RW-model equations, respectively. This yields the global picture given in the following table:

RW-model	$\stackrel{L-T}{\longrightarrow}$	Telegraphist equation	$\longleftrightarrow$	telegraph process
$\downarrow$		$\downarrow c \to 0$		$\downarrow$ CLT
Burgers' equation	$\stackrel{H-C}{\longrightarrow}$	Heat equation	$\longleftrightarrow$	white noise

The previous analysis clearly shows that the improved Greenshields' model Eq. (5.44) follows from the mesoscopic model of vehicular traffic given in Eqs. (5.60) and can be understood from a central limit procedure.

5.5 Application to serial production lines

The analogy between traffic and production flows discussed in Chapter 3 directly suggests to apply the multi-scale analysis to production lines composed of N machines $M_1, ..., M_N$, N large, which are coupled in series through $N-1$ buffers. It is known that from a practical point of view, it is not reasonable to conceive very long production lines as both, throughput and controllability of the process decreases with N [76]. The multi-scale analysis indicates that we have to add to these inconveniences another one namely, the fact that long lines are very likely to produce unsteady flow dynamics. To make use of the microscopic hopping model we look at machines as being ordered spots (particles) moving on the real line $\mathbb{R}$ with speed -1 when operational (and not blocked by a non-moving spot) and with speed 0 otherwise. Spots can not overtake and hence, conserve their initial ordering. The content of the buffer separating two adjacent machines is proportional to the euclidian distance D of the associated consecutive spots on the line. In particular, an empty buffer (say B_{k-1}) will correspond to two superposed spots (*i.e.*, $D(M_k, M_{k-1}) = 0$). Accordingly, the initial condition reflecting empty buffers corresponds to N spots located all together at some point x_0, say $x_0 = 0$. The evolution of the distance between consecutive spots encodes the evolution of the corresponding buffer contents. The work in process is proportional to the spread of the two extremal spots M_1 and M_N and the throughput of the line corresponds to the evolution of M_N.
Let us subdivide $\mathbb{R}$ into predefined cells $C_j \in \mathbb{Z}$ of length h (see figure 5.2). The space continuous evolution of the ordered spots is now approached by a space-discrete hopping dynamic. It consists of N spots which can, during some small time window, either jump from one cell C_i to C_{i-1} (if the internal state is -1 ="on") or stay in the cell C_i (if the internal state is 0 ="of"). The internal state thereby changes according to a two-state Markov process. In analogy to the traffic application discussed in section 3, we suppose now

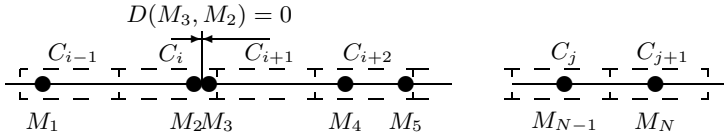

Fig. 5.2. The black spots on $\mathbb{R}$ are identified with machines that can move along the line with speed -1 when operational (and not blocked by a non-moving spot) and with speed 0 otherwise. This evolution is replaced by a simpler mean field hopping events dynamics, saying that spots in the "up" state can jump from cell C_i to C_{i-1} with some probability.

that at any instant of time t the machines can be classified into operational machines (state "up") and non-operational machines (state "down"). The former correspond to spots on the lattice which can perform downward jumps within the infinitesimal time window $[t, t + \mathrm{d}t]$ from the cells they are in, into their neighboring downward cells with some given probability. The latter one stay where they are during $\mathrm{d}t$ with probability 1. The modelling assumptions are:

(B1) The prone to failure machines changes their operational states ("up" and "down") according to independent two-states Markov chains with switching rates α and β.
(B2) Downstream machine M_{k+1} is starved when buffer B_k is empty. In this case, M_{k+1} will not be able to produce (*i.e.* it can not jump downwards to the next cell). Starving is supposed to occur with some mean frequency μ.
(B3) The buffer capacities are infinite (*i.e.* no blocking will occur).

(B1) implies transitions of the form "up" $\rightarrow$ "down" with rate α and "down" $\rightarrow$ "up" with rate β. (B2), together with (B3), state that only consecutive spots can interact in the following way, "(down, up)" $\rightarrow$ "(down, down)" with rate μ, where "(x,y)" means an ordered couple of consecutive machines with operational states "x" and "y", respectively.
Hence, using the convergence result of section 2 (exactly as we did for the traffic application in section 3), we deduce that under the stochastic microscopic assumptions (B1)–(B3), the resulting mesoscopic workload distribution is related to the RW model in the following sense: Let (ρ^-, ρ^+) be the solutions to the RW equations

$$\begin{cases} \partial_t \rho^-(x,t) - 1 \cdot \rho_x^-(x,t) = -\alpha\rho^-(x,t) + \beta\rho^+(x,t) + \mu\rho^-(x,t)\rho^+(x,t), \\ \partial_t \rho^+(x,t) + 0 \cdot \rho_x^+(x,t) = +\alpha\rho^-(x,t) - \beta\rho^+(x,t) - \mu\rho^-(x,t)\rho^+(x,t), \\ \big(\rho^-(x,0), \rho_x^+(x,0)\big) \qquad = \big(g_1(x), g_2(x)\big), \end{cases} \tag{5.77}$$

where the initial distribution $(g_1(x), g_2(x))$ has compact support. From the modelling assumptions it follows that $\rho^-(x,t)$ can be interpreted as the spots distribution (*i.e.* machines) which are in the "up" state and $\rho^+(x,t)$ the distribution of spots in the "down" state. Let us define $\rho(x,t) := \rho^+(x,t) + \rho^-(x,t)$ and denote by $supp\{\rho(t)\}$ the support of $x \mapsto \rho(x,t)$ at time t. The support of $\rho(x,t)$ stays finite thanks to the finite support assumption made on the initial condition. The simplified mean field picture gives now the following new expressions:

1. The euclidian distance between the first and the last spot is given by $supp\{\rho(t)\}$ and is a measure for the work in process at time t.
2. The evolution of the last spot M_N can be expressed as $\max\left\{x \in supp\{\rho(t)\}\right\}$ and corresponds to the throughput of the installation.
3. The location where the euclidian distance (*i.e.*, the buffer content) between the spots is smallest is $\sup\{x \in \mathbb{R} \mid \rho(x,t)\}$. This quantity corresponds to the location (or locations) where starvation is most likely to occur at time t.

The explicit solutions allow to compute these quantities numerically for given initial distributions. We refrain to write explicit expressions but we rather focus on the qualitative salient feature. We namely point out that the discussed diffusive relation with the Burgers equation (see discussion in 4.2.) shows, via the emerging shock wave solutions, that unsteady flow dynamics are likely to occurrence in long production lines.

5.6 Concluding remarks

One of the main aims in traffic theory is to unveil the decisive local interactions (a microscopic model) among traffic participants contributing all together to the complex emerging flow dynamics which we observe day by day. Such a microscopic model will certainly not reproduce all the observable facts but allows the recognition and the understanding of the prominent factors leading to some of the observed real world phenomena. In this chapter we have shown that emerging flow properties like shock waves and hysteresis can be explained on the basis of local kinetic features including only migrations, reactions and collisions.
Thanks to its simplicity, the microscopic model can, to some extent, be transferred to other domains where similar local interactions are to be expected. This transfer has been realized for production lines where new mean field expressions for the work in process and the throughput are derived.

5.7 Contributions of Chapter 5

- We derive the macroscopic single-lane traffic model of Lighthill, Whitham and Greenshields which links the car density ρ and the flow of cars J by the set of equations:

$$\partial_t \rho(x,t) + \partial_x J(x,t) = 0, \tag{5.78}$$
$$J(x,t) = V_{\max}\rho(x,t)\big(1-\rho(x,t)\big) - D\partial_x \rho(x,t). \tag{5.79}$$

  The derivation shows that the kinetic features leading to this semi-phenomenological traffic model are besides the migration term a reaction and a collision mechanism of mass action type.
- The micro-macro scaling passes through the intermediate mesoscopic regime where the phase-space dynamics are governed by the exactly solvable variant of the non-linear Boltzmann equations introduced by Ruijgrok and Wu:

$$\begin{cases} (\partial_t + v_1\partial_x)\rho^- = \mu\rho^-\rho^+ - \alpha\rho^- + \beta\rho^+ \\ (\partial_t + v_2\partial_x)\rho^+ = -\mu\rho^-\rho^+ + \alpha\rho^- - \beta\rho^+, \end{cases} \tag{5.80}$$

  where $(x,t) \in \mathbb{R}\times\mathbb{R}^+$, $\rho^- := \rho^-(x,t)$ and $\rho^+ := \rho^+(x,t)$ are the distribution functions of vehicles which *migrate* with velocities v_1 and v_2 respectively and where α, β and μ are positive constants governing the *reaction* and *collision* rates. For a specific range of the parameters α, β and μ, this mesoscopic model shows the signature of hysteresis which is observable in real traffic systems.

6

On the outflow process of a merge system for items with non-vanishing spatial extensions

Summary. In this study, a discrete material flow merge system connected to a downstream station is presented. The arrival process into the merging system is the superposition of N independent outflow processes of N different workstations and is approximated by a Poisson process. We show that when the items processed have finite spatial extensions, the Poisson structure of the arrival process into the merge is lost. The resulting non-Poisson outflow process from the merging system is explicitly calculated.

6.1 Introduction

Up to now we treated serial production flows thanks to the analogies with one-line traffic flows. In actual flow-lines however, complex configurations with merging, bifurcation or multiplexing of flows are the rule rather than the exception. The multiplexing of several and usually stochastic production flows into a single stream of items for example, is a very common situation in many shop floors [51]. Multiplexing arises typically when highly flexible and expensive stations are used to perform general tasks including quality control or cleaning operations (see figures 6.1 and 6.2). Clearly the close study of the production streams at splitting and merging points of the production network is mandatory. Here we concentrate on merging flows and their study will be related to the narrowing of cars passing from multi lane roads to one-lane roads.

To characterize the flows through serial production lines or lines with more complex topologies, the original configurations are usually decomposed into series of production dipoles (two machines separated by a buffer) and the global stationary performance (e.g. the throughput) are estimated by using self consistent approximation schemes based on aggregation of dipoles [49, 50].

In parallel with the development of new and more sophisticated production devices, the growing place taken by the telecommunication networks stimulates, since about thirty years, a strong activity to derive general properties

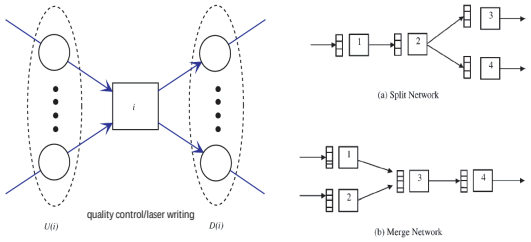

Fig. 6.1. Acyclic merging and splitting nodes in a buffered manufacturing network. For example, high speed quality control and/or laser writing installations (left) gives rise to both splitting and merging nodes (right).

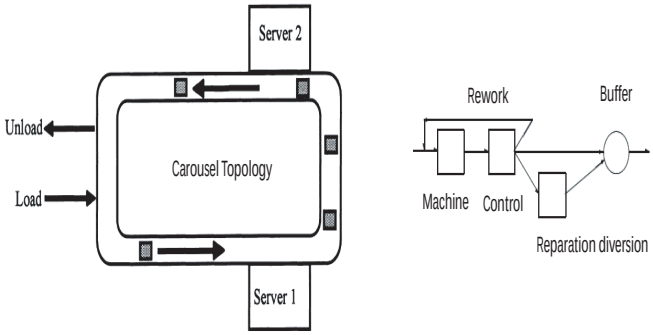

Fig. 6.2. Cyclic topology in a manufacturing network. For example, carousel topology for flexible installations (left) or reparation diversion and rework (right) give rise to cyclic structures.

for the information flows circulating in complex networks. A large corpus of literature devoted to the so called queueing network systems is available in this topic [7, 18, 56, 145]. While the probabilistic description enters naturally into the queueing network modelling, they do however reduce the circulating items to immaterial tokens (*i.e.* points). Tokens with vanishing spatial extensions can clearly be superposed and/or dispatched without any physical constraints. This offers the possibility to characterize these abstract flows by studying superpositions of several parallel point processes. This abstract point of view might be to simple for the production context. Consider indeed the multiplexing of several parallel flows of pallets (e.g., fig. 6.1). A consistent description of the flow dynamics at the merging point must imperatively take into account the finite spatial extensions of the pallets. The distribution of

time intervals between successive departures from a marge zone for example, definitely depends on the physical size of the objects.
This chapter is devoted to the characterization of such a merging flow dynamics in case the inflow process admits the simple Poisson structure. In general, one would expect that the superposition of several parallel flows produces an input into the merge system with complex statistical properties and that the Poisson assumption is rather restrictive. However, in situations where several, say N, parallel and approximately independent flows with small arrival rates λ_i are superposed, the resulting input flow into the merge system is well approximated by a Poisson stream with a global arrival intensity $\lambda = \Sigma_{i=1}^{N} \lambda_i$, [6]. We always assume that this situation is realized and hence, we suppose that a Poisson flow enters into the multiplexing structure.
Knowing the input process, we focus in the following on the outflow process of the merge system. Now at the shopfloor, the merging operation is generically performed by a conveyor system which converts the Poisson incoming stream into an outgoing generally non-Poisson flow. The corruption of the incoming Poisson structure originates from the fact that both, the size of the items and the conveyor velocity are finite. Indeed, as the items cannot overlap on the conveyor, their spatial extension together with the finite velocity of the conveyor introduces interactions between the items. As it will be shown in this chapter, the merging structure acts, roughly speaking, as a non-Markovian queueing system with service characteristics being directly related to the spatial extension of the incoming parts.
The aim of this Chapter is to study the detailed nature of the resulting effective queuing system and in particular to determine the statistical properties of its output flow. The knowledge of the probabilistic properties of the merging dynamics and in particular its output is strongly relevant for several applications among which we mention:

a) *Capacity of the merging zone.* As the merging zone acts merely as a queuing system, it is mandatory to determine the typical queue length in order to estimate the capacity of the merge system which avoids too frequent overflows.
b) *Output stream characteristics.* The detailed knowledge of the probabilistic nature of the output process is mandatory as it often will be the arrival process to a downstream queue. If, on the other hand, the output flow feeds a finished goods inventory, the knowledge of the outflow behavior may allow for variability reductions which reduces levels of optimal inventory. It is indeed established that the variability of the production flows enters directly into the calculation of the optimal hedging levels [4]. As we will show, the distribution of the output process and in particular its variability depends on the size of the circulating items. In fact, the output process is intermittent and is formed of platoons of items (*i.e.* random size batch process). The sizes of the platoons will be characterized in terms of the spatial size distributions of the incoming items and the conveyor velocity.

From an interdisciplinary point of view we remark that the understanding of merging flows of physical objects at bottlenecks is relevant for the modelling of the crowd dynamics of panicking pedestrians. Observed and simulated current-density relations of pedestrians which jam in escape situations unveil a *"slower-is-faster effect"* (see e.g., http://www.panics.org). This means that for sufficiently high densities, the escape rate (outflow current) decreases when the individuals augment their speeds (see figure 6.3). As far as we know, no analytical results concerning the outflow-properties of such crowd dynamics are known.

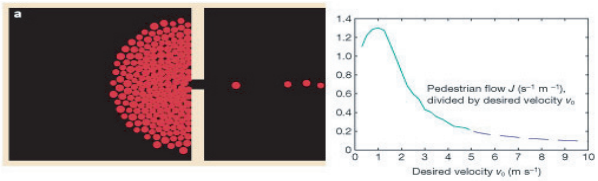

Fig. 6.3. Simulation-analysis of pedestrians moving with identical desired speed v_0 towards the exit. The figure is taken from the article *Simulating dynamical features of escape panics* by D. Helbing et al. in [23]. It shows the irregular outflow due to clogging.

The driving force behind the "slower is faster" effect is the existing discrepancy between the individual and the collective goals. Minimizing the individual outflow times does in fact not necessarily maximize the escape rate. It seams that such effects are implicitly known for a long time to architects which do build slowing-down obstacles in front of entrances since a while. Adding obstacles (*i.e.* slowing down mechanisms) in production processes in order to increase throughput is much less well known. A worthwhile exception is a production line of the Germane Infineon Technologies AG [122] where D. Helbing and D. Fasold managed to improve considerably the efficiency of the line by "slowing down" a few robots.
The chapter is organized as follows. In section 2 we state the problem of interest. In section 3 we analytically derive the stationary distribution of the outflow process and show that it tends to a Poisson process as the extensions of the items shrink to that of a material point. Based on these analytical results, several quantities of interest are derived and related to the coefficient of variation of the items size distribution. They include the number of items in the merge system, the mean and variance of the number of items in a batch of the outflow process and the busy period of the merge system. We conclude the chapter with section 4. The appendix of Chapter 6 contains a comparison of the analytical results with numerical simulation studies.

6.2 Problem Formulation

Suppose items arrive from N independent workstations with mean intensities $\lambda_1, ..., \lambda_N$ into a collecting buffer B (*i.e.* into a merging system) from where they are transported on a conveyor system to some workstation M. (see Fig. 6.4).

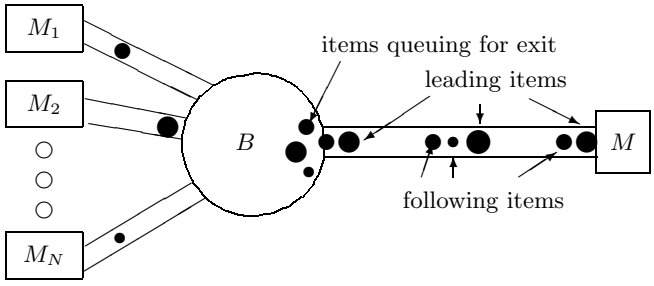

Fig. 6.4. Merging of N streams of possibly different items into a buffer B. The conveyor system transports the items from the buffer to the machine M with constant velocity v. The output process is divided in following and leading items.

The superposition of the N streams of items forms the input process to the buffer and we supposed that it behaves like a Poisson process with intensity $\lambda = \sum_{i=1}^{N} \lambda_i$. This assumption is very reasonable especially when the individual intensities λ_i are small with respect to the outflow capacity of the merging system. Indeed, Albin [6] showed that *the superposition of N independent renewal processes* having intensity λ/N and entering a service facility having service rate $\mu > \lambda$, *behaves*, for $N \to \infty$, *like a Poisson process* of intensity λ entering the same service facility. The departure process however, physically realized by a conveyor system, is Poisson only when the outgoing items do not interact during the outflow process (*i.e.* no outflow delay for items leaving the buffer due to other items queuing for exit in the buffer). In case of no interaction, the distribution of the outflow process coincides with the distribution of the arrival process. When interactions occur (*i.e.* queuing at the buffer exit), the conveyor system produces a stream of items, separated only by a conveyor dependant minimal headway h. Streams of following items flow toward M where they are processed further. We now divide items flowing out of the buffer into two classes:

1) items separated from its predecessor by the minimal headway h called *following items* and
2) items separated from its predecessor by headways exceeding h called *leading items*.

We address the problem of finding *the distribution of following and leading items after the merging* as a function of λ (*i.e.* the intensity of the arrival

stream of items into the buffer), the distribution of the possibly random finite extension (length) of the items L and the constant velocity v of the conveyor system. For ease of presentation, we suppose that the minimum headway h on the conveyor system is zero (*i.e.* $h = 0$). This assumption can easily be removed by replacing the length L of an item by a characteristic outflow length $L + h$.
Note that it is the finite spatial extensions of the items together with the finite velocity v of the conveyor system which blocks the output process during L/v (*i.e.* no other item than the outflowing one can leave the buffer during L/v). This problem is clearly related to the class of counter problems of recording apparatus when the finite resolving time is taken into account. A typical example is an α-particle counter which is impeded during a certain interval of time after a particle is recorded [30]. The direct connection with velocity traffic models modelling the narrowing of a multi-lane road to a one-lane road as described by A.J. Koning in [86] is even more relevant.

6.3 Exact analysis of the output process from the buffer

Enumerate the items in the order in which they leave the buffer. This enumeration $\{n\}$ is the index set of a sequence of random variables S_n which we interpret as the minimum exit time of item n from the buffer. This minimum exit time of item n from the buffer is easily measured on the shop floor. Indeed it corresponds to the time needed for the corresponding exit event to take place. This event starts when item n reaches the conveyor system and ends at the instant item n is entirely placed onto the conveyor system (see Fig. 6.5). Formally, $S_n = L_n/v$ with L_n being the (possibly random) characteristic length of item n and v the conveyor speed. The minimum exit times S_n are assumed to form a sequence of i.i.d. random variables (*i.e.* independent and identically distributed random variables) with cumulative distribution function G.

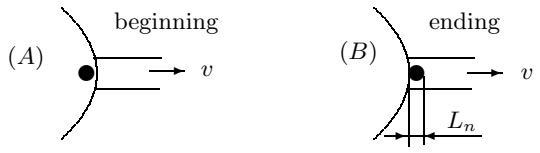

Fig. 6.5. The exit process of item n takes place during a time interval of length L_n/v. **(A)** Beginning of the exit event of item n from the buffer to the conveyor system with constant velocity v. **(B)** The exit of item n from the buffer is terminated.

Define O_n as the time instant at which item n starts to leave the buffer (output process) and suppose for convenience that $O_0 = 0$. Denote by D_n the

time instant item n starts to leave the buffer if its beginning was not delayed by the exit process of item $n-1$. The crucial observation is that when the characteristic lengths of all items vanish, the exit process is immediate and therefore $O_n = D_n$. Moreover in this case the output process (O_n) from the buffer and the arrival process into the buffer which by assumption is a Poisson point process with intensity λ have the same distribution (indeed, the output process equals the arrival process shifted by the deterministic time an item needs to travel through the buffer). The above observation amounts to saying that D_n is Poisson with intensity λ and we have similar as in [86] for $n \geq 1$ the relation:

$$O_n = \max\big(D_n, O_{n-1} + S_{n-1}\big), \tag{6.1}$$

that is to say that the nth item starts to flow out of the buffer at time D_n unless it is delayed by the exit process of item $n-1$. In the later case, n starts to leave the buffer at time $O_{n-1} + S_{n-1}$. Note that under the First in First out (FIFO) buffer discipline, which is assumed throughout the chapter, the ordering of O_n and D_n are the same (by definition of FIFO, the ordering given by the exit enumeration $\{n\}$ equals the ordering of the arrival process). The later ordering is clearly independent of the characteristic length and coincides therefore with the ordering given by D_n. The following auxiliary definition is now meaningful:

$$W_n = O_n - D_n \geq 0, \quad n \geq 1 \tag{6.2}$$

which is the time the outflow process of item n is delayed by the exit of item $n-1$. We are now ready to characterize the output process by applying Theorem 2.1. in [86] which for completeness is repeated here:

Theorem. Let $(O_n)_{n\in\mathbb{N}}$ be a sequence of random variables such that there exists a Poisson process $(D_n)_{n\in\mathbb{N}}$ with intensity λ, and a sequence $(S_n)_{n\in\mathbb{N}}$ of independent random variables with identical distribution function G independent of $(D_n)_{n\in\mathbb{N}}$, satisfying Eq. (6.1). If $\lambda\mathbb{E}(S_n) < 1$, where $\mathbb{E}(S_n)$ is the expectation of S_n, the time Y_n between the beginnings of the outflow processes of items $n-1$ and n given by

$$Y_n = O_n - O_{n-1} \tag{6.3}$$

has an equilibrium distribution as n tends to ∞ with cumulative distribution function

$$F(y) = \big(1 - e^{-\lambda(y-\theta)}\big)G(y) \tag{6.4}$$

where

$$\theta = \frac{1}{\lambda}\ln\Big(\frac{1-\lambda\mathbb{E}(S_n)}{\mathbb{E}(e^{-\lambda S_n})}\Big). \tag{6.5}$$

The theorem completely characterizes the outflow process and Eqs. (6.4, 6.5) explicitly unveil the influence of the items size distribution on it. The proof is based on the observation that the sequence of delays W_n is equivalent to a queuing process induced by the sequence $S_n - (D_n - D_{n-1})$. The distribution of W_n equals therefore the waiting time distribution W_n^q of the nth customer

of a $M/G/1$ queue with arrival intensity λ and service times S_n (see e.g., Feller [36] p.194, Definition 1 and Example (a)). Here "waiting time" means the time from the customer arrival to the epoch where his service *starts*. In this framework the hypotheses $\lambda\mathbb{E}(S_n) < 1$ reduces to the stability condition for the queue length not to explode. Rewritten as $\mathbb{E}(S_n) < 1/\lambda$, the stability condition tells us that the mean minimum exit time must be smaller than the mean inter arrival times of the items into the buffer.
In view of the theorem it is now immediate to check that for items with vanishing characteristic length (*i.e.* $L_n \to 0$, in probability) the output process equals D_n and is in particular a Poisson point process. Indeed:

$$S_n \overset{\text{in Prob.}}{\to} 0 \Rightarrow G(y) \to 1_{\{y\geq 0\}} \Rightarrow \theta \to 0 \Rightarrow F(y) = 1 - e^{-\lambda y}.$$

Hence, Eq. (6.4) reduces to the cumulative distribution function of an exponentially distributed random variable. In the case of non vanishing characteristic length (*i.e.* $L_n > 0 \Leftrightarrow \theta \neq 0$) Eq. (6.4) clearly shows that the output process is not a Poisson process.
Note that the value of θ given in (6.5) makes the (stationary) intensity of the outflow process O_n equal to the (stationary) intensity of the arrival process. Indeed,

$$\begin{aligned}\mathbb{E}(Y_n) &= \int \big(1 - F(y)\big)\mathrm{d}y = \int \big(1 - G(y) + G(y)e^{-\lambda(y-\theta)}\big)\mathrm{d}y \\ &= \mathbb{E}(S_n) + e^{\lambda\theta}\int G(y)e^{-\lambda y}\mathrm{d}y = \mathbb{E}(S_n) + \frac{e^{\lambda\theta}}{\lambda}\mathbb{E}(e^{-\lambda S_n}) = \frac{1}{\lambda}. \quad (6.6)\end{aligned}$$

Therefore stationary first order performance measures (*i.e.* performance measures involving only first order moments) such as the mean throughput of the downstream machine M, will not be affected by the non-markovian behaviour of the flows due to the spatial extensions of the products. This is not so for performance measures involving higher order moments. We elucidate this point by applying standard results available for the $M/G/1$ queue (with arrival rate λ and service S_n) to the merging process in the buffer. For example, exploiting the Pollaczek-Kinchine formula (see e.g., [102] pp.259) we may establish under equilibrium conditions:

(1) *the waiting time will increase with increasing variability of the items sizes.* The simple relation between the mean delays for exponential exits S_n and general exit distributions S_n (denoted resp. by $\mathbb{E}(W_n)[M/M/1]$ and $\mathbb{E}(W_n)[M/G/1]$):

$$\mathbb{E}(W_n)[M/G/1] = \mathbb{E}(W_n)[M/M/1]\frac{1 + c_v^2}{2} \quad (6.7)$$

where $c_v = \sqrt{\mathrm{Var}(S_n)}/\mathbb{E}(S_n)$ is the coefficient of variation of S_n. Hence delays will increase with increasing variability of the extensions of the circulating items.

(2) *the population in the merge system will increase with increasing variability of the items sizes.* The probability generating function $V(s)$ of the number of items in the buffer at the departure times $O_n + S_n$ of items is

$$V(s) = \frac{(1-\lambda\mathbb{E}(S_n))(1-s)\mathbb{E}(e^{(\lambda-\lambda s)S_n})}{\mathbb{E}(e^{(\lambda-\lambda s)S_n}) - s}. \tag{6.8}$$

As an illustration suppose for instance that the minimal exit time distribution S_n is erlangian with parameter $k \in \mathbb{N}$ (including the markovian case $k = 1$ and the deterministic case $k \to \infty$) we have:

$$V(s) = \frac{(1-\lambda\mathbb{E}(S_n))(1-s)}{1 - s\big(1 + (1-s)\frac{\lambda\mathbb{E}(S_n)}{k}\big)^k}, \tag{6.9}$$

from where it directly follows that the mean number of items in the buffer at the departure instants is:

$$M_k := \lim_{s\to 1} \frac{\mathrm{d}}{\mathrm{d}s} V(s) = \frac{\lambda\mathbb{E}(S_n)}{1-\lambda\mathbb{E}(S_n)}\Big(1 - \frac{\lambda\mathbb{E}(S_n)}{2}\big(1 - \frac{1}{k}\big)\Big). \tag{6.10}$$

M_k is visibly decreasing in k and indicates how a shrinking randomness in the exit process (variance of S_n decreases to zero as $k \to \infty$) can allow for smaller buffer design.

(3) *the outflow delays from the merge system will increase with increasing variability of items sizes.* The Laplace-Stielties Transform (LST) $W_q^*(s)$ of the outflow delays is:

$$W_q^*(s) = \int_0^\infty \mathrm{e}^{-st}\mathrm{d}W_n(t) = \frac{s(1-\lambda\mathbb{E}(S_n)}{s - \lambda\big(1 - \mathbb{E}(e^{-sS_n})\big)}. \tag{6.11}$$

By differentiating k times $W_q^*(s)$ with respect to s and putting $s = 0$ we can have the kth moment of W_q. For $k = 1$ and $k = 2$ we find in particular the mean and the variance which read as:

$$\mathbb{E}(W_q) = \frac{\lambda\mathbb{E}(S_n)}{2\mathbb{E}(S_n)\big(1-\lambda\mathbb{E}(S_n)\big)}\big(1 + c_v^2\big), \tag{6.12}$$

$$Var(W_q) = \frac{\lambda}{12(1-\lambda\mathbb{E}(S_n))^2}\Big[4(1-\lambda\mathbb{E}(S_n))\mathbb{E}(S_n)^3 + 3\lambda\mathbb{E}(S_n)^2\Big] \tag{6.13}$$

from where we in particular see, that the mean delays increase with increasing variability of S_n. The LST permits moreover to unveil the probabilistic information contained in θ. Indeed, for $s = \lambda$ we have:

$$W_q^*(\lambda) = \mathbb{E}(e^{-\lambda W_n}) = \frac{1-\lambda\mathbb{E}(S_n)}{\mathbb{E}(e^{-\lambda S_n})} = e^{\lambda\theta}; \tag{6.14}$$

rewriting Eq. (6.14) in the form:

$$\mathbb{E}(e^{-\lambda(W_n+\theta)}) = 1 \tag{6.15}$$

shows that θ is, thanks to the exponential form, a very sensitive measure for the sample delays.

(4) *the busy period of the merge system as a function of items sizes.* By Takàcs integral equation we know also the LST of the busy period T of the merge system (loosely speaking this is the period of time a connected outflow stream of items from the buffer is observed on the conveyor system):

$$T^*(s) = \int_0^\infty \mathrm{e}^{-st}\mathrm{d}T(t) = \mathbb{E}\Big(\exp\big(-(s+\lambda-\lambda T^*(s))S_n\big)\Big). \tag{6.16}$$

For the first two moments we find:

$$\mathbb{E}(T) = \frac{\mathbb{E}(S_n)}{1-\lambda\mathbb{E}(S_n)}, \tag{6.17}$$

$$\mathbb{E}(T^2) = \frac{\mathbb{E}(S_n^2)}{(1-\lambda\mathbb{E}(S_n))^3} = \frac{\mathbb{E}(T)^2(c_v^2+1)}{1-\lambda\mathbb{E}(S_n)}. \tag{6.18}$$

Introducing the coefficient of variation of T by putting $c_v(T) = \sqrt{\mathrm{Var}(T)}/\mathbb{E}(T)$, Eq. (6.18) can be rewritten in the form

$$c_v(T)^2 = \frac{c_v^2+\lambda\mathbb{E}(S_n)}{1-\lambda\mathbb{E}(S_n)}. \tag{6.19}$$

Therefore the variability of the busy period of the merge system increases with increasing variability of the extensions of the circulating items and is very sensitive in case the inflow intensity λ is close to $1/\mathbb{E}(S_n)$.

(5) *the number of items in a busy period as a function of items sizes.* The probability generating function $P(s)$ for the number of items which flow out during a busy period N satisfies the following functional equation:

$$P(s) = s\int_0^\infty \mathrm{e}^{-(\lambda-\lambda P(s))t}\mathrm{d}G(t) \tag{6.20}$$

with the explicit expressions for the first two moments:

$$\mathbb{E}(N) = \frac{1}{1-\lambda\mathbb{E}(S_n)}, \tag{6.21}$$

$$\mathbb{E}(N^2) = \frac{1-\lambda^2\mathbb{E}(S_n)^2+\lambda^2\mathbb{E}(S_n^2)}{(1-\lambda\mathbb{E}(S_n))^3}. \tag{6.22}$$

Introducing the coefficient of variation of N by putting $c_v(N) = \sqrt{\mathrm{Var}(N)}/\mathbb{E}(N)$, Eq. (6.22) can be rewritten in the form

$$c_v(N)^2 = \frac{\lambda\mathbb{E}(S_n)}{1-\lambda\mathbb{E}(S_n)}\big(c_v^2\lambda\mathbb{E}(S_n)+1\big). \tag{6.23}$$

Therefore the variability of N increases with increasing variability of the extensions of the circulating items and is (as the busy period) very sensitive in case the inflow intensity λ is close to $1/\mathbb{E}(S_n)$.

6.4 Beyond the merge

Let us now study more closely the distribution on the conveyor system below the merge. Recall that an item n finishes its outflow process at $O_n + S_n$; then it is proceeded on the conveyor system with constant speed v towards M. This process is supposed to be deterministic and independent of the downstream stage M. In particular, we suppose that M (or the buffer system of M) is capable to absorb the flow of products without inducing jamming on the conveyor system. Under this assumptions M will receive batches of workloads as illustrated in figure 6.4 rather than simple poisson flows of products. To make this statement more precise we emphasize the following corollary which is a direct consequence of the above theorem:

Corollary. The time headway between successive items flowing out of a buffer which itself is filled by a Poisson process of intensity λ is *not* in general *a Poisson process* but may be interpreted as the maximum of a shifted exponential random variable with parameter λ and a minimal time headway S_n. More precisely: there exists a sequence of mutually independent and exponentially distributed random variables $(T_n)_{n\in\mathbb{N}}$ with parameter λ, independent of $(S_n)_{n\in\mathbb{N}}$ such that for all $n \geq 1$, $Y_n = \max\left(T_n + \theta, S_n\right)$ almost surely and where θ is given by Eq. (6.5).
The corollary allows the following simple characterization of leading and following items:

1) Item n is a leading item iff $T_n + \theta > S_n$. In that case $Y_n = T_n + \theta$ and the time headway is $T_n + \theta$.
2) Item n is a following item iff $T_n + \theta \leq S_n$. In that case $Y_n = S_n$ and accordingly, the time headway is S_n.

Using this characterization Eq. (6.4) can be rewritten as:

$$\begin{aligned} F(y) &= \mathbb{P}(\max\left(T_n + \theta, S_n\right) \leq y) \\ &= \mathbb{P}(T_n + \theta \leq y \mid T_n + \theta > S_n)\, \mathbb{P}(T_n + \theta > S_n) \\ &\quad + \mathbb{P}(S_n \leq y \mid T_n + \theta \leq S_n)\, \mathbb{P}(T_n + \theta \leq S_n) \\ &= F_L(y)(1-\rho) + F_F(y)\rho \end{aligned} \tag{6.24}$$

with the obvious definitions:

$$\begin{aligned} F_L(y) &:= \mathbb{P}(T_n + \theta \leq y \mid T_n + \theta > S_n) \\ F_F(y) &:= \mathbb{P}(S_n \leq y \mid T_n + \theta \leq S_n) \\ \rho &:= \mathbb{P}(T_n + \theta \leq S_n). \end{aligned}$$

Eq. (6.24) interprets the distribution of outflowing items as a convex combination of the outflow of following and leading items. The somewhat lengthy calculations of Appendix A show that the ratio of following items ρ (*i.e.* the probability that n is a following item) is simply:

$$\rho = \lambda \mathbb{E}(S_n) \tag{6.25}$$

and that the distributions of leading and following items are given by:

$$F_L(y) = \frac{\int_0^y \lambda e^{-\lambda t} G(t) \mathrm{d}t}{\int_0^\infty e^{-\lambda t} \mathrm{d}G(t)}, \quad y \geq 0 \tag{6.26}$$

$$F_F(y) = \frac{G(y) - \int_0^y e^{-\lambda(t-\theta)} \mathrm{d}G(t)}{\lambda \int_0^\infty t \mathrm{d}G(t)}, \quad y \geq 0. \tag{6.27}$$

We define now in analogy to the $M/G/1$ queue the *busy period* and the *free period* of the merge system. The busy period commences at an instant a *leading* item, say item n, starts the outflow process and terminates at $O_{n+k} + S_{n+k}$ where $k \in \mathbb{N}$ is the smallest integer such that $n + k + 1$ is a leading item (*i.e.* it terminates at the instant the last *following* item connected to the stream of items induced by n is placed on the conveyor system). The free period is complementary to the busy period and formally given, using the same notations as above, by $O_{n+k+1} - O_{n+1}$.
From queueing theory we know that the epochs of arrivals of (lucky) customers finding the server unoccupied constitute a renewal process and that the free periods form a sequence of iid random variables (see e.g., Feller [36] p.197). Hence, the leading items initiate a busy period of the merge system and the arrival times of leading items form a renewal process. Its equilibrium distribution T can be found via Takàcs' integral equation (see e.g., [102] p.278) and the first two moments are given in Eqs. (6.17,6.18). Moreover, the number of items flowing out during a busy period follows the distribution given in Eq. (6.20) and depends visibly on the distribution G of the spatial extensions of the items. In conclusion, the downstream station M receives batches of workload which form a renewal process (called hereafter "batch arrival process"). The arrival of the first item in the batch at M is a renewal point of the batch arrival process. The outflow process (leading *and* following items) however is not a renewal process in general as Eq. (6.4) indicates (see also the remark in [86] Eq. (2.13)). The batch sizes depend on the spatial extensions of the items with the mean and the variance explicitly given in Eqs. (6.21,6.22). In case of vanishing spatial extensions, every item is a leading item, all batches have size one and the outflow process (which is now a renewal process) coincides in distribution with the batch arrival process.

6.5 Concluding remarks

In the setting of discrete materials flow production systems we considered the merging of N independent streams of items with finite spatial extensions into a single stream. Also the input process is well approximated by a Poisson process, the outflow process from the merging system is definitely not Poisson. In fact, the outflow is a Poisson point process only in the limit case of vanishing extensions of the items lengths. When the extensions of the processed items are finite and independently drawn from a random variable L, the resulting

outflow process may be interpreted as the maximum of a shifted exponential random variable and a minimal time headway $S = L/v$ where v is the conveyor speed governing the outflow process.
A distinction between items with minimal time headway (following items) and items exceeding the minimal headway (leading items) is drawn and their distributions are explicitly given. Leading items form a renewal process and the downstream stage receives at the renewal events (and under some hypotheses concerning the downstream stage) batches of workload with a size distribution depending on the extensions of the items. The size distribution is equivalent to the (well known) distribution of the number of served clients during a busy period of a $M/G/1$ queueing system.
The results constructively show the limited use of the standard Markov chain analysis at merging points of production systems when the circulating items are supposed to have finite spatial extensions. We analyze the non-markovian outflow process (O_n) by comparing it with a fictive poissonian outflow process (D_n). The method is different from the more common perturbation analysis of Markov processes and might find further impacts on non-markovian production flow modelling.

6.6 Contributions of Chapter 6

- Under the hypothesis of Poisson inflow D_n of items n into a merge, the outflow process O_n from the merge is defined via the recurrence relation

$$O_n = \max\big(D_n, O_{n-1} + L_{n-1}/v\big), \tag{6.28}$$

  where v is the conveyor speed after the merge and where L_n is the size distribution of item n. If G denotes the distribution function of the i.i.d. exit times from the merge of an item (*i.e.* $G(y) = \mathbb{P}(L_n \leq yv)$) and if the inflow rate λ verifies $\lambda\mathbb{E}(L_n/v) < 1$, then the inter-departure times of consecutive items $O_n - O_{n-1}$ have an equilibrium distribution as n tends to infinity with cumulative distribution function

$$F(y) = \big(1 - e^{-\lambda(y-\theta)}\big)G(y)$$

  where

$$\theta = \frac{1}{\lambda}\ln\Big(\frac{1 - \lambda\mathbb{E}(L_n/v)}{\mathbb{E}(e^{-\lambda L_n/v})}\Big).$$

- The prove of the above stationary distribution is based on the observation that the delay time W_n of item n, induced by the outflow process of item $n-1$, equals the waiting time distribution of the $n$the customer in a $M/G/1$ queue with arrival intensity λ and service time L_n/v. This offers to derive quantitative statements which we list here in their qualitative form:
  (0) We have $\mathbb{E}(Y_n) = \frac{1}{\lambda}$. Therefore, stationary performance measures involving only first order moments will not be affected by the delay dynamics.

(1) The waiting time in the buffer increases with increasing variability of S_n (*i.e.* with $\sqrt{\mathrm{Var}(S_n)}/\mathbb{E}(S_n)$).
(2) The mean population in the merge system increases with increasing variability of S_n.
(3) The mean outflow delays from the merge system increases with increasing variability of S_n.
(4) The variability of the busy period of the merge system increases with increasing variability of S_n.
(5) The variability of the number of out-flowing items in a busy period increases with increasing variability of S_n.

Part III

Mesoscopic Modelling of Stochastic Transport

Introductory remarks concerning Part III

Up to here, we considered flows of cars or products and proposed some modelling tools for their dynamical understanding. A very synthetic macroscopic understanding is thereby delivered by the deterministic flow-density relation (*i.e.* the fundamental-diagram in traffic theory) obtained through a multi-scale analysis. The important point for flow engineering is that such a deterministic macroscopic relation reestablishes – at least approximatively – the predictability of the complex many-body system.
In this part, we will do a step towards a more general view on *flow-density relations* of interacting particles and on *stochastic transport*. This step is mainly based on the assumption that the irregular motion of the transport processes under investigation can be reformulated as stochastic processes which are solutions to stochastic differential equations.
The assumption is fundamental and is related to the very existence of a macroscopic description of the system. This is indeed based on the possibility to select a small set of system-variables in such a way, that they obey approximately an autonomous set of deterministic variables. Their approximate nature appears in the existence of fluctuation terms, by which the eliminated variables make themselves felt. As a consequence the macroscopic variables are stochastic functions of time *i.e.*, continuous-time stochastic processes ([143] p.55-58). According to van Kampens notation, this stochastic description including both the deterministic law and the fluctuations about them is coined *mesoscopic* modelling [143].
Almost all the continuous-time stochastic process models of applied probability consist of some combination of the following:

- diffusion,
- deterministic motion and
- random jumps.

A glance at the literature reveal that the techniques used in connection with diffusion processes differ clearly from those employed with the other two classes. As remarked by M.H.A. Davis in [28], an important exception is

the large class of piecewise-deterministic Markov processes. This processes – also called random evolutions or Markov jump processes – cover virtually most non-diffusion applications and can be studied, similarly to diffusion processes, by means of the corresponding backward evolution operators. We will encounter both, diffusions and random evolutions leading respectively to parabolic and hyperbolic types of transport equations.
The stochastic formalism unifying on the mesoscopic level of description both types of transport are stochastic differential equations. They will appear in Chapter 7 and 8 in the form:

$$\frac{dX_t}{dt} = h(X_t, t) + \text{“noise”}, \tag{6.31}$$

where to the deterministic law $\dot{x} = h(x, t)$ – describing e.g. the evolution of the center of mass of n particles – is superposed the noise term. The deterministic part is the law that connects the change of a given system “in the immediate future” to the present state and arises naturally from the concept of causality. The choice of the noisy part is less straight forward and there is in fact a wide variety of stochastic processes which can be used to model stochastic transport.
In Chapter 7, the noisy term will be the so-called telegraph noise leading to a random evolution X_t (hyperbolic). The interesting link with Chapter 5 of part II is that under some hypothesis concerning the space inhomogeneity of the noise, the *flow-density relation* resulting from eq. (6.31) *does have a special algebraic structure*. To unveil this structure, which goes back to the so-called Darboux transformation introduced in 1882 (!) by G. Darboux [27], is the main topic pursued in Chapter 7.
In Chapter 8, the noisy term in eq. (6.31) will be Gaussian White Noise and accordingly X_t is a diffusion process (parabolic). Here the connection with part II is mainly through Chapter 4. In Chapter 4 we ask for the optimal control u^* minimizing some average cost functional. Eventually, the same question is addressed in Chapter 7 in the context of *diffusion mediated transport processes*. The fluctuations in these out-of equilibrium processes are vital for the occurrence of directed transport and new transport phenomena occur thanks to the interplay between the deterministic and the noisy part of eq. (6.31). Loosely speaking, we ask for the optimal force field (*i.e.* how do I have to chose the function h in eq. (6.31)) in order to minimize some *appropriate* average cost functional. In contrast to Chapter 4, the choice for the average cost functional is not clear in this case and its physically consistent derivation must be considered as a result.

7

Supersymmetric density-flow relations in random two-velocities processes

Summary. We discuss a random two-velocities process on the line with space dependent exogenous drift. For this process, the probability density and the associated "probability current" are shown to be in a supersymmetric relation.

7.1 Introduction

Consider the inhomogeneous diffusion of particles on $\mathbb{R}$ described by the stochastic differential equation (i.e. Langevin equation) in the form:

$$dX_t = g(X_t)dB_t \quad (S), \tag{7.1}$$

where dB_t stands for the standard Brownian motion, $g(x) > 0$ controls the diffusion process and where S means that the underlying stochastic integral is interpreted in its Stratonovitch form. The probability density $u(x,t)$ associated with the stochastic process Eq.(7.1) obeys to the Fokker-Planck equation [48]:

$$\partial_t u(x,t) = \frac{1}{2}\partial_x\big[g(x)\partial_x[g(x)u(x,t)]\big]. \tag{7.2}$$

The *parabolic nature* of Eq.(7.2) implies that probability propagates with an infinite velocity. This feature may lead to difficulties for the physical interpretation see for instance [59, 60].
To remove this structural difficulty, several alternatives to Eq.(7.1) have been proposed. Among the simplest possibilities, K.P. Hadeler [59] emphasizes that a tractable alternative which takes into account inertia and correlations are random velocity (RV) jump processes. Basically, these models lead to motion with finite propagation speeds and approaches Brownian motion in a diffusive limit [67]. The simplest model belonging to the RV-class is based on a two-velocity process on $\mathbb{R}$ given by the Langevin-type equation:

$$\dot{X}_t = g(X_t)I_t, \tag{7.3}$$

where I_t is now a dichotomous noise taking values in the set of velocities $\{-v, v\}$ and having exponentially distributed holding times with parameters $\lambda > 0$ (from v to $-v$) and $\mu > 0$ (from $-v$ to v). Langevin equations with this type of telegraphic noise are thoroughly studied in [72]. It is established that the probability densities $u^+ = u^+(x,t)$ (resp. $u^- = u^-(x,t)$) of a particle going to the right (resp. left) and subject to the dynamics Eq.(7.3) obey to the hyperbolic system of partial differential equations:

$$\partial_t u^+ + v\partial_x[g(x)u^+] = -\lambda u^+ + \mu u^-, \tag{7.4}$$
$$\partial_t u^- - v\partial_x[g(x)u^-] = +\lambda u^+ - \mu u^-. \tag{7.5}$$

From Eqs. (7.4) and (7.5), we can draw the following elementary remarks:

- The system given by Eqs.(7.4) and (7.5) exhibits a *hyperbolic structure*. Accordingly, the propagation of probability occurs at finite speed in contrast with the parabolic structure of Eq.(7.2).
- In both Eqs.(7.1) and (7.3), we can, supposing the integrability of $x \mapsto g^{-1}(x)$, introduce the new variable $Y = \int^X g^{-1}(x)\,dx$ and then consider, in terms of the variable Y, the associated (homogeneous) transport problem having a constant diffusion coefficient. Accordingly, without explicit mention, we shall always consider the case where $g(x) \equiv 1$.

An alternative interpretation of Eqs.(7.4) and (7.5) is given by S. Goldstein [54] who investigates particles performing independently persistent random walks on a lattice. A suitable continuum limit of this transport process also yields Eqs.(7.4) and (7.5) for the particles densities going to the right respectively to the left. The first direct treatment of the telegraph equation in continuous time as given in eq.(7.3) goes back to M. Kac [82] (see, [66] for a recent comprehensive overview on the history of random evolutions). As emphasized in [59, 60], the persistent random walk provides a better description of spatial spread in population dynamics than Brownian motion. Defining the total density $P(x,t)$ and the current $Q(x,t)$ as:

$$P(x,t) = u^+(x,t) + u^-(x,t), \tag{7.6}$$
$$Q(x,t) = u^+(x,t) - u^-(x,t), \tag{7.7}$$

one finds from Eqs.(7.4) and (7.5) the one-dimensional Cattaneo-like system [60]:

$$\partial_t P(x,t) + v\partial_x Q(x,t) = 0, \tag{7.8}$$
$$\partial_t Q(x,t) + v\partial_x P(x,t) = [\mu - \lambda]\,P(x,t) - [\lambda + \mu]\,Q(x,t), \tag{7.9}$$

which describes a macroscopic spatial spread of particles on $\mathbb{R}$. Separating the fields $P(x,t)$ and $Q(x,t)$ by differentiating Eqs.(7.8) and (7.9) with respect to t and x, it is immediate to obtain that $P(x,t)$ and $Q(x,t)$ both satisfy the same dissipative wave equation:

$$\partial_t^2\phi(x,t) + (\lambda+\mu)\partial_t\phi(x,t) = v^2\partial_x^2\phi(x,t) + (\lambda-\mu)v\frac{\partial}{\partial x}\phi(x,t). \qquad (7.10)$$

When $\lambda = \mu$, Eq.(7.10) reduces to the standard telegraphist equation [54, 82]. Since these pioneering works, numerous alternative derivations of Eq.(7.10) have been performed [108, 117]. A recent and comprehensive review devoted to this topic is delivered by G.H. Weiss [149] who emphasizes several relevant physical aspects of such transport processes.

While the space inhomogeneity in the Langevin Eqs.(7.1) and (7.3) is introduced via the $g(x)$ term as a noise *amplitude modulation* (see e.g., [121]), it is important to emphasize that Eq.(7.3) does also offer the possibility to consider inhomogeneity due to noise *spectral modulations* via spatial dependence of the terms $\lambda(x) > 0$ and $\mu(x) > 0$. Relatively little attention has so far been devoted to these spectral modulation cases. Noticeable exceptions being *i*) first passage time problems considered in [100] where inhomogeneities of the spectral type occur naturally and *ii*) non-Markovian dichotomous processes considered in [8] where the non-Markovian character of the holding times is translated into the dependence of the switching rates λ and μ on x. In addition the relevance of spectral modulation for flagellated bacteria such as *E. coli* or more generally for *chemotaxis* in living systems has also been recently pointed out in [109].

The aim of the present paper is to show that for a special class of noise spectral inhomogeneities (i.e. when $\lambda(x) + \mu(x) = \text{const.}$) the resulting density field $P(x,t)$ and its associated current field $Q(x,t)$ are connected via a supersymmetric relation similar to the one arising in quantum mechanics. This exceptional structure offers the possibility to apply powerful algebraic tools to discuss the relations between the transient behaviors of the fields $P(x,t)$ and $Q(x,t)$ for these inhomogeneous transport problems.

The presentation is organized as follows: In section 1 we introduce the general inhomogeneous random velocity process and derive formally the associated stationary probability measures. In section 2, the supersymmetric structure connecting the dynamics of $P(x,t)$ and $Q(x,t)$ is explicitly unveiled and a simple illustration is given.

7.2 Two-velocities process with inhomogeneous dichotomous noise

We consider as in [72] a stochastic process $\{X_t\}_{t\in\mathbb{R}^+}$ defined on a standard probability space $(\Omega, \mathcal{F}, \mathbb{P})$ with state space $(\mathbb{R}, \mathcal{B})$ and whose dynamical evolution is given by the piecewise deterministic evolution:

$$\dot{X}_t = h(X_t) + g(X_t)I_t(X_t) \qquad (7.11)$$

where h and g are given functions of class $\mathcal{C}^1(\mathbb{R})$ with $g > 0$ such that $x \mapsto 1/g(x)$ is integrable and where $I_t(X_t)$ is a state dependant dichotomous noise with values in $\{-1, +1\}$ (for simplicity velocity v is now set to

1). The random holding time of $I_t(x)$ in state 1 (resp. -1) is governed by a *space inhomogeneous* probability density of exponential type with parameters $\lambda(x) \in \mathcal{C}^1(\mathbb{R})$ (resp. $\mu(x) \in \mathcal{C}^1(\mathbb{R})$). For all $x \in \mathbb{R}$, $\lambda(x)$ (resp. $\mu(x)$) is strictly positive and gives the average frequency of switching from $\{1\}$ to $\{-1\}$ (resp. from $\{-1\}$ to $\{1\}$).
Observe that the pair process (X_t, I_t) is a Markov process. Its transition probability density is denoted by $\mathbb{P}(x, i, t|y, j, s)$, $x, y \in \mathbb{R}$, $i, j \in \{-1, 1\}$, $0 \leq s < t$. Fix a starting point $X_0 = x_0$ and an initial velocity $i_0 \in \{-1, 1\}$ and set:

$$u^+(x,t|0) := \mathbb{P}(X_t = x, I_t = +1, t|X_0 = x_0, I_0 = i_0, 0),$$
$$u^-(x,t|0) := \mathbb{P}(X_t = x, I_t = -1, t|X_0 = x_0, I_0 = i_0, 0).$$

It is easy to establish that, exactly as in the case of constant switching rates (see e.g., [72] p.260), the time evolution of $u^+(x,t|0)$ and $u^-(x,t|0)$ reads:

$$\begin{aligned}\partial_t u^+(x,t|0) &= -\partial_x\big[\big(h(x)+g(x)\big)u^+(x,t|0)\big] \\ &\quad -\lambda(x)u^+(x,t|0) + \mu(x)u^-(x,t|0), \qquad (7.12)\\ \partial_t u^-(x,t|0) &= -\partial_x\big[\big(h(x)-g(x)\big)u^-(x,t|0)\big] \\ &\quad +\lambda(x)u^+(x,t|0) - \mu(x)u^-(x,t|0). \qquad (7.13)\end{aligned}$$

Integrating out the initial conditions, one directly sees that these equations still hold for the unconditioned joint probabilities respectively denoted by $u^+(x,t)$ and $u^-(x,t)$. We further define a probability density $P(x,t)$ and the associated probability flow $Q(x,t)$ in the form:

$$P = P(x,t) := u^+(x,t) + u^-(x,t), \qquad (7.14)$$
$$Q = Q(x,t) := u^+(x,t) - u^-(x,t). \qquad (7.15)$$

Using Eqs.(7.12) and (7.13), the resulting Cattaneo-like system for these new fields P and Q reads:

$$\partial_t P + \partial_x\big[h(x)P + g(x)Q\big] = 0, \qquad (7.16)$$
$$\partial_t Q + \partial_x\big[g(x)P + h(x)Q\big] = -(\lambda(x) - \mu(x))P - (\lambda(x) + \mu(x))Q. \qquad (7.17)$$

For inhomogeneous rates $\lambda(x)$ and $\mu(x)$, the elimination from Eqs.(7.16) and (7.17) of one of the fields P or Q to obtain a simple hyperbolic system of the telegraphist type is not possible in general. However, supposing that $g(x)^2 > h(x)^2$ for all $x \in \mathbb{R}$, the stationary solutions $P_s(x)$ and $Q_s(x)$ can be formally obtained in the closed form:

$$Q_s(x) = -\frac{h(x)}{g(x)}P_s(x) + \frac{C}{g(x)}, \qquad (7.18)$$

$$\begin{aligned}P_s(x) &= \frac{g(x)}{g(x)^2 - h(x)^2}\exp\Big(\int_0^x \mathrm{d}y \frac{(\mu(y)+\lambda(y))h(y) + (\mu(y)-\lambda(y))g(y)}{g(y)^2 - h(y)^2}\Big) \\ &\times\Big[N - C\int_0^x \big[\mathrm{d}y \frac{\mu(y)+\lambda(y)+h'(y)-h(y)g'(y)/g(y)}{g(y)} \\ &\qquad \times \exp\big(-\int_0^y \mathrm{d}z \frac{(\mu(z)+\lambda(z))h(z) + (\mu(z)-\lambda(z))g(z)}{g(z)^2 - h(z)^2}\big)\big]\Big] \qquad (7.19)\end{aligned}$$

with N and C being two constants. When interpreting $P_s(x)$ as a probability measure (and not as a particle density function), N stands for a normalization constant which exists whenever we can find a positive K such that:

$$(\mu(x) + \lambda(x))h(x) < (\lambda(x) - \mu(x))g(x), \quad \forall x > K, \tag{7.20}$$

$$(\mu(x) + \lambda(x))h(x) > (\lambda(x) - \mu(x))g(x), \quad \forall x < -K. \tag{7.21}$$

The Eqs.(7.20) and (7.21) express, for $h \neq 0$, the deterministic stability condition introduced in [72]. For $h = 0$, which is the case we will focus on, the following observations can be given:
A finite stationary solution $P_s(x)$ exists only when the switching rates satisfy $\mu(x) < \lambda(x)$ for all sufficiently large x and $\mu(x) > \lambda(x)$ for all sufficiently large $|x|$, $x < 0$. Therefore the noise spectral modulation can generate noise induced spatial structures. Moreover, when the conditions Eqs.(7.20) and (7.21) are satisfied, the integration constant C vanishes (see [72] p. 266) and hence $Q_s(x) \equiv 0$.

7.3 Transient behavior and Supersymmetry

The importance of studying transient behaviour of probability densities associated with stochastic differential equations is largely commented in far from equilibrium processes (see for instance the recent works devoted to Brownian ratchets and stochastic resonance [124]). In particular, diffusion processes are abundantly described and explicit transient solutions of Fokker-Planck equations have been derived using, among other approaches, the connection with supersymmetric quantum mechanics [80]. Explicit transient solutions of the Chapmann-Kolmogorov equation associated to stochastic differential equations of the type given in Eq.(7.11) are so far much less discussed. Exceptions worthwhile mentioning are the cases i) $h(x) = 0$ with homogenous rates λ and μ leading to the telegraphist eq.(7.10) and ii) $h(x) = -\gamma x$ with γ a constant and with homogenous rates λ and μ discussed in [135] and more recently in [8] and [16]. As pointed out in [135], the basic difficulty when $h \neq 0$ is due to the lack of self-adjointness in the system of equations (7.12) and (7.13). Here we consider the case $h(x) = 0$ together with space inhomogeneous $\lambda(x)$ and $\mu(x)$ with the restriction $\lambda(x) + \mu(x) = \beta =$ constant. The resulting class of Langevin-type equations (indexed by $\beta \in \mathbb{R}^+$) enjoys the following remarkable properties:

i) The probability densities $P(x,t)$ and the associated probability flows $Q(x,t)$ obey second order PDE's with a spatial part similar to Fokker-Planck equations corresponding to diffusive processes with a drift term.
ii) The probability density $P(x,t)$ and the associated probability flow $Q(x,t)$ are in a supersymmetric relation.

To exhibit these properties, we introduce the potential $V(x) = \int_{-\infty}^{x}(\lambda(y) - \mu(y))\mathrm{d}y$, and write the Cattaneo-like system Eqs.(7.16) and (7.17) as:

$$\partial_t P + \partial_x Q = 0, \tag{7.22}$$

$$Q(x,t) + \frac{1}{\beta}\partial_t Q = -\frac{1}{\beta}\Big(\partial_x P + P\partial_x V\Big). \tag{7.23}$$

Observe that the above system is identical to the modified Smoluchowski diffusion equation discussed in [130] which approximately describes the motion of a particle moving in a potential $V(x)$ subject to Brownian movement at a constant temperature. This observation leads us to introduce:

a) a drift force $W(x) := \mu(x) - \lambda(x) = -\partial_x V$ and
b) a constant parameter $\beta := \mu(x) + \lambda(x)$ which plays the role of an effective temperature [130].

With these definitions and when separating the fields P and Q by differentiating Eqs.(7.22) and (7.23) with respect to t and x, one ends with the following damped wave equations:

$$\partial_t^2 P + \beta\partial_t P = \partial_x^2 P - \partial_x[W(x)P], \tag{7.24}$$

$$\partial_t^2 Q + \beta\partial_t Q = \partial_x^2 Q - W(x)\partial_x Q. \tag{7.25}$$

Note that Eqs.(7.24) and (7.25) are identical when $W(x) =$ constant. Moreover due to the underlying probabilistic interpretation, the conservation of the positivity of the solutions of Eqs.(7.24) is guaranteed even for inhomogeneous $\lambda(x)$ and $\mu(x)$. A purely analytical approach to establish the positivity has been discussed in [70] and is the basis for the associated H-theorem exposed in [17].
As mentioned in point i) above, the RHS of Eq.(7.24) (resp. Eq. (7.25)) formally coincide with the Fokker Planck forward equation (resp. backward equation) associated with the diffusion process:

$$dX_t = \frac{1}{\beta}W(X_t)\mathrm{d}t + \frac{1}{\sqrt{\beta}}dB_t, \tag{7.26}$$

resp.

$$dX_t = -\frac{1}{\beta}W(X_t)\mathrm{d}t + \frac{1}{\sqrt{\beta}}dB_t \tag{7.27}$$

with $\mathrm{d}B_t$ being standard Brownian motion and $\pm W(x)/\beta$ drift terms.
Let us now unveil the supersymmetric relation between P and Q. We write:

$$\mathbf{\Psi} = \begin{pmatrix}\psi^-(x,t)\\ \psi^+(x,t)\end{pmatrix} := \exp\big[\frac{1}{2}\big(V(x) - V(x_0)\big)\big]\begin{pmatrix}Q(x,t)\\ P(x,t)\end{pmatrix}, \tag{7.28}$$

where $x_0 \in \mathbb{R}$ is a fixed starting point of the particle. With this notations, Eqs.(7.24) and (7.25) can be written as:

$$\begin{pmatrix}\partial_{t,t}^2 + \beta\partial_t & 0\\ 0 & \partial_{t,t}^2 + \beta\partial_t\end{pmatrix}\mathbf{\Psi} = -\begin{pmatrix}H_- & 0\\ 0 & H_+\end{pmatrix}\mathbf{\Psi}, \tag{7.29}$$

with

$$H_{\pm} := -\partial_{x,x}^2 + \frac{1}{4}W(x)^2 \pm \frac{1}{2}W'(x) \tag{7.30}$$

and where $W'(x)$ stands for the derivation with respect to x. This is precisely the formalism of supersymmetry (SUSY) applied in quantum mechanics (QM) (see [80, 21] for recent reviews). In particular $H_{\pm}$ are the SUSY partner Hamiltonians acting on $L^2(\mathbb{R})$ and the drift terms $\pm W(x)$ are the so-called SUSY partner potentials. Hence the operators H_+ resp. H_- appear to be partner Hamiltonians similar to those in Wittens model of SUSY QM [152] and Eq.(7.29) establishes the mentioned supersymmetric relation between P and Q.
Recall that the SUSY partner Hamiltonians $H_{\pm}$ with spectrum $\mathrm{Spec}(H_{\pm})$ are related by means of the differential operator A and its adjoint $A^{\dagger}$ by:

$$H_+ = AA^{\dagger}, \;\; H_- = A^{\dagger}A, \tag{7.31}$$

where:

$$A := \partial_x + \frac{1}{2}W(x), \;\; A^{\dagger} = -\partial_x + \frac{1}{2}W(x). \tag{7.32}$$

It follows that the partner Hamiltonians are positive and essentially isospectral (i.e. the strictly positive eigenvalues of H_- and H_+ coincide). Hence, the transient behavior of the probability density P and the flow Q are identical and the relaxation to the equilibrium is governed by the value of β and the smallest non zero eigenvalue of the Hamiltonians. Indeed, for a large class of time independent potentials W the spectrum of $H_{\pm}$ is of the form (see e.g., [72] Chapt. 6.7):

$$\mathrm{Spec}\big(H_{\pm}\big) \setminus \{0\} = \{\nu_1, ..., \nu_n, ...\} \cup [a, \infty[\tag{7.33}$$

where $[a, \infty[$, $a \in \mathbb{R} \cup \{\infty\}$ is the continuous (possibly empty) range of eigenvalues of $H_{\pm}$ and where $\{\nu_1, ..., \nu_n, ...\}$ is the countable (possibly empty or finite) set of eigenvalues of $H_{\pm}$ satisfying $0 < \nu_1 \leq ...\nu_n \leq ... \leq a$. For given initial conditions $\psi^{\pm}(x, 0)$ and $\psi_t^{\pm}(x, 0)$ the solution to Eqs.(7.29) can formally be expanded in a series of eigenfunctions as

$$\psi^{\pm}(x,t) = \sum c_{\nu}(t)\phi_{\nu}^{\pm}(x) + \int_a^{\infty} c_{\nu}(t)\phi_{\nu}^{\pm}(x)\mathrm{d}\nu \tag{7.34}$$

where the summation is taken over all discrete eigenvalues, the integral is taken over the continuous range of eigenvalues and where the square integrable eigenfunctions $\phi_{\nu}^{\pm}$ are supposed to be normalized. Depending on the sign of $\Delta_{\nu} := \beta^2 - 4\nu$ the $c_{\nu}(t)$, solving the characteristic equation $c''(t) + \beta c'(t) + \nu c(t) = 0$, are given by:

$$\begin{array}{lll}
\text{i)} & c_{\nu}(t) = \exp(-\frac{\beta}{2}t)\big(A_{\nu}\cosh(t\sqrt{\Delta_{\nu}}/2) + B_{\nu}\sinh(t\sqrt{\Delta_{\nu}}/2)\big) & \text{if } \Delta_{\nu} > 0 \\
\text{ii)} & c_{\nu}(t) = \exp(-\frac{\beta}{2}t)\big(A_{\nu}\cos(t\sqrt{-\Delta_{\nu}}/2) + B_{\nu}\sin(t\sqrt{-\Delta_{\nu}}/2)\big) & \text{if } \Delta_{\nu} < 0 \\
\text{iii)} & c_{\nu}(t) = \exp(-\frac{\beta}{2}t)\big(A_{\nu} + B_{\nu}t\big) & \text{if } \Delta_{\nu} = 0
\end{array}$$

and where the A_ν's and B_ν's are determined by the initial conditions. If the smallest non-zero eigenvalue $\nu_1 \in \mathrm{Spec}\big(H_\pm\big) \setminus \{0\}$ is less than $\beta^2/4$ (hence c_{ν_1} is not oscillating and of the form given in i)) the relaxation to stationary state is governed by $\big(-\beta+\sqrt{\beta^2-4\nu_1}\big)/2$. In the contrary ($\nu_1 \geq \beta^2/4$) the approach to equilibrium is governed by $\beta/2$ and oscillates (when the inequality is strict) with a frequency $\sqrt{\nu_1-\beta^2/4}$.

In the language of SUSY QM, the case where zero is an eigenvalue (i.e., $0 \in \mathrm{Spec}(H_-) \cup \mathrm{Spec}(H_+)$) is coined "good SUSY" and when all eigenvalues are strictly positive SUSY is "broken". Recall that for a non vanishing asymptotic behavior of the drift force $W(x)$, the dichotomy between "good" and "broken" SUSY can be discussed using:

$$\text{broken SUSY} \Leftrightarrow \mathrm{sign}\big(\lim_{x\to\infty} W(x)\big) = \mathrm{sign}\big(\lim_{x\to-\infty} W(x)\big).$$

and

$$\text{good SUSY} \Leftrightarrow \mathrm{sign}\big(\lim_{x\to\infty} W(x)\big) \neq \mathrm{sign}\big(\lim_{x\to-\infty} W(x)\big).$$

The two previous alternatives allow to draw the following conclusions concerning the existence of stationary solutions:

1a) In the case of good SUSY, with

$$\mathrm{sign}\big(\lim_{x\to\infty} W(x)\big) = -1 \quad \text{and} \quad \mathrm{sign}\big(\lim_{x\to-\infty} W(x)\big) = 1$$

we have:

$$0 = \inf\{\nu \mid \nu \in \mathrm{Spec}(H_+)\} < \inf\{\nu \mid \nu \in \mathrm{Spec}(H_-)\},$$

and therefore a non-trivial stationary distribution for P (solving $A^\dagger P = 0$) exists but no (non-trivial) stationary flow Q (i.e. $C = 0$) does exist. The solution P equals P_s given by Eq.(7.19) with N being the normalization constant.

1b) In the case of good SUSY, with

$$\mathrm{sign}\big(\lim_{x\to\infty} W(x)\big) = 1 \quad \text{and} \quad \mathrm{sign}\big(\lim_{x\to-\infty} W(x)\big) = -1$$

we have:

$$0 = \inf\{\nu \mid \nu \in \mathrm{Spec}(H_-)\} < \inf\{\nu \mid \nu \in \mathrm{Spec}(H_+)\},$$

and therefore a non-trivial stationary distribution for Q (solving $AQ = 0$) exists ($C \neq 0$) but no (non-trivial) stationary distribution P does exist. The solution Q equals Q_s given by Eq.(7.18).

2) In the case of broken SUSY, there is no (non-trivial) stationary distribution neither for P nor for Q.

Remark. It is worthwhile noting that in the SUSY formalism the "deterministic stability condition", expressed in Eqs.(7.20) and (7.21), correspond exactly to the case 1a) above and expresses the fact that only H_+ possesses a normalizable zero energy ground state eigenfunction.
Example. As an illustration of case 1a, consider the transition rates:

$$\lambda(x) = \frac{1}{2} + \frac{1}{2}\tanh(x), \quad \mu(x) = \frac{1}{2} - \frac{1}{2}\tanh(x). \tag{7.39}$$

The physical relevance of this example for inhomogeneous transmission lines is given in [68]. Note that the interchange of the transition rates yields an example for case 1b. We have $\beta = 1$ and the resulting exogenous drift function $W(x) = -\tanh(x)$ is a special case of the shape invariant, good SUSY, Rosen-Morse II potential (see e.g., table 4.1 in [21]). Apart from the ground state eigenvalue $0 \in \mathrm{Spec}(H_+)$ the spectrum is purely continuous and is given by $\nu = \frac{1}{4} + \tilde{\nu}^2, \quad \tilde{\nu} \geq 0$. We specify the initial conditions by setting $P(x,0) = Q(x,0) = \delta_0(x)$ (corresponding to $x_0 = 0$ and $i_0 = +1$ in Eqs.(7.12,7.13)) where $\delta_0(x)$ is the ordinary delta-function and by setting $P_t(x,0) = Q_t(x,0) = 0$. The solution for P, calculated in [153] (see also [71] model B) reads:

$$P(x,t) = \frac{1}{\cosh(x)}\Big(\frac{1}{\pi} + \frac{\mathrm{e}^{-t/2}}{2\pi}\int_0^\infty \big[\cos(\tilde{\nu}t) + \frac{1}{2\tilde{\nu}}\sin(\tilde{\nu}t)\big] \times\big(\phi^+_{-\tilde{\nu}}(x)\phi^+_{\tilde{\nu}}(0) + \phi^+_{\tilde{\nu}}(x)\phi^+_{-\tilde{\nu}}(0)\big)\,\mathrm{d}\tilde{\nu}\Big) \tag{7.40}$$

where the $\phi^+_{\tilde{\nu}}$ are given in terms of the hypergeometric functions:

$$\phi^+_{\tilde{\nu}}(x) = \exp(i\tilde{\nu}x)\cosh(x)\,{}_2F_1\Big(-1/2, 3/2; 1 + i\tilde{\nu}; \frac{1+\tanh(x)}{2}\Big). \tag{7.41}$$

The SUSY-structure implies that $Q = P_s\overline{Q}$ with $\overline{Q}$ solving Eq.(7.24) wherein W is replaced by $-W$. Hence, for Q we obtain (see [71] model C):

$$Q(x,t) = \frac{\mathrm{e}^{-t/2}}{2\pi}\int_0^\infty \big[\cos(\tilde{\nu}t) + \frac{1}{2\tilde{\nu}}\sin(\tilde{\nu}t)\big] \times\big(\phi^-_{-\tilde{\nu}}(x)\phi^-_{\tilde{\nu}}(0) + \phi^-_{\tilde{\nu}}(x)\phi^-_{-\tilde{\nu}}(0)\big)\,\mathrm{d}\tilde{\nu} \tag{7.42}$$

where the $\phi^-_{\tilde{\nu}}$ are given in terms of the hypergeometric functions:

$$\phi^-_{\tilde{\nu}}(x) = \exp(i\tilde{\nu}x)\cosh(x)\,{}_2F_1\Big(1/2, 1/2; 1 + i\tilde{\nu}; \frac{1+\tanh(x)}{2}\Big). \tag{7.43}$$

7.4 Concluding remarks

Hyperbolic transport equations such as the telegraph equation, describe processes where perturbations in the physical field propagate with finite speed.

This make them more suitable for the modelling of spacial spread of inertial objects than parabolic equations such as the heat equation, where the perturbations propagate with infinite speed. This is most easily seen by comparing the discrete derivations of the hyperbolic respectively the parabolic equations starting from the correlated respectively from the non-correlated random walks. The non-Markovian nature introduced via the inertia (*i.e.* the correlation) into the hyperbolic type equations make them potentially more difficult to handle mathematically than parabolic equations. Hence it is of interest to search for relations simplifying the hyperbolic transport from a mathematical and stochastic point of view. Such a relation between the probability density field and the associated probability flow field has been unveiled in this Chapter allowing for example to identify the transient behavior of both fields.

7.5 Contributions of Chapter 7

- Starting with the Langevin-type equation

$$\dot{X}_t = I_t, \tag{7.44}$$

where I_t is a dichotomous noise taking values in $\{-1, 1\}$ and having exponentially distributed holding times with space-inhomogeneous parameters $\lambda(x) > 0$ (from 1 to -1) and $\mu(x) > 0$ (from -1 to 1) verifying $\lambda(x) + \mu(x) = \beta = const$, we show that the probability density P and the probability flow Q associated to the random evolution X_t verify

$$\begin{pmatrix} \partial_{t,t}^2 + \beta\partial_t & 0 \\ 0 & \partial_{t,t}^2 + \beta\partial_t \end{pmatrix} \mathbf{\Psi} = - \begin{pmatrix} H_- & 0 \\ 0 & H_+ \end{pmatrix} \mathbf{\Psi}, \tag{7.45}$$

where

$$H_\pm := -\partial_{x,x}^2 + \frac{1}{4}W(x)^2 \pm \frac{1}{2}W'(x), \;\; W(x) := \mu(x) - \lambda(x) \tag{7.46}$$

and

$$\mathbf{\Psi}(x,t) := \exp\left[\frac{1}{2}\left(\int_0^x W(y)dy\right)\right] \begin{pmatrix} Q(x,t) \\ P(x,t) \end{pmatrix}. \tag{7.47}$$

- We remark that the above relations eqs. (7.45) and (7.47) are identical to the ones studied in supersymmetric (SUSY) Quantum Mechanics and draw the relevant transient and stationary conclusions. As far as transience is concerned, the SUSY formalism is well adapted to discuss the relaxation speed to equilibrium via the spectral properties of $H_\pm$. The relation also shows that questions related to the existence of stationary solutions can be handled by a simple asymptotic investigation of the drift force $W(x)$. The formalism provides us moreover with a whole class of exactly solvable potentials studied in great detail in SUSY QM.

8

Relative Entropy and Efficiency Measure for diffusion-mediated transport processes

Summary. We propose an efficiency measure for diffusion-mediated transport processes including molecular-scale engines such as Brownian motors (BMot) moving in ratchet potentials acting as mechanical "rectifiers". The efficiency measure is based on the concept of "minimal energy required to complete a task" and is defined via a class of stochastic optimal control problems. The underlying objective function depends on both the external force field (i.e. the fluctuation rectifier in the case of BMot) and the amplitude of the environmental noise. Ultimately, the efficiency measure can be directly interpreted as the relative entropy between two probability distributions, namely: the distribution of the particles in presence of the external rectifying force field and a reference distribution describing the behavior in absence of the rectifier.

8.1 Introduction

Despite to an already vast available literature, the fact that micro-particles immersed in a noisy environment can be transported by an ad-hoc rectification of the fluctuations, continue to attract attention directed towards applications [123]. The operations of these diffusion-mediated devices which essentially act as mechanical diodes, require basically *i*) a fluctuating environment and *ii*) a fluctuation rectifier which is driven by an external energy input. This mechanism is able to generate a net particles current (see figure 8.1 for a simple realization of a ratchet mechanism) which can be sustained even in the presence of an opposing force *i.e.*, an external load. It is therefore possible to extract a net useful work from these devices, a property appealing for applications in the molecular and microscopic size ranges.

The possibility to extract work legitimates to use the word **motors** and also suggests that a suitable efficiency measure, namely the **motor efficiency** (ME) should be defined for these devices – this is the goal of the present contribution.

Yet, the issue of efficiency of molecular motors has been and remains an important topic of its own (see e.g., [123] Chapt.6.9 and [112, 133]). The main

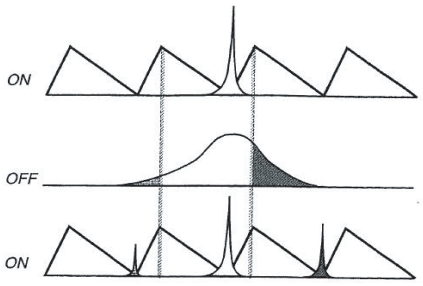

Fig. 8.1. The so-called flashing ratchet at work. The figure represents three snapshots of the potential and the density of particles and is taken from J.M.R. Parrondos and S. Dinis recent paper [113] (2004). Initially the potential is on (upper figure) and all the particles are located around one of the minimum of the potential. Then the potential is switched off and the particles diffuse freely. Once the potential is connected again, the particles in the darker region move to the right-hand minimum whereas those within the small grey region move to the left. Due to the asymmetry of the potential, the ensemble of particles move, in average, to the right.

difficulty here is that on the microscopic scale the fluctuations do, simultaneously, favor and hinder the transport process. The external energy injected into the system is indeed dissipated via two mechanisms, *i*) the driving energy itself responsible for the transport process and *ii*) the heating of the medium which hinders the directed transport thanks to the fluctuation-dissipation relation.

In view of the conjugate actions played by the fluctuations, the study of energetics requires a precise formulation of what the energy output of the system really is. Here we essentially adopt the point of view of I. Dérenyi et al. [74] which identifies the energy output with the *minimum energy input* E_{in}^{min} required to accomplish the same task as the molecular motor. Following [74], the generalized efficiency η is defined as:

$$\eta = E_{in}^{min}/E_{in}, \tag{8.1}$$

where E_{in} is the external energy input.
The aim of this chapter is to derive a *systematic method*, to characterize the efficiency of the molecular motor. This will be achieved via a stochastic optimal control approach in which the objective function combines the conjugate actions of transport and dissipation.
Formally, assume that a molecular motor operates according to the Langevin dynamics:

$$\gamma \mathrm{d}X_t = (-V'(X_t, t) - F)\mathrm{d}t + \sigma(X_t, t)dB_t, \tag{8.2}$$

which describes a Brownian particle in an overdamped regime (*i.e.* inertia is neglected). The stochastic equation is interpreted in the Stratonovich sense

(see [101] for an account of Itô-Stratonovich modelling in the context of molecular motors) and models the so-called Brownian motor (BMot). Here dB_t stands for $1D$ standard Brownian motion, $\sigma(x,t) = \sqrt{2\gamma k_B T(x,t)}$ controls the diffusion process with k_B being Boltzmann's constant, $T(x,t)$ the absolute temperature field and γ is the viscous friction coefficient. F is a constant force modelling an external load and $V(x,t)$ is the "ratchet" potential through which the fluctuations are "rectified".
The net effect of the rectifying force given by $-V'(X_t,t)$ is to drive an initial probability distribution δ_{x_0} at time $t=0$ to a final distribution μ_τ at time $\tau > 0$. In practice, there is a great freedom in choosing rectifying forces able to complete this task. Hence the natural idea behind the efficiency concept is to compare $-V'(x,t)$ to an optimal drift field $u(x,t)$ which operates a similar task (namely transporting δ_{x_0} to μ_τ within a time τ) and simultaneously minimizes the objective functional:

$$u \mapsto J_\tau(u) = \frac{1}{2}\mathbb{E}_{x_0}\int_0^\tau \Big(\frac{u(X_t^u,t)}{\sigma(X_t^u,t)}\Big)^2 \mathrm{d}t, \tag{8.3}$$

where X_t^u is evolving as:

$$\gamma \mathrm{d}X_t^u = (u(X_t^u,t) - F)\mathrm{d}t + \sigma(X_t^u,t)dB_t. \tag{8.4}$$

Note that the objective functional (sometimes called cost functional) depends on the stochastic dynamics via both the drift u and the diffusion σ fields. Due to the structure of the cost functional, transport with small diffusion is very costly – a property which reflects the diffusion-mediated transport processes where fluctuations directly participate to the driving of particles. Define now the optimal rectifier $u^*(x,t)$ force field to be the one, able to achieve the transporting task, namely $\delta_{x_0} \mapsto \mu_\tau$ while minimizing the global value function $J_\tau(u^*)$ given by Eq. (8.3). With such an optimal rectifier at hand, the generalized efficiency of a BMot subject to a potential V satisfying $0 < J_\tau(V') < \infty$, is now simply defined as:

$$\eta(\tau) = \frac{J_\tau(u^*)}{J_\tau(V')}. \tag{8.5}$$

The ME $\eta(\tau)$ compares the expected costs incurred by both the optimal trajectories $X_t^{u^*}$ and the actual motor trajectories X_t and therefore takes fully into account the probabilistic nature of the underlying process. This is, we believe, the conceptual advantage of the present approach over the one proposed in [74] where the minimum energy input is defined via a purely mechanical view not explicitly invoking the underlying stochastic dynamics.
From a mathematical point of view, the efficiency parameter given by Eq. (8.5) is well defined. It directly relies on the possibility to assign to given initial and final distributions (here δ_{x_0} and μ_τ) a unique Markov process – a problem first formulated by Schrödinger in [131]. A mathematically rigorous exposition of this program is given by P. Dai Pra [119]. The optimal control

interpretation of the stochastic dynamics is thereby realized by the concept of logarithmic transformations introduced by Jamisson [78] and Flemming [46] (see also 5.4.). Using this approach, the minimal value $J_\tau(u^*)$ – entering the definition of $\eta(\tau)$ – coincides with the relative entropy $K(\mu_\tau, \overline{\mu}_\tau)$ between the distributions μ_τ and $\overline{\mu}_\tau$ with $\overline{\mu}_\tau$ being the probability distribution at time τ describing the position $\overline{X}_\tau$ of a particle evolving under the control free dynamics

$$\gamma \mathrm{d}\overline{X}_t = -F\mathrm{d}t + \sigma(\overline{X}_t, t)\mathrm{d}B_t, \quad X_0 = x_0 \in \mathbb{R}. \tag{8.6}$$

The efficiency of the Brownian motor then reads as

$$\eta(\tau) = K(\mu_\tau, \overline{\mu}_\tau)/J_\tau(V'). \tag{8.7}$$

This way of writing the ME, which is equivalent to Eq. (8.5), does not explicitly use the underlying control and is therefore intrinsic. Its connection with the control problem relies on the remarkable property that both:

i) the quasi-free evolution, *i.e.* the evolution in absence of an external potential given by Eq. (8.6) and
ii) the evolution under the optimal control u^*

produce identical families of "most probable paths" [119]. The concept of "most probable path" is based on a variational principle applicable for Langevin equations driven by White Gaussian Noise. The associated transition probability measures (*i.e.* the solutions of the relevant Fokker-Planck equations) can be expressed as the weighted sum over random trajectories with given initial and final conditions. The relative weights entering into the summation directly depend upon the drift and the diffusion coefficients and are expressed by the Onsager-Machlup functional [32]. Intuition suggests that the more probable a particular trajectory is, the more effectively it will contribute to the global value function. The fact that the most probable path under u^* coincides with the most probable path under the quasi-free dynamics physically shows that the optimal control u^* does in fact interfere as little as possible with the most probable trajectory of the quasi-free dynamics.
The chapter is organized as follows. In section 2, we specify the hypothesis of the BM-model, state the optimal control problem and recall its solution. In section 3 we calculate the efficiency for a generic class of examples and indicate how to construct optimal rectifiers.

8.2 Problem Formulation

Consider the controlled diffusion process $X^u(t)$ defined on some probability space $(\Omega, \mathcal{F}, \mathbb{P})$ that solves the following Stratonovich stochastic differential equation:

$$\gamma \mathrm{d}X^u_t = (u(X^u_t, t) - F)\mathrm{d}t + \sigma(X^u_t, t)\mathrm{d}B_t. \tag{8.8}$$

Formally, the above Langevin equation is obtained by replacing in Eq. (8.2) the force field $-V'(x,t)$ by a control $u(x,t)$. The efficiency measure to be constructed relies on the following optimal control problem:

Problem (P)**.** Find an admissible control $u^*(x,t)$ such that:

(1) $X_0^{u^*}$ is distributed according to δ_{x_0} and $X_\tau^{u^*}$ according to μ_τ,
(2) between all admissible controls satisfying (1), the control u^* minimizes the energy cost functional:

$$u \mapsto J_\tau(u) = \frac{1}{2}\mathbb{E}\int_0^\tau \Big(\frac{u(X_t^u,t)}{\sigma(X_t^u,t)}\Big)^2 \mathrm{d}t. \tag{8.9}$$

Remarks.

a) In order for Eq. (8.8) to admit a unique, t-continuous strong solution $X^u(t)$, σ and u must satisfy the following classical assumptions: σ and u are linearly bounded in x uniformly for $t \in [0,\tau]$ and satisfy a Lipschitz condition in x for every fixed $t \in [0,\tau]$. These conditions ensure the uniqueness of X_t^u and are supposed to hold from now on. In the autonomous case i.e., when both u and σ do not explicitly depend on time, existence and uniqueness of the solution are already guaranteed for $u, \sigma \in \mathcal{C}^1(\mathbb{R})$ [72].
b) A control $u(X_t(\cdot),t) : \Omega \to \mathbb{R}$ is admissible if: (i) u satisfies the regularity conditions stated in a), (ii) u is adapted to the filtration $\mathcal{F}_t = \sigma\{X_t^u\}$ and (iii) $J_\tau(u) < \infty$. The potential V entering into Eq. (8.2) is supposed to be admissible and non trivial i.e. $J_\tau(V') > 0$.
c) A similar approach also holds for non-deterministic initial distributions μ_0. The only restriction on μ_0 is the existence of a finite second moment, i.e. $\int x^2 \mu_0(\mathrm{d}x) < \infty$. In this case, the problem (P) does still have a well defined solution.
d) The Stratonovich stochastic differential equation (8.8) – commonly encountered in physical modelling where the White Gaussian Noise is viewed as the limit of shortly correlated colored noises – is equivalent to the Itô stochastic differential equation:

$$\gamma \mathrm{d}X_t^u = \big[u(X_t^u,t) - F + \frac{1}{2}\sigma'(X_t^u,t)\sigma(X_t^u,t)\big]\mathrm{d}t + \sigma(X_t^u,t)dB_t \tag{8.10}$$

which, due to the fact that the noise term is a martingale, is more frequently used in control theory.

For $0 \le s < t \le \tau$ and $y, x \in \mathbb{R}$, denote by $q(s,y,t,x)$ the fundamental solution to the backward Fokker-Planck equation of the Markov process $\overline{X}_t$ defined in Eq. (8.6):

$$\frac{\partial}{\partial t} q(s,y,t,x) = Lq(s,y,t,x), \quad 0 \le s < t \le \tau \tag{8.11}$$

$$q(s,y,s,x) = \delta_{x,y} \tag{8.12}$$

where the operator $L(\cdot)$ is:

$$L(\cdot) = [-F + \frac{1}{2}\sigma'(x,t)\sigma(x,t)]\frac{\partial(\cdot)}{\partial x} + \frac{1}{2}\sigma(x,t)^2\frac{\partial^2(\cdot)}{\partial x \partial x}. \tag{8.13}$$

For μ and ν, two probability distributions on the real line, write $\mathrm{d}\nu/\mathrm{d}\mu$ for the Radon-Nykodim derivative of ν with respect to μ (*i.e.* ν is assumed to be absolutely continuous with respect to μ). Introduce now the relative entropy (also known as the Kullback "distance" [88]) $K(\mu,\nu)$ which quantifies the "discrepancy" between μ and ν:

$$K(\mu,\nu) = \int_{\mathbb{R}} \log\left(\frac{\mathrm{d}\mu}{\mathrm{d}\nu}\right)\mathrm{d}\mu. \tag{8.14}$$

The "distance" $K(\cdot,\cdot)$ is commonly used for fitting and classifying statistical models, hypothesis testing and risk minimization. In the context of our minimization problem (P), we have the following central result (Theorem 3.1 in [119]):

Theorem. Suppose that $K(\mu_\tau, \overline{\mu}_\tau) < \infty$ and define $h : \mathbb{R} \times [0,\tau] \to \mathbb{R}$ by

$$h(x,t) = \int_{\mathbb{R}} q(t,x,\tau,z)\frac{\mathrm{d}\mu_\tau}{\mathrm{d}\overline{\mu}_\tau}(z)\mathrm{d}z.$$

Then

a) $u^*(x,t) = \sigma^2(x,t)\frac{\partial}{\partial x}\log(h(x,t))$ solves the control problem (P) and
b) $J_\tau(u^*) = K(\mu_\tau, \overline{\mu}_\tau)$.

This result has three implications of practical relevance for the transport processes under study, namely:

1) It establishes that the ME $\eta(\tau)$ takes values between zero and one (remember that $J_\tau(u)$ is positive). Moreover, $\eta(\tau)$ takes its maximum value 1 exactly if the motor realizes its task ($\delta_{x_0} \to \mu_\tau$) in the energetically most favorable way.
2) It allows an intrinsic (*i.e.* control free) definition of the efficiency:

$$\eta(\tau) = K(\mu_\tau, \overline{\mu}_\tau)/J_\tau(V'), \tag{8.15}$$

   which relates the relative entropy between the distribution of the particle subject to V and the distribution of the quasi-free particle with the expected cumulated costs $J_\tau(V')$.
3) It furnishes an explicit formula for u^* which can be used as a theoretical guideline to physically realize *optimal* motors.

8.3 Applications for a class of pulsating ratchets

In the couple of examples which follow, we suppose that the Brownian particle is released at time $t = 0$ from $X_0 = 0$ and evolves under the isothermal dynamics:

$$\gamma \mathrm{d}X_t = \big[-V'(X_t, \varphi(t)) - F \big] \mathrm{d}t + \gamma \sqrt{2D_0} dB_t, \tag{8.16}$$

with $D_0 = \frac{k_B T}{\gamma}$ constant. The next example 8.3.1 deals with a pulsating potential $V(x, \varphi(t))$ which is space periodic with period L and where $\varphi(t)$ is either a periodic or a stochastic function of time. We calculate η in the central limit regime. In 8.3.2 we impose the optimal efficiency $\eta = 1$ (*i.e.* the BMot operates under optimal conditions) and derive the associated optimal force field.

8.3.1 The efficiency for a pulsating ratchet in the central limit regime

Consider a Brownian particle evolving according to the working model for pulsating ratchets given by Eq. (8.16) (see e.g., [123] Chapt. 3.3 for a classification scheme for BMot). We make the simplifying assumption that $\varphi(t)$ is either periodic in t with a unique periodic long-time behavior or a stationary stochastic process independent of the Brownian motion dB_t. This allows, on a sufficiently coarse grained space-scale ($\gg L$), to approximately view the evolution as the succession of single, independent and identically distributed hopping events ([123] p.88). Invoking the central limit theorem, the particle distribution for large τ approaches a Gaussian measure μ_τ with density:

$$f(x, \tau) = \frac{1}{\sqrt{4\pi D_{eff} \tau}} \exp\big(- \frac{[(a\tau - x)^2]}{4 D_{eff} \tau} \big), \tag{8.17}$$

where $a = \lim_{t \to \infty} X_t / t$ is the average particle current and $D_{eff} = \lim_{t \to \infty} \big(\langle X_t^2 \rangle - \langle X_t \rangle^2 \big) / (2t)$ is the effective diffusion coefficient – both quantities can be measured in actual applications [146].
According to Eq. (8.6), the quasi-free particle evolves under the dynamics:

$$\overline{X}_t = -\frac{F}{\gamma} t + \sqrt{2D_0} B_t. \tag{8.18}$$

Its distribution $\overline{\mu}_\tau$ at τ is therefore a Gaussian measure with density:

$$\overline{f}(x, \tau) = \frac{1}{\sqrt{4\pi D_0 \tau}} \exp\big(- \frac{[x - \frac{F}{\gamma}\tau]^2}{4 D_0 \tau} \big). \tag{8.19}$$

The relative entropy of the two Gaussian measures Eqs. (8.17) and (8.19) reads as:

$$\begin{aligned} K(\mu_\tau, \overline{\mu_\tau}) &= \int_{\mathbb{R}} \ln \big(f(x,\tau) / \overline{f}(x,\tau) \big) f(x,\tau) \mathrm{d}x \\ &= \frac{(F/\gamma - a)^2}{4D_0} \tau + \\ &\quad \Big\{ \frac{1}{2} \ln \big(\frac{D_0}{D_{eff}} \big) + \frac{D_{eff} - D_0}{2D_0} \Big\}. \end{aligned} \tag{8.20}$$

This expression, valid for large τ, enables to separately appreciate the influence of the potential V on the particles current and on the rectifying process. The first term describes the external energy input necessary to maintain the particles current a. The symmetry in the difference $F/\gamma - a$ shows that exceeding or undergoing the quasi-free current F/γ by the amount $|F/\gamma - a|$ requires the same energy input. The second contribution – non-negative as the former one – is related to the part of the energy input required to get an effective diffusion D_{eff}. In contrast to the current difference $F/\gamma - a$, the diffusion difference $D_0 - D_{eff}$ contributes non-symmetrically to the relative entropy. Setting:

$$H(D_{eff}) := \ln\big(\frac{D_0}{D_{eff}}\big) + \frac{D_{eff} - D_0}{D_0}, \tag{8.21}$$

we indeed have:

$$H(D_0 - \Delta) > H(D_0 + \Delta), \quad \Delta \in (0, D_0). \tag{8.22}$$

Hence, rectifying the diffusion to ensure that $D_{eff} = D_0 - \Delta$ with $\Delta \geq 0$ costs more than to let it increase by the same amount (i.e. $D_{eff} = D_0 + \Delta$). In the limiting case where V "ties down" the effective diffusion to zero, we have $H(0) = \infty$ and consequently, the relative entropy $K(\mu_\tau, \overline{\mu_\tau})$ becomes infinite. On the other hand, the cost functional for the given potential is:

$$\begin{aligned} J_\tau(V') &= \frac{1}{4\gamma k_B T_0}\mathbb{E}\int_0^\tau V'(X_t)^2 \mathrm{d}t \\ &= \frac{\tau}{4\gamma^2 D_0}\mathbb{E}\frac{1}{\tau}\int_0^\tau V'(X_t)^2 \mathrm{d}t, \end{aligned} \tag{8.23}$$

which due to ergodicity behaves asymptotically as:

$$J_\tau(V') \simeq \frac{\tau}{4\gamma^2 D_0}\langle V'^2\rangle, \tag{8.24}$$

where the ensemble mean $\langle V'^2\rangle$ is taken over one space period of V. Using Eqs. (8.20) and (8.24), we have:

$$\eta(\tau) = \frac{K(\mu_\tau, \overline{\mu}_\tau)}{J_\tau(V')} = \frac{(F - \gamma a)^2}{\langle V'^2\rangle} + \mathcal{O}(\frac{1}{\tau}) \tag{8.25}$$

where explicitly the $\mathcal{O}(\frac{1}{\tau})$ term is given by:

$$\mathcal{O}(\frac{1}{\tau}) = \frac{1}{\tau}\frac{2\gamma^2 D_{eff}}{\langle V'^2\rangle}\big(1 + \frac{D_0}{D_{eff}}\big[\ln\big(\frac{D_0}{D_{eff}}\big) - 1\big]\big). \tag{8.26}$$

In the central limit regime, reached for $\tau \to \infty$, only the part contributing to the transport process influences the efficiency measure, namely:

$$\eta(\tau) = \frac{(F - \gamma a)^2}{\langle V'^2\rangle}, \quad \text{for,} \quad \tau \to \infty. \tag{8.27}$$

Remarks.

a) The efficiency $\eta(\tau)$ compares an effective driving force, namely the difference between the load and the drag force with the external force field.
b) The parameters F, γ, V', D_0, a and D_{eff} entering into Eqs. (8.26) and (8.27) are experimentally measurable as it is discussed in [146]. Hence, the efficiency $\eta(\tau)$ can be calculated for actual applications. Note in addition that the time series of motor positions, measurable with the current bioengineering technology, allow to solve a reverse problem, namely to reconstruct the rectifying potential V [81].
c) When $\varphi(t) \equiv 0$, Eq. (8.16) models a so-called tilted pulsating potential. In this case the asymptotic analysis can be pushed further. Indeed in this cases both a and D_{eff} are analytically related to the modelling parameters entering into Eq. (8.16) through [110]:

$$a = \frac{1 - e^{-LF/k_BT}}{\frac{1}{L}\int_0^L \mathrm{d}x I_+(x)}, \tag{8.28}$$

$$D_{eff} = D_0 \frac{\frac{1}{L}\int_0^L \mathrm{d}x I_+(x)^2 I_-(x)}{\left(\frac{1}{L}\int_0^L \mathrm{d}x I_+(x)\right)^3} \tag{8.29}$$

with

$$I_\pm(x) = \frac{1}{D_0}\int_0^L \mathrm{d}y \exp(\pm V(x) \mp V(x \mp y) - yF)/(k_BT). \tag{8.30}$$

From Eq. (8.28) we directly see that for a vanishing load $F \to 0$, the efficiency consistently vanishes. Indeed no work can be done in absence of load.

8.3.2 Conceiving efficient Brownian Motors.

As stated by Derényi et al. in [74], it is only a matter of time before molecular motors will be currently manufactured. One therefore is potentially interested in building highly efficient transport motors. Starting from the quasi-free dynamics:

$$\mathrm{d}\overline{X}_t = -\frac{F}{\gamma}\mathrm{d}t + \sqrt{2D_0}\mathrm{d}B_t \tag{8.31}$$

with F, γ and D_0 constant, let us construct an optimal force field $u^*(x,t)$ realizing $\eta(\tau) = 1$. The fundamental solution to the associated backward evolution equation Eq. (8.12) is:

$$q(s,y,t,x) = \frac{1}{\sqrt{4\pi D_0(t-s)}} \exp\Big(-\frac{[((x-y) - \frac{F}{\gamma}(t-s))^2]}{2D_0(t-s)}\Big) \tag{8.32}$$

and $\overline{\mu}_\tau$ is Gaussian with density $\overline{f}(x,\tau) = \int_{\mathbb{R}} q(0,y,\tau,x)\delta_0(\mathrm{d}y) = q(0,0,\tau,x)$. The minimum energy control $u^*(x,t)$ is now:

$$u^*(x,t) = 2D_0 \frac{\partial}{\partial x} \ln\Big(\int_{\mathbb{R}} q(t,x,\tau,z) \frac{f(z,\tau)}{q(0,0,\tau,z)} \mathrm{d}z \Big) \tag{8.33}$$

which after lengthy but elementary calculations yields:

$$u^*(x,t) = \frac{D_0\Big(\frac{F}{\gamma}t - x - \tau(a - \frac{F}{\gamma})\Big)}{D_0(\tau - t) + D_{eff}\tau}. \tag{8.34}$$

Setting $\frac{F}{\gamma} = a$ and $D_{eff} = D_0$ and prolonging $u(x,t)$ periodically in x resp. t with period L resp. τ to $\mathbb{R} \times \mathbb{R}_+$, we find the optimal drift field:

$$u^*(x,t) = \frac{at - x}{2\tau - t}, \;\; 0 \le x \le L, \;\; 0 \le t \le \tau$$
$$u^*(x + L, t) = u^*(x,t), \;\; u^*(x, t + \tau) = u^*(x,t).$$

As it stands, $u^*(x,t)$ is linear in x and depends explicitly on time. Note that the space-linearity is expected from the fact that in this case the initial and final measures are both Gaussian. The time-dependent drift field $u^*(x,t)$ defines an evolution belonging to the class of travelling ratchets (according to the classification in [123]) and might serve as a simple guideline in the attempts to actually realize isothermal molecular motors.

8.4 Concluding remarks

The stochastic optimal control formalism is well suited to define an efficiency measure for diffusion-mediated transport processes governed by the Langevin dynamics. The objective function to be minimized combines, in a single functional, the competing effects of the drift and diffusion forces responsible for the transport process. The explicit construction of the optimal force field that minimizes the objective functional, offers a rigorous and systematic way to conceive efficient diffusion-mediated transport devices.

8.5 Contributions of Chapter 8

- The main contribution of this chapter is to connect stochastic control theory and diffusive transport. The connection is realized via a new concept for the transport efficiency measure which is defined using stochastic optimal control techniques.
- The efficiency concept is applied to a class of pulsating ratchets defined by the diffusive dynamics (see eq. 8.16 for details):

$$\gamma \mathrm{d}X_t = \big[-V'(X_t, \varphi(t)) - F \big] \mathrm{d}t + \gamma \sqrt{2D_0} dB_t. \tag{8.35}$$

  For this case, the efficiency takes – in the central limit regime – the following form:

$$\eta(\tau) = \frac{(F - \gamma a)^2}{\langle V'^2 \rangle}, \quad \text{for } \tau \to \infty. \tag{8.36}$$

In words, the efficiency $\eta(\tau)$ compares the square of the effective driving force, namely the difference between the load F and the drag force γa with the average of the squared external force field V'.

- We show that diffusive transport using the time-dependent force field $u^*(x,t)$

$$u^*(x,t) = \frac{at - x}{2\tau - t}, \quad 0 \le x \le L, \quad 0 \le t \le \tau$$
$$u^*(x + L, t) = u^*(x,t), \quad u^*(x, t + \tau) = u^*(x,t).$$

is optimal in the sense of our definition in case the initial and final measures are both Gaussian.

Part IV

Conclusions and Perspectives

9

Conclusions and perspectives in a word on complexity

In order to understand things, science has proceeded for a long time by subdividing problems into smaller pieces and by coming to know those pieces completely. This programme has met with considerable success in many instances, but it fails to account for properties that emerge from the interrelation between constituents that can be seen in the system as a whole only [132]. Systems with emergent properties are indeed more than the sum of their components. In a socio-ecological context such a system is given by the industrial revolution – our introductory example. A typical report on the history of the industrial revolution describes the probable interplay between a succession of events. Each event has a small probability and limited impact in itself. Their juxtaposition and chaining however lead to the observed global phenomenon. During the last 30 years, the study of such emergent properties has made popular the concept of complex systems in various scientific fields [136]. The concept is based on systemic approaches (also synergetic approaches) which include multi-scale analysis and the classification of critical phenomena as bifurcations between phases [137, 61]. A glance at the available research literature in flow and production engineering shows that this system approach is less well established than in the Natural Sciences. A worthwhile exception is the holistic program presented in Warneckes "The Fractal Company" [147] (1993). The author exposes convincingly the need for new approaches and directions in performance optimization, staff management and manufacturing structures. Existing forms of performance optimization have indeed attained a degree of sophistication, where every supplementary effort offers only diminishing marginal utility.
The quest for new approaches in manufacturing modelling has been a leitmotif during the realization of this work. The fairly new analogies and connections presented here include:

Chapter 3. A connection between production flows and car traffic via optimal velocity models.

Chapter 4. A rigorous calculation of the "optimal velocity" strategy using optimal stochastic control techniques.
Chapter 5. A multi-scale analysis applied to car traffic and serial production lines.
Chapter 6. An analogy between the outflow process of a merge system and the flow dynamics of cars at the narrowing of a multi-lane road into a one-lane road.

These analogies and connections permitted us to add to the realm of stochastic transport the following theoretical contributions:

Chapter 7. We reported on the structural similarity between density and flow variables in a inhomogeneous hyperbolic transport model which is also encountered in Quantum Mechanics.
Chapter 8. We established a connection between the efficiency concept of diffusion mediated transport and stochastic optimal control.

These 8 points do certainly not exhaust all the manifold aspects of production systems and stochastic transport processes. They in fact show that there is plenty of research to do with benefic implications for both, the engineering and the scientific community. To be more concrete, let us mention a few open problems based on the several chapters which compose this work:

Chapter 3. The analogy with traffic theory led us to the notions of stable and unstable flow phases in production lines governed by a dimensionless flow parameter.
- Can we extend these notions to a production line where we fully take into account the prone to failure character of the machines?
- In principle, the optimal production rate model given by coupled maps dynamics can be extended to production systems with arbitrary topology including feedback loops and multiplexing structures. Can we distinguish and characterize different flow phases in such an extended case?

Chapter 4. The optimal control of the two-stage failure prone production line led us to the notion of four thresholds control.
- Is an ad hoc four-thresholds control for longer tandem lines capable to outperform other already existing controls?
- If this is the case, can we develop accurate aggregation methods for longer lines which reduce the production planing problem for the whole line to the two stage problem and can we still calculate the four-thresholds for the intermediate buffers?

Chapter 5. The multi-scale analysis is based on a microscopic model including the kinetic features of migration, reaction and collision.
- Can we do the multi-scale analysis when adding to these features a blocking mechanism *i.e.*, an extra collision term which prevent the hopping particles not only from being too close to each other but also from being too far away from each other?

Chapter 6. The outflow process of the merge system is based on the FIFO (first in first out) assumption and does not take into account friction forces between out-flowing items.

- Can we deduce the stationary output flow from a merge when the FIFO assumption is relaxed?
- Can we deduce the stationary output flow from a merge when the interactions not only cause outflow delays (waiting "politely" your turn to leave at the exit) but frictions ("fighting" for your turn to leave at the exit)?

Chapter 7. The probability density and the associated probability flow of a non-diffusive space-inhomogeneous transport process are supersymmetrically related.

- Can we realize supersymmetric density flow relations for jump diffusions and derive exactly solvable examples?
- Can we use the supersymmetric relation to construct simple ratchet like systems – based on space-inhomogeneous switching rates – which deliver prescribed stationary particles flows?

Chapter 8. The proposed efficiency measure for diffusion mediated transport is connected to the notion of (information theoretical) relative entropy and the optimal transport of probability masses.

- Can we connect the efficiency measure η to the existing efficiency concepts based on the thermodynamical entropy?
- Can we use the formalism of optimal (probability mass) transport to generalize the efficiency concept to non-diffusive stochastic processes?

It would be embarrassing to give to these questions a general research direction. However, if I was asked what is my best guess for new promising concepts to tackle with complex manufacturing systems and transport processes my answer would certainly include "Multi-agent network systems". They form a vivant branch in the realm of interacting many-body systems, where the interacting parts are doted with specific decision-making capacities. This concept seems to me viable in the long term and will form one of my personal research interests for the near future.

Part V

Appendix

10

Appendix Chapter 4

In the setting of chapter 4, we derive the stationary CDF's for the four remaining possible configurations (2) $z < Y < y < Z$, (3) $Y < z < y < Z$, (4) $Y < z < Z < y$, and (5) $z < Y < Z < y$ in case $v_1^+ = v_2^+$. The case $v_1^+ \neq v_2^+$ can be treated analogously.

(2) Fix the configuration $z < Y < y < Z$ in $[0, H]$. According to eqs. (4.16-4.18) the control-scheme in table (4.1) has to be replaced by the scheme in table (10.1). The thresholds ordering $z < Y < y < Z$ affects the C-K

	$0 < x <$	$z < x <$	$\mathbf{Y} < x <$	$\mathbf{y} < x <$	$Z < x < H$
Control $u(x,1,1)$	(v_1^+, v_2^-)	(v_1^+, v_2^+)	(v_1^+, v_2^+)	(v_1^+, v_2^+)	(v_1^-, v_2^+)
Control $u(x,1,0)$	$(v_1^+, 0)$	$(v_1^+, 0)$	$(\mathbf{v_1^-}, \mathbf{0})$	$(v_1^-, 0)$	$(v_1^-, 0)$
Control $u(x,0,1)$	$(0, v_2^-)$	$(0, v_2^-)$	$(\mathbf{0}, \mathbf{v_2^-})$	$(0, v_2^+)$	$(0, v_2^+)$
	$z^1 \quad D^1$	$z^2 \quad D^2$	$\mathbf{z^3} \quad \mathbf{D^3}$	$\mathbf{z^4} \quad D^4$	$z^5 \quad D^5 \quad z^6$

Table 10.1. The control-scheme for fixed thresholds $z^2 = z$, $z^3 = Y$, $z^4 = y$, $z^5 = Z$ with $0 < z < Y < y < Z < H$. The differences from the scheme given in table 4.1 are written in bold characters.

equations for $x \in D^3$ and the matching constraints at z^3 and z^4. Therefore, the stationary CDF is as before except that one has to change the rates in eqs. (4.60) for $k = 3, 4$ and in eq. (4.47) for $k = 3$ according to the rates given in table (10.1).

(3) Fix the configuration $Y < z < y < Z$ in $[0, H]$. According to eqs. (4.16-4.18) the control-scheme in table (4.1) has to be replaced by the scheme in table (10.2). With respect to the control-scheme 4.1, the thresholds ordering

	$0 < x <$	$\mathbf{Y} < x <$	$\mathbf{z} < x <$	$\mathbf{y} < x <$	$Z < x < H$
$u(x,1,1)$	(v_1^+, v_2^-)	$(\mathbf{v_1^+}, \mathbf{v_2^-})$	(v_1^+, v_2^+)	(v_1^+, v_2^+)	(v_1^-, v_2^+)
Control $u(x,1,0)$	$(v_1^+, 0)$	$(\mathbf{v_1^-}, \mathbf{0})$	$(\mathbf{v_1^-}, \mathbf{0})$	$(v_1^-, 0)$	$(v_1^-, 0)$
$u(x,0,1)$	$(0, v_2^-)$	$(0, v_2^-)$	$(\mathbf{0}, \mathbf{v_2^-})$	$(0, v_2^+)$	$(0, v_2^+)$
	z^1 D^1	$\mathbf{z^2}$ $\mathbf{D^2}$	$\mathbf{z^3}$ $\mathbf{D^3}$	$\mathbf{z^4}$ D^4	z^5 D^5 z^6

Table 10.2. The control-scheme for fixed thresholds $z^2 = Y$, $z^3 = z$, $z^4 = y$, $z^5 = Z$ with $0 < Y < z < y < Z < H$. The differences from the scheme given in table 4.1 are written in bold characters.

$Y < z < y < Z$ affects the C-K equations for $x \in D^k$ $k = 2, 3$ and the matching constraints at z^2, z^3 and z^4. Therefore, the stationary CDF is as before except that one has to introduce the following modifications:

- for $x \in D^2$, the solution is given by eqs. (4.42) and (4.44) (with $k = 2$) in case Eq. (4.43) is satisfied and by Eqs. (4.42) and (4.45) (with $k = 2$) in case it is not. In both cases, the rates are given in table (10.2) and the constants S_2 and K_2 are related by Eq. (4.40).
- for $x \in D^3$ the solution is given by Eqs. (4.47) and (4.48) in case $\lambda_2\mu_1 v^3_{1;(1,0)} \neq \lambda_1\mu_2 v^3_{2;(0,1)}$ and by Eqs. (4.47) and (4.50) in case $\lambda_2\mu_1 v^3_{1;(1,0)} = \lambda_1\mu_2 v^3_{2;(0,1)}$. In both cases, the rates are given in table (10.2).
- matching at $z^2 = Y$. As $v_1^+ > v_2^-$, the matching condition at Y is given by Eq. (4.62) for $k = 2$ and with the rates according to table (10.2).
- matching at $z^3 = z$. The matching condition at z is given by Eq. (4.54) for $k = 3$ and with the rates according to table (10.2). In addition, the threshold probability z_{11} is given by Eq. (4.52) with $k = 3$.
- matching at $z^4 = y$. The matching condition at Y is given by Eq. (4.60) for $k = 4$ and with the rates given in table (10.2).

(4) Fix the configuration $Y < z < Z < y$ in $[0, H]$. According to Eqs. (4.16-4.18) the control-scheme in table (4.1) has to be replaced by the scheme in table (10.3). With respect to the control-scheme 4.1, the thresholds ordering $Y < z < Z < y$ affects the C-K equations for $x \in D^k$ $k = 2, 3, 4$ and the matching constraints at z^2, z^3, z^4 and z^5. Therefore, the stationary CDF is as before except that one has to introduce the following modifications:

- for $x \in D^2$ the solution is given by Eqs. (4.42) and (4.44) (with $k = 2$) in case Eq. (4.43) is satisfied and by Eqs. (4.42) and (4.45) (with $k = 2$) in case it is not. In both cases, the rates are given in table (10.3) and the constants S_2 and K_2 are related by Eq. (4.40).

	$0 < x <$	$\mathbf{Y} < x <$	$\mathbf{z} < x <$	$\mathbf{Z} < x <$	$\mathbf{y} < x < H$
$u(x,1,1)$	(v_1^+, v_2^-)	$(\mathbf{v_1^+}, \mathbf{v_2^-})$	(v_1^+, v_2^+)	$(\mathbf{v_1^-}, \mathbf{v_2^+})$	(v_1^-, v_2^+)
Control $u(x,1,0)$	$(v_1^+, 0)$	$(\mathbf{v_1^-}, \mathbf{0})$	$(\mathbf{v_1^-}, \mathbf{0})$	$(v_1^-, 0)$	$(v_1^-, 0)$
$u(x,0,1)$	$(0, v_2^-)$	$(0, v_2^-)$	$(\mathbf{0}, \mathbf{v_2^-})$	$(\mathbf{0}, \mathbf{v_2^-})$	$(0, v_2^+)$
	z^1 D^1	$\mathbf{z^2}$ $\mathbf{D^2}$	$\mathbf{z^3}$ $\mathbf{D^3}$	$\mathbf{z^4}$ $\mathbf{D^4}$	$\mathbf{z^5}$ D^5 z^6

Table 10.3. The control-scheme for fixed thresholds $z^2 = Y$, $z^3 = z$, $z^4 = Z$, $z^5 = y$ with $0 < Y < z < Z < y < H$. The differences from the scheme given in table 4.1 are written in bold characters.

- for $x \in D^3$ the solution is given by Eqs. (4.47) and (4.48) in case $\lambda_2\mu_1 v^3_{1;(1,0)} \neq \lambda_1\mu_2 v^3_{2;(0,1)}$ and by Eqs. (4.47) and (4.50) in case $\lambda_2\mu_1 v^3_{1;(1,0)} = \lambda_1\mu_2 v^3_{2;(0,1)}$. In both cases, the rates are given in table (10.3).
- for $x \in D^4$ the solution is given by Eqs. (4.42) and (4.44) (with $k = 4$) in case Eq. (4.43) is satisfied and by Eqs. (4.42) and (4.45) (with $k = 4$) in case it is not. In both cases, the rates are given in table (10.3) and the constants S_4 and K_4 are related by Eq. (4.41).
- matching at $z^2 = Y$. As $v_1^+ > v_2^-$, the matching condition at Y is given by Eq. (4.62) for $k = 2$ and with the rates according to table (10.3).
- matching at $z^5 = y$. As $v_1^- < v_2^+$, the matching condition at y is given by Eq. (4.61) for $k = 5$ and with the rates according to table (10.3).
- matching at $z^3 = z$. The matching condition at z is given by Eq. (4.54) for $k = 3$ and with the rates according to table (10.3). In addition, the threshold probability z_{11} is given by Eq. (4.52) with $k = 3$.
- matching at $z^4 = Z$. The matching condition at Z is given by Eq. (4.54) for $k = 4$ and with the rates according to table (10.3). In addition, the threshold probability Z_{11} is given by Eq. (4.53) with $k = 4$.

(5) Fix the configuration $z < Y < Z < y$ in $[0, H]$. According to Eqs. (4.16-4.18) the control-scheme in table (4.1) has to be replaced by the scheme in table (10.4). With respect to the control-scheme 4.1, the threshold ordering $z < Y < Z < y$ affects the C-K equations for $x \in D^k$ $k = 3, 4$ and the matching constraints at z^3, z^4 and z^5. Therefore, the stationary CDF is as before except that one has to introduce the following modifications:

- for $x \in D^3$ the solution is given by Eqs. (4.47) and (4.48) in case $\lambda_2\mu_1 v^3_{1;(1,0)} \neq \lambda_1\mu_2 v^3_{2;(0,1)}$ and by Eqs. (4.47) and (4.50) in case $\lambda_2\mu_1 v^3_{1;(1,0)} = \lambda_1\mu_2 v^3_{2;(0,1)}$. In both cases, the rates are given in table (10.4).
- for $x \in D^4$ the solution is given by Eqs. (4.42) and (4.44) (with $k = 4$) in case Eq. (4.43) is satisfied and by Eqs. (4.42) and (4.45) (with $k = 4$)

	$0 < x <$	z	$< x <$	$\mathbf{Y}$	$< x <$	$\mathbf{Z}$	$< x <$	$\mathbf{y}$	$< x < H$
Control $u(x,1,1)$	(v_1^+, v_2^-)		(v_1^+, v_2^+)	(v_1^+, v_2^+)		$(\mathbf{v_1^-}, \mathbf{v_2^+})$		(v_1^-, v_2^+)	
$u(x,1,0)$	$(v_1^+, 0)$		$(v_1^+, 0)$	$(\mathbf{v_1^-}, \mathbf{0})$		$(v_1^-, 0)$		$(v_1^-, 0)$	
$u(x,0,1)$	$(0, v_2^-)$		$(0, v_2^-)$	$(\mathbf{0}, \mathbf{v_2^-})$		$(\mathbf{0}, \mathbf{v_2^-})$		$(0, v_2^+)$	
	z^1	D^1	z^2	D^2	$\mathbf{z^3}$	$\mathbf{D^3}$	$\mathbf{z^4}$	$\mathbf{D^4}$	$\mathbf{z^5}$ D^5 z^6

Table 10.4. The control-scheme for fixed thresholds $z^2 = z$, $z^3 = Y$, $z^4 = Z$, $z^5 = y$ with $0 < z < Y < Z < y < H$. The differences from the scheme given in table 4.1 are written in bold characters.

in case it is not. In both cases, the rates are given in table (10.4) and the constants S_4 and K_4 are related by Eq. (4.41).

- matching at $z^3 = Y$. The matching condition at Y is given by Eq. (4.60) for $k = 3$ and with the rates according to table (10.4).
- matching at $z^4 = Z$. The matching condition at Z is given by Eq. (4.54) for $k = 4$ and with the rates according to table (10.4). In addition, the threshold probability Z_{11} is given by Eq. (4.53) with $k = 4$.
- matching at $z^5 = y$. As $v_1^- < v_2^+$, the matching condition at y is given by Eq. (4.61) for $k = 5$ and with the rates according to table (10.4).

11

Appendix Chapter 6

11.1 Numerical simulation

To appreciate the accuracy of the analytical approach exposed in Chapter 6, we compared the analytical distributions F, F_L and F_F with the results of a discrete event simulation software (here, "Taylor ED"). We simulated the outflow events of about 60000 items from a merge buffer in the case where S_n is i) constant and ii) exponentially distributed. The empirical distributions presented in the figures below are in excellent agreement with the theoretical distributions.

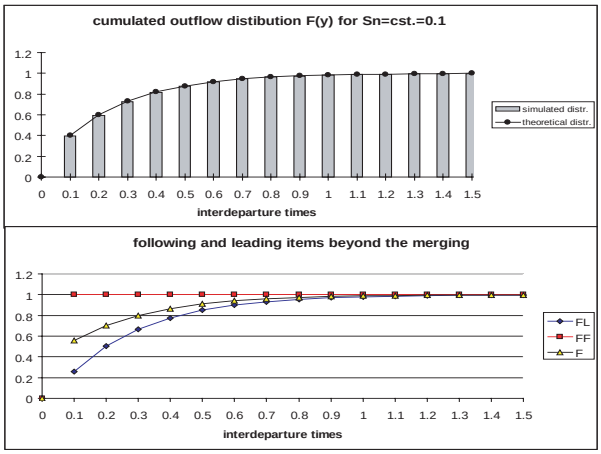

Fig. 11.1. Upper diagram: Empirical and theoretical cumulated distributions for a constant minimum exit time ($S_n = 0.1$). Lower diagram: The theoretical cumulated distribution F splits up into the distributions of the outflow times of leading (FL) and following (FF) items. As $S_n = 0.1$, inter-departure times from the merge are bigger than 0.1.

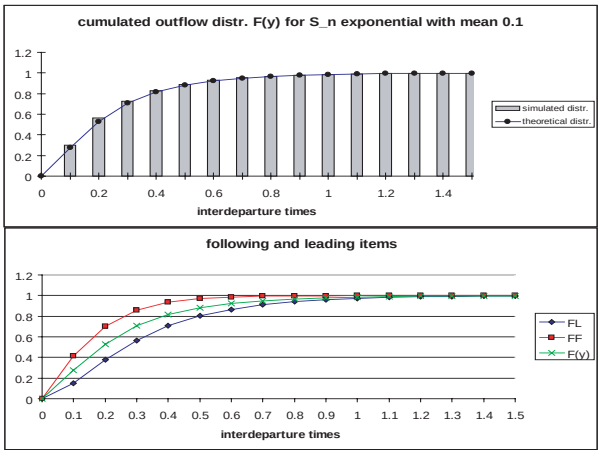

Fig. 11.2. "Upper" diagram: Empirical and theoretical cumulated distributions for a exponentially distributed minimum exit time ($\mathbb{E}(S_n) = 0.1$). Lower diagram: The theoretical cumulated distribution F splits up into the outflow times of leading (FL) and following (FF) items ($\mathbb{E}(S_n) = 0.1$).

12

Appendix Chapter 8

12.1 Conditioned Probabilities

Given the independent random variables $S, T : \Omega \to \mathbb{R}$ defined on some probability space $(\Omega, \mathcal{F}, \mathbb{P})$ such that T is exponentially distributed with parameter λ and such that the positive random variable S has the given cumulative distribution G we show that:

$$\begin{aligned} \rho &:= \mathbb{P}(T + \theta \leq S) = \lambda \mathbb{E}(S), && (12.1) \\ F_L(y) &:= \mathbb{P}(T + \theta \leq y \mid T + \theta > S) \\ &= \frac{\int_0^y \lambda e^{-\lambda t} G(t) \mathrm{d}t}{\int_0^\infty e^{-\lambda t} \mathrm{d}G(t)}, \quad y \geq 0, && (12.2) \\ F_F(y) &:= \mathbb{P}(S \leq y \mid T + \theta \leq S) \\ &= \frac{G(y) - \int_0^y e^{-\lambda(t-\theta)} \mathrm{d}G(t)}{\lambda \int_0^\infty t \mathrm{d}G(t)}, \; y \geq 0 && (12.3) \end{aligned}$$

where θ is given by Eq. (6.5). Note that θ is negative. Indeed, based on the well known inequality $e^{-x} \geq 1 - x$ it is immediate to see that $1 > \frac{1-\lambda \mathbb{E}(S)}{\mathbb{E}(e^{-\lambda S})}$ and hence that $\theta < 0$. This result is used twice in the following calculations where we replace the lower integration boundary $\max(\theta, 0) \overset{\text{not.}}{=} \theta \vee 0$ by 0.

We have:

$$\begin{aligned}
\mathbb{P}(T+\theta \le S) &= \int_0^\infty \mathbb{P}(S \ge x+\theta)\lambda e^{-\lambda x}\mathrm{d}x \\
&= \int_0^\infty (1-G(x+\theta))\lambda e^{-\lambda x}\mathrm{d}x \\
&= 1 - \int_0^\infty \lambda e^{-\lambda x}\big(\int_0^{x+\theta} \mathrm{d}G(t)\big)\mathrm{d}x \\
&= 1 - \int_0^\infty \big(\int_0^\infty \lambda e^{-\lambda x} 1_{x\ge t-\theta}\mathrm{d}x\big)\mathrm{d}G(t) \\
&= 1 - \int_0^\infty \lambda\big(\int_{t-\theta}^\infty e^{-\lambda x}\mathrm{d}x\big)\mathrm{d}G(t) \\
&= 1 - \int_0^\infty e^{-\lambda(t-\theta)}\mathrm{d}G(t) \qquad (12.4)
\end{aligned}$$

where on the first line we used the independence of S and T and on the forth resp. fifth line Fubinis' theorem resp. a usual integration by parts formula.

Hence replacing θ into the above formula we find:

$$\begin{aligned}
\rho &= 1 - \exp\big(\ln \frac{1-\lambda\mathbb{E}(S)}{\mathbb{E}(e^{-\lambda S})}\big)\int_0^\infty e^{-\lambda t}\mathrm{d}G(t) \\
&= 1 - \frac{1-\lambda\mathbb{E}(S)}{\mathbb{E}(e^{-\lambda S})}\mathbb{E}e^{-\lambda S} = \lambda\mathbb{E}(S)
\end{aligned}$$

thereby establishing the first formula Eq. (12.1). Next we have:

$$\begin{aligned}
F_L(y) &:= \mathbb{P}(T+\theta \le y \mid T+\theta > S) \\
&= \frac{\mathbb{P}(S < T+\theta \le y)}{\mathbb{P}(T+\theta > S)}.
\end{aligned}$$

Using Eq. (12.4) we see that the above denominator is given by $e^{\lambda\theta}\int_0^\infty e^{-\lambda t}\mathrm{d}G(t)$. For the numerator we have:

$$\begin{aligned}
\mathbb{P}(S < T+\theta \le y) &= \int_0^\infty \mathbb{P}(S < x+\theta \le y) 1_{\{x\le y-\theta\}}\lambda e^{-\lambda x}\mathrm{d}x \\
&= \int_0^{y-\theta} G(x+\theta)\lambda e^{-\lambda x}\mathrm{d}x \\
&= e^{\lambda\theta}\int_{\theta\vee 0}^{y} G(t)\lambda e^{-\lambda t}\mathrm{d}t
\end{aligned}$$

which establishes the second formula Eq. (12.2). Finally,

$$\begin{aligned}
F_F(y) &:= \mathbb{P}(S \le y \mid T+\theta \le S) \\
&= \frac{\mathbb{P}(T+\theta \le S \le y)}{\mathbb{P}(T+\theta \ge S)} \qquad (12.5)
\end{aligned}$$

Using Eq. (12.4) we see that the above denominator (which in fact is ρ) can be written as $\int_0^\infty t\mathrm{d}G(t)$. For the numerator we have:

$$
\begin{aligned}
\mathbb{P}(T+\theta \le S \le y) &= \int_0^\infty \mathbb{P}(x+\theta \le S \le y) 1_{\{x \le y-\theta\}} \lambda e^{-\lambda x} \mathrm{d}x \\
&= \int_0^{y-\theta} (G(y) - G(x+\theta)) \lambda e^{-\lambda x} \mathrm{d}x \\
&= G(y)(1-e^{-\lambda(y-\theta)}) - \lambda \int_0^{y-\theta} G(x+\theta) e^{-\lambda x} \mathrm{d}x \\
&= G(y)(1-e^{-\lambda(y-\theta)}) - \lambda \int_{\theta \vee 0}^{y} G(u) e^{-\lambda(u-\theta)} \mathrm{d}u \\
&= G(y)(1-e^{-\lambda(y-\theta)}) - \lambda e^{\lambda\theta} \int_0^\infty 1_{u \le y} \int_0^\infty 1_{t<u} e^{-\lambda u} \mathrm{d}G(t) \mathrm{d}u \\
&= G(y)(1-e^{-\lambda(y-\theta)}) - \lambda e^{\lambda\theta} \int_0^\infty \int_0^\infty 1_{t<u \le y} e^{-\lambda u} \mathrm{d}u \mathrm{d}G(t) \\
&= G(y)(1-e^{-\lambda(y-\theta)}) + e^{\lambda\theta} \int_0^y \left(e^{-\lambda y} - e^{-\lambda t}\right) \mathrm{d}G(t) \\
&= G(y)(1-e^{-\lambda(y-\theta)}) + e^{-\lambda(y-\theta)} G(y) - \int_0^y e^{-\lambda(t-\theta)} \mathrm{d}G(t) \\
&= G(y) - \int_0^y e^{-\lambda(t-\theta)} \mathrm{d}G(t)
\end{aligned}
$$

establishing the third formula Eq. (12.3).

13

Curriculum vitae

FILLIGER Roger, 23.10.1971-,
rue du milieu 20-22
CH-1400 Yverdon-les-Bains
roger.filliger@epfl.ch
Birthplace: Ennetmoos NW;

Recent professional activities:

- 01-05: PhD thesis at the EPF Lausanne under the direction of Prof. M-O. Hongler.
- 01-05: Part-time tutorial work at the STI-IPR-LPM Lab in Lausanne, EPFL and at the math. Institute of the University of Neuchâtel.
- 99-01: Tutorial work at the math. Institute of the University of Neuchâtel.
- 1999 Diploma in mathematics delivered by the University of Neuchâtel. Diploma work with Prof. A. Valette in the domain of operator algebras.
- 1995 Bachelor in mechanical engineering delivered by the ETS Lucerne. Diploma work with Prof. R. Schmutz in the domain of optimization of hydrodynamic devices.

Publications

- M.-O. Hongler and R. Filliger. Mesoscopic derivation of a fundamental diagram of one-lane traffic. *Physics Letters A*, 301: 597–602, 2002.
- R. Filliger and M.-O. Hongler. Supersymmetry in random two velocity processes. *Physica A*, 332: 141-150, 2004.
- R. Filliger. Discrete Derivation of Ruijgroks and Wus non-linear two velocity Boltzmann model with an application to traffic-flow modelling. *SIAM, Multiscale Modeling and Simulation*, 2(3): 440-451, 2004.
- R. Filliger and M.O. Hongler. Optimal thresholds control for failure prone tandem production systems. *to appear in IIE Transactions*, 2005.
- R. Filliger and M.-O. Hongler. Free-versus jamming-flow in buffered production lines. *Europ. J. Oper. Res.*, 167: 116-128, 2004.
- R. Filliger and M.O. Hongler. Relative Entropy and Efficiency Measure for diffusion-mediated transport processes. *J. Phys. A: Math. Gen.* 38: 1247-1255, 2005.
- R. Filliger and M.O. Hongler. Syphon dynamics - a soluble model of multi-agents cooperative behavior. *in press: Europhysics letters*, 2005.
- M.O. Hongler and R. Filliger. An exactly soluble Kolmogorov model for two interacting species. *to appear in: The mathematical scientist.*, 2005.

Proceedings

- R. Filliger and M.O. Hongler. Mesoscopic derivation of a fundamental diagram of one-lane traffic. *Preprint for the XXV^{th} Math encounter at the CCM "Centro de Ciencias Matematicas" at the University of Medeira, August 2004.*
- R. Filliger and M.O. Hongler. Controlled unreliable two-stage transfer lines with finite buffer. *Proceedings of the 5^{th} conference ROADEF, Avignon*, 296-297, 2003.
- R. Filliger and M.O. Hongler. Free versus jamming-flow in buffered production lines. *Proceedings of the 4^{th} conference MOSIM 2003, Toulouse*, 76-81, 2003.
- R. Filliger and M.O. Hongler. On the outflow process of a merge system for items with non-vanishing spacial extensions. *Proceedings of the 5^{th} conference MOSIM 2004, Nantes*,609-615, 2004.
- R. Filliger and M.O. Hongler. On the outflow process of a merge systems. *Preprint for the $XXVII^{th}$ Math encounter at the CCM, Oct. 2004.*
- R. Filliger and M.O. Hongler. Relative Entropy and Efficiency Measure for diffusion-mediated transport processes. *Preprint for the $XXVII^{th}$ Math encounter at the CCM, Oct. 2004.*

Acknowledgements

I want to express my deep gratitude to my adviser, Professor Max-Olivier Hongler. Without his tremendous help, his always welcoming availability and his encyclopedic physical knowledge, this thesis would be skeletonic or even non-existent. I thank him for having accepted me as a PhD student, for having introduced and guided me on my way through the fascinating world of scientific research and for having initiated, supported and amended this work and my proper scientific forthcoming. I am thankful for his kindness and friendship which made of my staying here at the EPFL a fruitful and happy period.

I thank Fabrice Dusonchet for fruitfully sharing time and space in our common office. His great sense of humor and our numerous extra-professional activities helped me through many situations. I thank you also for the many helpful advises and hints to find the way out from intricate computer problems.

My thanks go also to Professor Jaques Jacot who receives in the LPM Lab scientists and engineers coming from different fields thereby forming the necessary soil for fruitful interdisciplinary work.

I thank the Professors Ch. van den Broeck, Y. Dallery, J. Jacot and T. Mountford for accepting to make part of my thesis jury.

I thank Karine Genoud for professionally handling all the administrative work I have generated during my staying.

I thank Michelle Jacot for having indicated to me the PhD position at the LPM.

I thank Van Hongler for clarifying and arranging a few important points concerning my future scientific forthcoming.

My deepest gratitude goes to my parents for their constant encouragement and their huge confidence.

Finally thanks go to my invaluable social network formed by all my friends which contributed indirectly to this work through their very existence.

Lausanne, January 2005 *Roger Filliger*

References

1. D. Chowdhury, L. Santen and A. Schadschneider. Stochastical physics of vehicular traffic and some related systems. *Physics Reports*, 329:199–329, 2000.
2. K. Konishi, H. Kokame and K. Hirata. Coupled-map car-following model and its delayed-feedback control. *Physical Review E*, 60:4000–4007, 1999.
3. M. Bando, K. Hasebe, A. Nakayama, A. Shibata and A. Sugiyama. Dynamical model of traffic congestion and numerical simulation. *Physical Review E*, 51:1035, 1995.
4. P. Ciprut, M.-O. Hongler and Y. Salama. Hedging points for non-markovian piecewise deterministic production processes. *Discrete Events Dynamical Systems: Theory and Applications*, 8:365–375, 1998.
5. R. Akella and P.R. Kumar. Optimal control of Production rate in a Failure Prone Manufacturing System. *IEEE Trans. on Automatic Control*, 31 (2):116–126, 1986.
6. S.L. Albin. On Poisson Approximations for Superposition arrival processes in Queues. *Management Science*, 28 (2):126–137, 1982.
7. A.M. Makowski, F. Baccelli and A. Shwartz. The fork-join queue and related systems with synchronization constraints: Stochastic ordering and computable bounds. *Adv. Appl. Prob.*, 21 (3):629–660, 1989.
8. M. Annunziato. Non-Gaussian equilibrium distribution arising from the Langevin equation. *Physical Review E*, 65:0211130, 2002.
9. T. Antal and G.M. Schütz. Asymmetric exclusion process with next-nearest-neighbor interaction. *Phys. Rev. E*, 62.
10. H. Arendt. *Vita Activa: Vom tätigen Leben.* Serie Piper, 1967.
11. P. Bak. *How Nature Works.* Oxford University Press,Oxford, 1997.
12. R. Bellman. *Dynamic Programming.* Princton University Press, 1957.
13. T. Bielecki and P.R. Kumar. Optimality of zero-inventory policies for unreliable manufacturing systems. *Operations research*, 36 (4):532–541, 1988.
14. J.A. Buzacott and J.G. Shanthikumar. *Stochastic Models of Manufacturing Systems.* Prentice Hall, Englewood Cliffs, New Jersey, 1993.
15. John A. Buzacott. *The evolution of manufacturing system models: A personal view.* In: Stochastic modeling and optimization of manufacturing systems and supply chains. Chapter 3, Edited by: J.G. Shanthikumar, D.D. Yao and W. H. M. Zijm. Kluwer Academic Publisher, Bosten, Dordrecht, London, 2003.

16. M.O. Cáceres. Computing a non-Maxwellian velocity distribution from first principles. *Physical Review E*, 67:016102, 2003.
17. J. Camacho and D. Jou. H theorem for telegrapher type kinetic equations. *Physics Letters A*, 171:26–30, 1992.
18. H. Chen and D.D. Yao. *Fundamentals of queueing Networks.* Springer-Verlag, 2001.
19. P. Coillard and J.-M. Proth. Sur l'effet des stocks tampons dans une fabrication en ligne. *Rev. Belge Stat, Inf. et R.O.*, 24:1, 1983.
20. Factory Logic Software Company. The Bullwhip Effect. *Factory Logic Newsletter, http://www.factorylogic.com/newsletter.asp*, 1 (24), 2004.
21. F. Cooper, A. Khare, and U. Sukhatme. *SUSY in Quantum Mechanics.* World Scientific, 2001.
22. D. Armbruster, D. Marthaler and C. Ringhofer. Kinetic and Fluid Model hierarchies for supply chains. *SIAM: Multiscale Modelling and Simulation*, 2 (1):43–61, 2003.
23. D. Helbing, I. Farkas and T. Vicsek. Simulating dynamical features of escape panics. *Nature*, 407:487–590, 2000.
24. C. Daganzo. Requiem for second-order fluid with approximation to traffic flow. *Transportation Research B*, 29:277–286, 1995.
25. C.F. Daganzo. *A theory of supply chain.* Springer: Lecture notes in Economics and Mathematical Systems 526, 2003.
26. Y. Dallery and S. B. Gerschwin. Manufacturing flow Line Systems: A review of Models and Analytical Results. *Queueing Systems: Theory and Appl.(QUESTA)*, 12:3–94, 1992.
27. G. Darboux. . *C.R. Acad. Sci*, 94:1456, 1882.
28. M.H.A. Davis. Piecewise-deterministic Markov Processes: A general Class of non-diffusive Stochastic Models. *J. R. Statist. Soc. B*, 46:353–388, 1984.
29. B. Derrida. An exactly soluble non-equilibrium system: the asymmetric simple exclusion process. *Physics Reports*, 301:65–83, 1998.
30. C. Domb. Some probability distributions connected with recording apparatus. *Proceedings of the Cambridge Philosophical Society*, 43:335–341, 1948.
31. D. Dubois and Forestier J.P. Productivity and in process averages of 2 machines separated by a storage zone. *RAIRO-Automatique-Systems Analysis and Control*, 16 (2):105–132, 1982.
32. D. Durr and A. Bach. The Onsager-Machlup functional as Lagrangian for the most probable path of a diffusion process. *Comm. Math. Phys.*, 60:153–170, 1978.
33. F. Dusonchet. *Dynamic scheduling for production systems operating in a random environment. These No. 2825.* Press Polytechnique de l'EPFL., 2004.
34. JM.N. Eleftheriu. *On the analysis of hedging point policies of multi-stage production manufacturing systems.* UMI Dissertation Services, 1996.
35. Y. Lee et al. Universal Features in the Growth Dynamics of Complex Organizations. *Phys. Rev. Lett.*, 81 (15):32753278, 1998.
36. W. Feller. *An Introduction to Probability Theory and its applications, Vol. II.* J. Wiley and Sons, 1971.
37. R. Filliger. Mapel file generating the solutions to the optimal control problem. *http://lpmwww.epfl.ch/users/filliger/OptimalThresholds.html.*
38. R. Filliger. Discrete derivation of Ruijgrok and Wu's non-linear two-velocity model with an application to traffic flow modelling. *SIAM. MMS*, 2 (3):440–451, 2004.

39. R. Filliger and M.-O. Hongler. Mesoscopic derivation of a fundamental diagram of one-lane traffic. *Physics letters A*, 301:408–412, 2002.
40. R. Filliger and M.-O. Hongler. On the outflow process of a merge system for items with non-vanishing spacial extensions. *Actes de la 5e conf. francophone MOSIM 2004, Nantes, France*, 2:609–615, 2004.
41. R. Filliger and M.-O. Hongler. Supersymmetry in random two-velocity processes. *Physica A*, 332:141–150, 2004.
42. R. Filliger and M.-O. Hongler. Cooperative flow dynamics in production lines with buffer level dependent production rates. *EJOR*, 167:116–128, 2005.
43. R. Filliger and M.-O. Hongler. Optimal thresholds control for failure prone tandem production systems. *Submitted for publication in: IIE*, 2005.
44. R. Filliger and M.-O. Hongler. Relative Entropy and Efficiency Measure for diffusion-mediated transport processes. *J. Phys. A: Math. Gen.*, 38:1247–1255, 2005.
45. F.L. Hall, B.L. Allen and M.A. Gunter. Empirical analysis of freeway flow-density relationships. *Transp. Res. A*, 20:197–210, 1986.
46. W.H. Flemming and H.M. Soner. *Controlled Markov Processes and Viscosity Solutions*. Springer-Verlag, 1993.
47. G. van Ryzin, S.X.C. Lou and S.B. Gershwin. Production control for a tandem two-machine system. *IIE Transactions*, 25 (5):5–20, 1993.
48. C.W. Gardiner. *Handbook of Stochastic Methods.* Springer-Verlag, 1985.
49. S. B. Gershwin and M. H. Burman. A Decomposition Method for Analyzing Inhomogeneous Assembly/Disassembly Systems. *Annals of Operations Research*, 93:91–116, 2000.
50. S.B. Gershwin. Assembly/disassembly systems: an efficient decomposition algorithm for tree structured networks. *IIE Transactions*, 23 (4):302–314, 1991.
51. S.B. Gershwin. *Manufacturing Systems Engineering*. Prentice Hall, 1994.
52. I. Goldhirsch. Rapid granular flows. *Annual Review of Fluid Mechanics*, 35:267–293, 2003.
53. NJ.A. Goldstein. *Semigroups of Linear Operators and Applications*. Oxford University Press, New York, 1985.
54. S. Goldstein. On diffusions by discontinuous movements and on the telegraph equation. *Quarterly Journal of Mechanics and Applied Mathematics*, 4 (2):129–156, 1951.
55. B.D. Greenshields. A study of traffic capacity. *Proceedings of the Highway Research Board*, 14:448–477, 1935.
56. D. Gross and C.M. Harris. *Fundamentals of queueing theory*. Wiley Inter-Science, 1998.
57. H.M. Gupta and J.R. Campanha. Firms growth dynamics, competition and power-law scaling. *Physica A*, 323:626–634, 2003.
58. H-S. Ahn, I. Duenyas and M.E. Lewis. Optimal control of a two-stage tandem queuing system with flexible servers. *Probability in the Engineering and Information Sciences*, 16:453–469, 2002.
59. K.P. Hadeler. *Reaction telegraph equations and random walk systems*. Springer Verlag, 1993.
60. K.P. Hadeler. *Reaction Transport Systems in Biological Modelling*. Lecture Notes in Mathematics 1714: Springer Verlag, 1997.
61. H. Haken. *Synergetics*. Springer-Verlag, Heidelberg, 2004.
62. H. Hayakawa and K Naganishi. Theory of traffic jam in one lane model. *Phy. Rev. E*, 57:3839–3845, 1998.

63. D. Helbing. Gas-kinetic derivation of Navier-Stokes-like traffic equations. *Phys. Rev. E*, 53:23662381, 1996.
64. D. Helbing. Traffic and related self-driven many-particle systems. *Reviews of Modern Physics*, 73 (4):1067–1141, 2001.
65. D. Helbing. Modelling supply networks and business cycles as unstable transport phenomena. *New Journal of Physics*, 5:90.1–90.28, 2003.
66. R. Hersh. The birth of random evolutions. *Mathematical Intelligencer*, 25:53–60, 2003.
67. Hillen, Thomas and Othmer, H.G. The diffusion limit of transport equations derived from velocity jump processes. *SIAM J. Appl. Math.*, 61(3):751–775, 2000.
68. M.-O. Hongler. Supersymmetry and Signal Propagation in inhomogenous Transmission Lines. *Physica A*, 137:407–416, 1986.
69. M.-O. Hongler. *Lecture Notes in Physics: Chaotic and Stochastic Behaviour in Automatic Production Lines.* Springer-Verlag, 1994.
70. M.-O. Hongler and L. Streit. Generalized Master Equations and the Telegrapher's Equation. *Physica A*, 165:196–206, 1990.
71. M.O Hongler and R.C. Desai. Decay of unstable states in presence of fluctuations. *Helv.Phys. Acta.*, 59:367–389, 1986.
72. W. Horsthemke and R. Lefever. *Noise-Induced Transitions.* Springer-Verlag, 1984.
73. J.-Q. Hu. A Decomposition Approach to Flow Control in Tandem Production Systems. *Proc. of the 34th Conf. on Decision and Control*, New Orleans:3140–3143, 1995.
74. I. Derényi, M. Bier and R.D. Astumian. Generalized Efficiency and its Application to Microscopic Engines. *Physical Review Letters*, 83 (5):903–906, 1999.
75. O.L.R. Jacobs. *Introduction to Control Theory.* Oxford University Press, 1973.
76. J. Jacot. Privat communication. *LPM Lab*, 2004.
77. M.A. Jafari and J.G. Shanthikumar. Exact and approximate solutions to two-stage transfer lines with general uptime and downtime distributions. *IIE Transactions*, 19 (4):412–420, 1987.
78. B. Jamison. The Markov Processes of Schrödinger. *Z. Wahrscheinlichkeitstheorie verw. Gebiete*, 32:323–331, 1995.
79. D. Jou. . *Private communication*, 2004.
80. G. Junker. *SUSY Methods in Quantum and Statistical Physics.* Springer-Verlag, 1996.
81. K. Visscher, M. Schnitzer and S. Block. Single kinesin molecules studied with a molecular force clamp. *Nature*, 400:184–189, 1999.
82. M. Kac. A stochastic Model related to the telegrapher's equation. *Rocky Mt. J. Math.*, 4:497–509, 1974.
83. Boris S. Kerner. *The Physics of Traffic.* Springer, Series : Understanding Complex Systems, 2004.
84. C. Kippnis and C. Landim. *Scaling limits of Interacting Particle Systems.* Springer-Verlag, 1998.
85. A. Klar and R. Wegener. A Hierarchy of models of multilane vehicular traffic. *SIAM*, 59:983–1001, 1999.
86. A.J. Koning. On single-lane roads. *Adv. Appl. Prob.*, 21:142–158, 1989.
87. R.D. Kühne and M.B. Rödiger. Macroscopic simulation model for freeway traffic with jams and stop-start waves. *B.L. Nelson, W.D. Kelton, and G.M.*

Clark, eds. Proceedings of the 1991 Winter Simulation Conference, Phoenix, Arizona., page 762, 1991.
88. S. Kullback. *Information Theory and Statistics*. Dover, New York, 1968.
89. T.G. Kurtz. Extensions of Trotter's Operator Semigroup Approximation Theorems. *J. of Funct. Anal.*, 3:354–375, 1969.
90. L. Neubert, L. Santen, A. Schadschneider, M. Schreckenberg. Stochastic theory of freeway traffic. *Phys. Rev. E*, 60:6480, 1999.
91. R. Gamkrelidze L. Pontriaguine, V. Boltianski and E. Michtchenko. *Théorie math. des processus optimaux*. MIR, Moscou, 1974.
92. David S. Landes. *The Unbound Prometheus:Technological Change and Industrial Development in Western Europe from 1750 to the Present*. Cambridge University Press, 1969.
93. T. Li. Global solutions and zero relaxation limit for a traffic flow model. *SIAM J. Appl. Math.*, 61 (3):1042–1061, 2000.
94. T.M. Liggett. *Stochastic Interacting Systems*. Springer-Verlag, 1999.
95. M.J. Lighthill and G.B. Whitham. On kinematic waves II: A theory of traffic flow on long crowded roads. *Proceedings of the Royal Society of London A*, 229:317–345, 1955.
96. M. Chipot, D. Kinderlehrer and M. Kovalczyk. A variational principle for molecular motors. *Meccanica*, 38:505–518, 2003.
97. M. Schreckenberg, A. Schadschneider, K. Nagel, and N. Ito. Discrete stochastic models for traffic flow. *Phys. Rev. E*, 51.
98. R. Mahnke and J. Kaupuzs. Stochastic theory of freeway traffic. *Phys. Rev. E*, 59 (1):117–125, 1999.
99. Malathronas J.P., Perkins J.D., Smith R.L. The availability of a system of 2 unreliable machines connected by an intermediate storage tank. *IIE Transactions*, 15(3):195–201, 1983.
100. J. Masoliver and G.H. Weiss. First passage times for a generalized telegrapher's equation. *Physica A*, 183:537–548, 1992.
101. M. Matsuo and S. Sasa. Stochastic energetics of non-uniform temperature systems. *Physica A*, 276:188–200, 1999.
102. Medhi. *Stochastic Models in Queueing Theory. Second Edition*. Academic Press, 2003.
103. M.O. Hongler, H.M. Soner and L. Streit. Stochastic Control for a class of Random Evolution Models. *Applied mathematics and Optimization*, 49:113–121, 2004.
104. N. van Foreest, M. Mandjess and W. Scheinhardt. Analysis of a Feedback Fluid Model for Heterogeneous TCP Sources. *Stochastic Models*, 19 (3):299–324, 2003.
105. T. Nagatani. Traffic jams induced by fluctuation of a leading car. *Physical Review E*, 61;4:3534–3540, 1999.
106. N.C. Tsourveloudis, E. Dretoulakis and S. Ioannidis. Fuzzy work-in-process inventory control of unreliable manufacturing systems. *Information Sciences*, 127:69–83, 2000.
107. P. Nelson. A kinetic model of vehicular traffic and its associated bimodal equilibrium solutions. *Transport Theory and Statistical Physics*, 24:383–409, 1995.
108. E. Orsingher. Hyperbolic-equations arising in random models. *Stochastic Processes and their Applications*, 21 (1):93–106, 1985.

109. H.G. Othmer and T. Hillen. The diffusion limit of Transport Equations II: Chemotaxis equations. *SIAM J. Appl. Math.*, 62 (4):1222–1250, 2002.
110. P. Reimann, C. van den Broeck, H. Linke, P. Hänggi, M. Rubi and A. Pérez-Madrid. Giant Acceleration of Free Diffusion by Use of Tilted Periodic Potential. *Physical Review Letters*, 87:010602, 2001.
111. H.T. Papadapoulos, C. Heavy, and J. Browne. *Queueing Theory in Manufacturing Analysis and Design.* Chapman and Hall, Cambridge, 1993.
112. J.M.R. Parrondo and B.J. De Cisneros. Energetics of Brownian Motors: a review. *Applied Physics A*, 75:179–191, 2002.
113. J.M.R. Parrondo and L. Dinis. Brownian motion and Gambling: from ratchets to paradoxical games. *Contemporary Physics*, 45:147–157, 2004.
114. S.L. Paveri-Fontana. On Boltzmann-like treatments for traffic flow. *Transportation Research*, 9:225–235, 1975.
115. H.J. Payne. *Math. Models of Public Systems, Vol.1, pp.51.* Edited by G.A. Bekey, 1971.
116. A. Pazy. *Semigroups of Linear Operators and Applications to Partial Differential Equation.* Appl. Math. Sciences 44, Springer-Verlag, 1983.
117. M.A Pinsky. *Lectures on Random Evolutions.* World Scientific Publishing, 1991.
118. S. G. Powell and K. L. Schultz. Throughput in Serial Lines with State-Dependent Behavior. *Management Science*, 50 (8):1095–1105, 2004.
119. P. Dai Pra. A stochastic control approach to reciprocal diffusion processes. *Applied mathematics and Optimization*, 23:313–329, 1991.
120. I. Prigogine and R.Herman. *Kinetic theory of vehicular traffic.* American Elsevier Publishing Co., 1971.
121. N.E. Ratanov. Telegraph Evolutions in Inhomogeneous Media. *Markov Processes and Rel. Fields*, 5:53–68, 1999.
122. M. Rauner. Langsam gehts schneller. *Sonntags Zeitung*, 13.6.:79–81, 2004.
123. P. Reimann. Brownian Motors: noisy transport far from equilibrium. *Phys. Rep.*, 361:57, 2002.
124. P. Reimann and P. Hänggi. Introduction to the physics of Brownian Motors. *Appl. Phys. A: Material Science and Processing*, 75:169–178, 2002.
125. F. Rezakhanlou. Propagation of chaos for particle systems associated with discrete Boltzmann equation. *Stochastic Processes and their Appl.*, 64:55–72, 1996.
126. W.A. Rosenkrantz and Li Zhang Bing. Diffusion approximation for a class of Markov Processes satisfying a nonlinear Fokker-Plank equation. *Nonlinear Analysis. Theory, Methods and Applications*, 7 (10):1089–1099, 1983.
127. W.A. Rosenkrantz and C.C.Y. Dorea. Limit Theorems for Markov Processes via a variant of the Trotter-Kato theorem. *J. Appl. Prob.*, 17:704–715, 1980.
128. Th.W. Ruijgrok and T.T. Wu. A completely solvable model of the nonlinear Boltzmann equation. *Physica*, 113 A:401–416, 1982.
129. S. Cheybani, J. Kertesz, M. Schreckenberg. Stochastic boundary conditions in the deterministic Nagel-Schreckenberg traffic model. *Phys. Rev. E*, 63.
130. R.A. Sack. A modification of Smoluchowski's diffusion equation. *Physica*, XXII:917–918, 1956.
131. E. Schrödinger. Über die Umkehrung der Naturgesetzte, Sitzung der Preuss. Akad. Wissen., Berlin. *Phys. Math.*, 144, 1931.
132. F. Schweitzer. *Self-Organization of Complex Structures: From Individual to Collective Dynamics.* Gordon and Breach, London, 1997.

133. K. Sekimoto. Kinetic characterization of heat bath and the energetics of thermal ratchet models. *Journal of the Physical Society of Japan*, 66(5):1234–1237, 1997.
134. S.P. Sethi and Q. Zhang. *Hierarchical Decision Making in Stochastic Manufacturing Systems*. Birkhauser, 1994.
135. P. Sibani and N.G. van Kampen. An exactly soluble Relaxation Problem. *Physica A*, 122:397–412, 1983.
136. S. Solomon and E. Shir. Complexity; a Science at 30. *Europhysics news*, March/April:54–57, 2003.
137. D. Sornette. *Critical Phenomena in Natural Sciences*. Springer, 2000.
138. S.Tadiki, M. Kikuchi, Y. Sugiyama and S. Yukawa. Noise induced Congested Traffic Flow in Coupled Map optimal velocity model. *Journal of the Physical Society of Japan*, 68.
139. Y. Sugiyama and H. Yamada. *in Traffic in Granular Flow 97, p.301. Eds.: Schreckenberg and Wolf*. Springer, Singapore, 1998.
140. S.X.C. Lou, S.P. Sethi and Q. Zhang. Optimal feedback production planning in a stochastic two-machine flowshop. *European Journal of Operational Research*, 73:331–345, 1994.
141. C. Tsallis. Entropic nonextensivity: a possible measure of complexity. *Chaos Solitons and Fractals*, 13 (3):371–391, 2002.
142. C. Tsallis. Nonextensive statistical mechanics: a brief review of its present status. *Anais da Academia Brasileira de Ciencias*, 74 (3):393–414, 2002.
143. N.G. van Kampen. *Stochastic Processes in Physics and Chemistry*. North-Holland, 1981.
144. M.H. Veatch and L.M. Wein. Optimal control of a two-station tandem Production/Inventory System. *Operations Research*, 42 (2):337–350, 1994.
145. J. Walrand. *An Introduction to Queueing Networks*. Prentice-Hall Int. Editions, 1988.
146. H. Wang. Mathematical theory of molecular motors and a new approach for uncovering motor mechanism. *IEE Proc.-Nanobiotechnol.*, 150 (3):127–133, 2003.
147. H.J. Warnecke. *The Fractal Company: A Revolution in Corporate Culture*. Springer, 1993.
148. Ding wei Huang and Chung wei Tsai. Low-density limit of the nagel-schreckenberg model. *Phys. Rev. E*, 63:012101, 2001.
149. G.H. Weiss. Some applications of persistent random walks and the telegrapher's equation. *Physica A*, 311:381–410, 2002.
150. W.F-Phillips. A kinetic model of vehicular traffic and its associated bimodal equilibrium solutions. *Transpn. Plan. Technol.*, 5:131, 1979.
151. J. Wijngaard. The effect of interstage buffer storage on the output of two unreliable production units in series, with different production rates. *AIIE Transactions*, 11 (1):42–47, 1979.
152. E. Witten. Dynamical breaking of supersymmetry. *Nuc. Phys. B*, 202:513–554, 1981.
153. E. Wong. The construction of a class of stationary Markov processes. *Symp. Appl. Math.*, 16:264, 1964.
154. B. Zimmern. Etude de la propagation des arrèts aléatoires dans une chaîne de production. *Rev. de Stat. Appl.*, 4:85–104, 1956.

Index

abstract Cauchy problem, 68
adaptability, 26
admissible control, 117
anisotropic
  collision, 67
  interactions, 73
approach to equilibrium, 110

breakdowns of machines, 23
Brownian
  particle, 114
  motion, 103
  motor, BMot, 113
bullwhip effect, 23
busy period, 96

Cattaneo system, 104
chemotaxis, 105
clogging at bottlenecks, 4
competition, 7
complex behavior, 63
cost, 41
  average cost criterion, 44
  discounted cost criterion, 44
  functional, 115
  structure, 42
current-density relations, 5

diffusive re-scaling, 77
dimensionless stability condition, 31
discrete
  time sampling, 34
  derivation, 64
  feedback system, 34
  material flow merge, 85
  space-discrete hopping model, 63
dissipative structures, 4
dynamical phenomena, 4
dynamics
  collective dynamics, 63
  control free dynamics, 116
  cooperative dynamics, 22
  crowd dynamics, 8
  stochastic dynamics, 72

efficiency measure, 113
  motor efficiency, ME, 113
equation
  Boltzmann-like equation, 63
  Burgers, 72
  Chapman-Kolmogorov, C-K, 42
  continuity equation, 77
  dynamic programming equation, 45
  fluid-dynamic equations, 64
  Fokker-Planck equation, 103, 116
  Hamilton-Jacobi-Bellmann, 41
  hyperbolic, 104
  Kolmogorov forward equations, 65
  Langevin, 103, 114, 117
  Master equation, 79
  parabolic, 103
  Pollaczek-Kinchine, 92
  Smoluchowski diffusion, 108
  stochastic diff. equation, 78, 116
  Takàcs integral equation , 94
  telegraphist equation, 76
external load, 113

$\mathcal{F}$, 32
factory system, 4
feedback, 40
  optimal feedback control, 40
flexibility, 22
flow, 21
  compressibility, 28
  diagram, 22, 35
  flow balance, 52
  inversion, 57
  jamming flows, 31
  merging flows, 85
  patterns, 7
  shop, 23
flow regimes
  free flow production regime, 29
  free flow regime, 22
  jamming flow regime, 22
  No-jamming condition, 35
  soft-running regime, 36
fluctuation rectifier, 113
fluctuation-dissipation relation, 114
fluid modelling approach, 42
free period, 96

γ, viscous friction coefficient, 115
Gaussian White Noise, 79, 116
generator
  infinitesimal, 68, 79
  matrix, 65

human operators, 22, 36
hypergeometric functions, 111

Industrial Revolution, 3
inhomogeneous diffusion, 103
interacting particle system, 63
interruptions, 39
  blocking, 4, 39
  operation dependent, 43
  starving, 4, 39
  time dependent, 43
items
  following item, 95
  following items, 89
  leading item, 95
  leading items, 89

just in time, 32

k_B Boltzmann's constant, 115
kinetic features
  collision, 63
  migration, 63
  reaction, 63
Kullback distance, 118

Laplace-Stielties Transform, LST, 93

Markov network models, 8
mechanical diodes, 113
Micro-Meso-Macro link, 63
  micro-macro paradigm, 63
  multi-scale analysis, 80
most probable paths, 116
MS, manufacturing system, 4
multiplexing, 8, 85

nearest neighbor-influence, 28

Onsager-Machlup functional, 116
optimal
  control, 9
  production rate model, 27
  transportation, 9
  velocity model, 25
  control, 41, 115
  policy, 41, 44
  Stochastic optimal control, 6
  thresholds, 59
OR, Operations Research, 7
outflow delays W_n, 91

People based manufacturing, 40
performance measures, 36
  dynamic performance factor, 28
  stationary first order, 92
persistent random walk, 104
phenomenological, 25
process
  arrival process, 87
  controlled diffusion process, 116
  diffusion-mediated transport, 113
  exit process, 90
  jump processes, 103
  outflow process, 90
  Poisson process, 85
  stationary stochastic, 119
  transport process, 114

two-velocity process, 103
psychological effects, 26
pull production, 32
pulsating potential, 119

quantum mechanics, QM, 109
Queueing Systems, 5

Radon-Nykodim derivative, 118
reaction time, 32
relative entropy, 118
representation formula, 69
response delay time, 25
Rosen-Morse II potential, 111

self-organizing effects, 5
semipermeable membranes, 53
sensitivity, 26
shock wave, 67, 82
slower-is-faster effect, 8, 88
spectral modulation, 105
stationary, 52
distribution, 49, 58, 110
performance measures, VII
solution, 107
Statistical Physics, 5
supply chains, 9
SUSY
broken SUSY, 110
good SUSY, 110
partner Hamiltonians, 109
partner potentials, 109
supersymmetric relation, 107
supersymmetry, SUSY, 109
synergetic approach, 22

telegraph process, 79
tilted pulsating potential, 121
time-localized perturbation, 29
traffic
Greenshields traffic model, 75
hysteresis, 73
macroscopic approach, 72
mesoscopic approach, 74
microscopic approach, 72
multi-lane road, 90
stochastic microscopic model, 74
stop-and-go traffic, 73
traffic system, 71
Traffic Theory, 5
traffic-flow modelling, 71
transformation
Hopf-Cole transformation, H-C, 76
logarithmic transform., L-T, 76, 116
transient
behaviour, 107
performance measures, VII, 33
solutions, 107
travelling ratchets, 122
Trotter–Kato approx. theorem, 68

u^*, optimal drift field, 115
unavailability factor, 32

value function, 45

work-cells, 4

$\mathcal{Z}$, 31